Number 44 Year 2023

Journal of New Theory

ISSN: 2149-1402

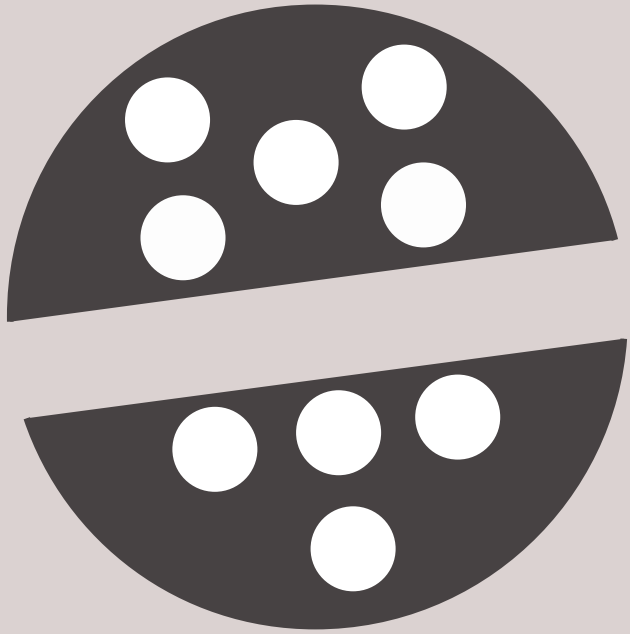

Editor-in-Chief
Naim Çağman

www.dergipark.org.tr/en/pub/jnt

CONTENTS

Journal of New Theory (abbreviated as J. New Theory or JNT) is a mathematical journal focusing on new mathematical theories or their applications to science.
J. New Theory is an international, peer-reviewed, and open-access journal.
JNT was founded on 18 November 2014, and its first issue was published on 27 January 2015.
Language: As of 2023, JNT accepts contributions in American English only.
Editor-in-Chief: Naim Çağman
E-mail: journalofnewtheory@gmail.com
APC: JNT incurs no article processing charges.
Review Process: Blind Peer Review
DOI Numbers: The published papers are assigned DOI numbers.
The policy of Screening for Plagiarism: JNT accepts submissions for pre-review only if their reference-excluded similarity rate is a **maximum of 30%**.

Publication Ethics: The governance structure of Journal New Theory and its acceptance procedures are transparent and designed to ensure the highest quality of published material. JNT adheres to the international standards developed by the Committee on Publication Ethics (COPE).

Aim & Scope

Journal of New Theory aims to share new ideas in pure or applied mathematics with the world of science.

Journal of New Theory publishes original research articles and reviews from all science branches that use mathematics theories.

Journal of New Theory is concerned with the studies in the areas of **MSC2020**, but not limited to:

Mathematical Sciences > Applied Mathematics > Approximation Theory and Asymptotic Methods
Mathematical Sciences > Applied Mathematics > Biological Mathematics
Mathematical Sciences > Applied Mathematics > Calculus of Variations, Mathematical Aspects of Systems Theory and Control Theory
Mathematical Sciences > Applied Mathematics > Complex Systems in Mathematics
Mathematical Sciences > Applied Mathematics > Dynamical Systems in Applications
Mathematical Sciences > Applied Mathematics > Financial Mathematics
Mathematical Sciences > Applied Mathematics > Mathematical Methods and Special Functions

Mathematical Sciences > Applied Mathematics > Operations Research İn Mathematics
Mathematical Sciences > Applied Mathematics > Theoretical and Applied Mechanics in Mathematics
Mathematical Sciences > Applied Mathematics > Applied Mathematics (Other)
Mathematical Sciences > Numerical and Computational Mathematics > Experimental Mathematics
Mathematical Sciences > Numerical and Computational Mathematics > Finite Element Analysis
Mathematical Sciences > Numerical and Computational Mathematics > Mathematical Optimization
Mathematical Sciences > Numerical and Computational Mathematics > Numerical Analysis
Mathematical Sciences > Numerical and Computational Mathematics > Numerical Solution of Differential and Integral Equations
Mathematical Sciences > Numerical and Computational Mathematics > Symbolic Calculation
Mathematical Sciences > Numerical and Computational Mathematics > Numerical and Computational Mathematics (Other)
Mathematical Sciences > Pure Mathematics > Algebra and Number Theory
Mathematical Sciences > Pure Mathematics > Algebraic and Differential Geometry
Mathematical Sciences > Pure Mathematics > Category Theory, K Theory, Homological Algebra
Mathematical Sciences > Pure Mathematics > Combinatorics and Discrete Mathematics (Excl. Physical Combinatorics)
Mathematical Sciences > Pure Mathematics > Group Theory and Generalizations
Mathematical Sciences > Pure Mathematics > Lie Groups, Harmonic and Fourier Analysis
Mathematical Sciences > Pure Mathematics > Mathematical Logic, Set Theory, Lattices and Universal Algebra
Mathematical Sciences > Pure Mathematics > Operator Algebras and Functional Analysis
Mathematical Sciences > Pure Mathematics > Ordinary Differential Equations, Difference Equations and Dynamical Systems
Mathematical Sciences > Pure Mathematics > Partial Differential Equations
Mathematical Sciences > Pure Mathematics > Real and Complex Functions (Incl. Several Variables)
Mathematical Sciences > Pure Mathematics > Topology
Mathematical Sciences > Pure Mathematics > Pure Mathematics (Other)
Mathematical Sciences > Statistics > Applied Statistics
Mathematical Sciences > Statistics > Biostatistics
Mathematical Sciences > Statistics > Computational Statistics
Mathematical Sciences > Statistics > Forensic Evaluation, Inference and Statistics
Mathematical Sciences > Statistics > Large and Complex Data Theory
Mathematical Sciences > Statistics > Operation
Mathematical Sciences > Statistics > Probability Theory

Mathematical Sciences > Statistics > Quantitative Decision Methods
Mathematical Sciences > Statistics > Risk Analysis
Mathematical Sciences > Statistics > Soft Computing
Mathematical Sciences > Statistics > Spatial Statistics
Mathematical Sciences > Statistics > Statistical Analysis
Mathematical Sciences > Statistics > Statistical Data Science
Mathematical Sciences > Statistics > Statistical Experiment Design
Mathematical Sciences > Statistics > Statistical Quality Control
Mathematical Sciences > Statistics > Statistical Theory
Mathematical Sciences > Statistics > Stochastic Analysis and Modelling
Mathematical Sciences > Statistics > Theory of Sampling
Mathematical Sciences > Statistics > Statistics (Other)

Journal Boards

Section Editors

Muhammad Riaz
Department of Mathematics, Punjab University, Quaid-e-Azam Campus, Lahore, Pakistan
mriaz.math@pu.edu.pk
Topology, Fuzzy Sets and Systems, Machine Learning, Computational Intelligence, Linear Diophantine Fuzzy Set

Pabitra Kumar Maji
Department of Mathematics, Bidhan Chandra College, Asansol, Burdwan (W), West Bengal, India.
pabitra_maji@yahoo.com
Soft Sets, Fuzzy Soft Sets, Intuitionistic Fuzzy Sets, Fuzzy Sets, Decision Making Problems

Kalyan Mondal
Department of Mathematics, Jadavpur University, Kolkata, West Bengal, India
kalyanmathematic@gmail.com
Neutrosophic Sets, Rough Sets, Decision Making, Similarity Measures, Neutrosophic Soft Topological Space

Sunil Jacob John
Department of Mathematics, National Institute of Technology Calicut, Calicut Kerala, India
sunil@nitc.ac.in
Topology, Fuzzy Mathematics, Rough Sets, Soft Sets, Multisets

Murat Sarı
Department of Mathematics, Istanbul Technical University, İstanbul, Türkiye
muratsari@itu.edu.tr
Computational Methods, Differential Equations, Heuristic Methods, Biomechanical Modelling, Economical and Medical Modelling

Alaa Mohamed Abd El-Latif
Department of Mathematics, Faculty of Arts and Science, Northern Border University, Rafha, Saudi Arabia
alaa_8560@yahoo.com
Fuzzy Sets, Rough Sets, Topology, Soft Topology, Fuzzy Soft Topology

Ahmed A. Ramadan
Mathematics Department, Faculty of Science, Beni-Suef University, Beni-Suef, Egypt
aramadan58@gmail.com
Topology, Fuzzy Topology, Fuzzy Mathematics, Soft Topology, Soft Algebra

Journal of New Theory
ISSN: 2149-1402

44 (2023) 1-9
Journal of New Theory
https://dergipark.org.tr/en/pub/jnt
Open Access

BL-Algebras with Permuting Tri-Derivations

Damla Yılmaz[1]

Article Info
Received: 29 Apr 2023
Accepted: 11 Jul 2023
Published: 30 Sep 2023
doi:10.53570/jnt.1289799
Research Article

Abstract — Basic logic algebras (BL-algebras) were introduced by Hajek. Multi-value algebras (MV-algebras), Gödel algebras, and product algebras are particular cases of BL-algebras. Moreover, BL-algebras are algebraic structures, and their principal examples are the real interval $[0,1]$ with the structure given by a continuous t-norm and abelian l-groups. In this article, we consider a type of derivation structure on BL-algebras. We study $(\odot,\vee)$-permuting tri-derivations of BL-algebras and their examples and basic properties. We obtain results regarding the trace of $(\odot,\vee)$-permuting derivations on Gödel BL-algebras. Finally, the article presents that the results herein can be generalized in future research.

Keywords *BL-algebra, permuting tri-derivation, Boolean algebra, isotone, trace*

Mathematics Subject Classification (2020) 08A05, 03G25

1. Introduction

The interest in multi-value algebras (MV-algebras) introduced by Chang [1] continues to increase. One of the most important examples of MV-algebra is the interval $[0,1]$ of the commutative l-group: $(M,\max,\min,+,',0)$ equipped with a continuous t-conorm and continuous t-norm defined by $m\oplus n=\min\{m+n,1\}$ and $m\odot n=\max\{m+n-1,0\}$ and with the negation defined by $m'=1-m$. After MV-algebras, Gödel algebras and product algebras have been investigated [2–5]. These three structures form the most important algebraic model structure for fuzzy logic, which are Lukasiewicz logic, Gödel logic and product logic, respectively. These logics studying these algebras are of logical interest, as well as their connection to some mathematical structures, as they correspond to the most important continuous t-norms on $[0,1]$ and their associated residues. Basic logic algebras (BL-algebras) [6] has been introduced by Hajek. MV-algebras, Gödel algebras, and product algebras are particular cases of BL-algebras. Various derivation studies [7–9] have been done on BL-algebras. In this article, we investigate a derivation type defined by some authors [10–13] in rings, lattices, and MV-algebras. More precisely, we define a type of permuting tri-derivations on BL-algebras and study some of its properties.

This article is organized as follows: The next section reminds some results and basic properties of BL-algebras. Section 3 defines $(\odot,\vee)$-permuting tri-derivation structure in BL-algebras and obtains their some results. Moreover, it explores many properties by the trace of the $(\odot,\vee)$-permuting tri-derivation on BL-algebras. Finally, the conclusion briefly overviews this type of algebra and discusses future studies.

[1]damla.yilmaz@erzurum.edu.tr (Corresponding Author)
[1]Department of Mathematics, Faculty of Science, Erzurum Technical University, Erzurum, Türkiye

2. Preliminaries

This section provides some basic notions to be needed for the next section. A t-norm $\otimes$ on the real interval $[0,1]$ is a commutative and associative operation on $[0,1]$ such that

i. If $\beta \leq \delta$, then $\beta \otimes \eta \leq \delta \otimes \eta$, for all $\beta, \delta, \eta \in [0,1]$

ii. $1 \otimes \beta = \beta$, for all $\beta \in [0,1]$

From i and ii, $0 \otimes \beta = 0$, for all $\beta \in [0,1]$. A t-norm $\otimes$ on $[0,1]$ is continuous if it is continuous in the usual sense as a function $\otimes : [0,1] \times [0,1] \to [0,1]$. On $[0,1]$, Lukasiewicz t-norm, Gödel t-norm, and Product t-norm, the most important continuous t-norms, are defined as follows, respectively:

$$\beta \odot \delta = \max\{\beta + \delta - 1, 0\}$$

$$\beta \odot \delta = \min\{\beta, \delta\}$$

and

$$\beta \odot \delta = \beta\delta$$

Note that every continuous t-norm $\otimes$ on $[0,1]$ induces a binary operation $\to$ defined by

$$\beta \to \delta = \max\{\eta \in [0,1] | \, \beta \otimes \eta \leq \delta\}$$

called the associated residuum. The binary operation satisfies the statement $\beta \otimes \delta \leq \eta$ if and only if (iff) $\beta \leq \delta \to \eta$, for all $\beta, \delta, \eta \in [0,1]$. These three norms above are related to fuzzy logic along with the residues Lukasiewicz implication, Gödel implication, and Product implication, defined as follows, respectively:

$$\beta \to \delta = \min\{1, 1 - \beta - \delta\}$$

$$\beta \to \delta = \begin{cases} 1, & \beta \leq \delta \\ \delta, & \text{otherwise} \end{cases}$$

and

$$\beta \to \delta = \begin{cases} 1, & \beta \leq \delta \\ \frac{\delta}{\beta}, & \text{otherwise} \end{cases}$$

If $\otimes$ is a continuous t-norm on $[0,1]$ and $\to$ is the associated residuum, then the structure

$$([0,1], \max, \min, \otimes, \to, 0, 1)$$

is the starting point in describing and investigating Basic Logic and corresponds to the basic logic system: BL-algebras.

Definition 2.1. [6] A basic logic algebra (BL-algebra) is a structure $(\Lambda, \wedge, \vee, \odot, \to, 0, 1)$ such that

i. $(\Lambda, \wedge, \vee, 0, 1)$ is a bounded lattice

ii. $(\Lambda, \odot, 1)$ is a commutative monoid

iii. $\beta \leq \delta \to \eta$ iff $\delta \odot \beta \leq \eta$ (residuation)

iv. $\beta \wedge \eta = \beta \odot (\beta \to \eta)$ (divisibility)

v. $(\beta \to \eta) \vee (\eta \to \beta) = 1$ (prelinearity)

For any $\beta, \eta \in \Lambda$, we define

$$\beta^* = \beta \to 0, \quad \beta \oplus \eta = \left(\beta^* \odot \eta^*\right)^*, \quad \text{and} \quad \beta \ominus \eta = \beta \odot \eta^*$$

We recall that a BL-algebra Λ is an MV-algebra iff $(\beta^*)^* = \beta$, for all $\beta \in \Lambda$ [4]. A Gödel algebra is a

BL-algebra Λ satisfying the condition $\beta \odot \beta = \beta$, for all $\beta \in \Lambda$ [6]. Moreover, a product algebra is a BL-algebra Λ satisfying the conditions *i.* $\beta \wedge \beta^* = 0$ and *ii.* $(\delta^*)^* \odot (\beta \odot \delta \to \eta \odot \delta) \leq \beta \to \eta$, for all $\beta, \eta, \delta \in \Lambda$ [6].

Proposition 2.2. [2] Suppose that Λ is a BL-algebra and $\beta, \eta, \delta \in \Lambda$. Thus, the followings hold:

i. $\beta \leq \eta$ iff $\beta \to \eta = 1$

ii. $\beta \to (\eta \to \delta) = (\beta \odot \eta) \to \delta = \eta \to (\beta \to \delta)$

iii. If $\beta \leq \eta$, then $\eta \to \delta \leq \beta \to \delta$, $\delta \to \beta \leq \delta \to \eta$, $\beta \odot \delta \leq \eta \odot \delta$, and $\eta^* \leq \beta^*$

iv. $\beta \leq (\eta \to \beta) \to \beta$, $\eta \leq (\eta \to \beta) \to \beta$, and $\beta \vee \eta = ((\beta \to \eta) \to \eta) \vee ((\eta \to \beta) \to \beta)$

v. $\beta \odot \eta \leq \beta$, $\beta \odot \eta \leq \eta$, $\beta \odot \eta \leq \beta \wedge \eta$, $\beta \odot 0 = 0$, and $\beta \odot \beta^* = 0$

vi. $1 \to \beta = \beta$, $\beta \to \beta = 1$, $\beta \leq \eta \to \beta$, $\beta \to 1 = 1$, and $0 \to \beta = 1$

vii. $\beta \odot \eta = 0$ iff $\beta \leq \eta^*$

viii. $\beta \odot (\eta \wedge \sigma) = (\beta \odot \eta) \wedge (\beta \odot \sigma)$

ix. $\beta \odot (\eta \vee \sigma) = (\beta \odot \eta) \vee (\beta \odot \sigma)$

A BL-algebra satisfying $\beta \vee \beta^* = 1$ is called a Boolean algebra. For a BL-algebra Λ, if

$$B(\Lambda) = \{\beta \in \Lambda : \beta \oplus \beta = \beta\} = \{\beta \in \Lambda : \beta \odot \beta = \beta\}$$

then $(B(\Lambda), \oplus, *, 0)$ is the largest subalgebra of Λ and a Boolean algebra. Hence, $B(\Lambda)$ is called Boolean center of Λ.

Theorem 2.3. [2] Let Λ be a BL-algebra and $\beta, \eta \in \Lambda$. Then, the following conditions are equivalent:

i. $\beta \in B(\Lambda)$

ii. $\beta \odot \beta = \beta$ and $\beta^{**} = \beta$

iii. $\beta \odot \beta = \beta$ and $\beta^* \to \beta = \beta$

iv. $\beta^* \vee \beta = 1$

v. $(\beta \to \eta) \to \beta = \beta$

vi. $\beta \wedge \eta = \beta \odot \eta$

3. $(\odot, \vee)$-Permuting Tri-derivations on BL-algebras

This section defines $(\odot, \vee)$-permuting tri-derivation structures in BL-algebras and explores their some results. It investigates the properties provided by the trace of the $(\odot, \vee)$-permuting tri-derivation on BL-algebras. Throughout this paper, Λ denotes a BL-algebra unless otherwise specified.

Definition 3.1. A map $\Phi : \Lambda \times \Lambda \times \Lambda \to \Lambda$ is called a permuting mapping if $\Phi(\beta, \delta, \theta) = \Phi(\beta, \theta, \delta) = \Phi(\delta, \beta, \theta) = \Phi(\delta, \theta, \beta) = \Phi(\theta, \beta, \delta) = \Phi(\theta, \delta, \beta)$, for all $\beta, \delta, \theta \in \Lambda$.

Furthermore, a map $\varphi : \Lambda \to \Lambda$ defined by $\varphi(\beta) = \Phi(\beta, \beta, \beta)$ is referred to as the trace of Φ such that Φ is a permuting mapping. Hereinafter, for brevity, we use the notation $\varphi\beta$ instead of $\varphi(\beta)$.

Definition 3.2. Let $\Phi : \Lambda \times \Lambda \times \Lambda \to \Lambda$ be a permuting mapping. If Φ satisfies the following condition

$$\Phi(\beta \odot \eta, \delta, \theta) = (\Phi(\beta, \delta, \theta) \odot \eta) \oplus (\beta \odot \Phi(\eta, \delta, \theta))$$

for all $\beta, \eta, \delta, \theta \in \Lambda$, then Φ is called a permuting tri-derivation. Clearly, if Φ is a permuting tri-

derivation on Λ, then the following relations hold:

$$\Phi(\beta, \delta \odot \eta, \theta) = (\Phi(\beta, \delta, \theta) \odot \eta) \oplus (\delta \odot \Phi(\beta, \eta, \theta))$$

and

$$\Phi(\beta, \delta, \theta \odot \eta) = (\Phi(\beta, \delta, \theta) \odot \eta) \oplus (\theta \odot \Phi(\beta, \delta, \eta))$$

for all $\beta, \eta, \delta, \theta \in \Lambda$.

Example 3.3. Let $\Lambda = \{0, \beta, \theta, 1\}$ such that $0 < \beta < \theta < 1$ and the binary operations $\odot$ and $\rightarrow$ be defined as follows:

$\odot$	0	β	θ	1
0	0	0	0	0
β	0	β	β	β
θ	0	β	θ	θ
1	0	β	θ	1

and

$\rightarrow$	0	β	θ	1
0	1	1	1	1
β	0	1	1	1
θ	0	β	1	1
1	0	β	θ	1

Then, $(\Lambda, \wedge, \vee, \odot, \rightarrow, 0, 1)$ is a BL-algebra. Define a map $\Phi : \Lambda \times \Lambda \times \Lambda \rightarrow \Lambda$ by

$$\Phi(x_1, x_2, x_3) = \begin{cases} \beta, & (x_1, x_2, x_3) \in \left\{ \begin{array}{c} (\beta,\beta,\beta),(\beta,\beta,\theta),(\beta,\theta,\beta),(\theta,\beta,\beta),(\beta,\beta,1), \\ (\beta,1,\beta),(1,\beta,\beta),(\theta,\theta,1),(\theta,1,\theta),(1,\theta,\theta) \end{array} \right\} \\ \theta, & (x_1, x_2, x_3) = (\theta, \theta, \theta) \\ 0, & \text{otherwise} \end{cases}$$

It is easy to observe that Φ is a $(\odot, \vee)$-permuting tri-derivation on Λ.

Proposition 3.4. Assume that Φ is a $(\odot, \vee)$-permuting tri-derivation on Λ, φ is the trace of Φ, and $\beta, \delta, \theta \in \Lambda$. Then, the following conditions are valid:

i. $\varphi 0 = 0$

ii. $\varphi\beta \odot \beta^* = \beta \odot \varphi\beta^* = 0$

iii. $\varphi\beta = \varphi\beta \vee (\beta \odot \Phi(\beta, \beta, 1))$

iv. If $\beta \in B(\Lambda)$, then $\beta \leq (\Phi(\beta, \beta, \beta^*))^*$

v. If $\beta \in B(\Lambda)$, then $\Phi(\beta, \delta, \theta) \leq \beta$ and $\Phi(\beta^*, \delta, \theta) \leq \beta^*$

Proof.

i. For all $\beta \in \Lambda$,

$$\begin{aligned} \Phi(\beta, \beta, 0) &= \Phi(\beta, \beta, 0 \odot 0) \\ &= (\Phi(\beta, \beta, 0) \odot 0) \vee (0 \odot \Phi(\beta, \beta, 0)) \\ &= 0 \vee 0 = 0 \end{aligned}$$

Since φ is the trace of Φ,

$$\begin{aligned} \varphi 0 &= \Phi(0, 0, 0) \\ &= \Phi(0 \odot 0, 0, 0) \\ &= (\Phi(0, 0, 0) \odot 0) \vee (0 \odot \Phi(0, 0, 0)) \\ &= 0 \vee 0 = 0 \end{aligned}$$

ii. For all $\beta \in \Lambda$,

$$\begin{aligned} 0 &= \Phi(\beta, \beta, 0) \\ &= \Phi(\beta, \beta, \beta \odot \beta^*) \\ &= (\Phi(\beta, \beta, \beta) \odot \beta^*) \vee (\beta \odot \Phi(\beta, \beta, \beta^*)) \end{aligned}$$

Hence, $\varphi\beta \odot \beta^* = 0$ and $\beta \odot \Phi(\beta, \beta, \beta^*) = 0$. Similarly, $\beta \odot \varphi\beta^{^*} = 0$, for all $\beta \in \Lambda$.

iii. For all $\beta \in \Lambda$,

$$\begin{aligned}\varphi\beta &= \Phi(\beta, \beta, \beta)\\ &= \Phi(\beta, \beta, \beta \odot 1)\\ &= (\Phi(\beta, \beta, \beta) \odot 1) \vee (\beta \odot \Phi(\beta, \beta, 1))\\ &= \varphi\beta \vee (\beta \odot \Phi(\beta, \beta, 1))\end{aligned}$$

iv. Let $\beta \in B(\Lambda)$. Since $\Phi(\beta, \beta, \beta^*) \odot \beta = 0$, then $\Phi(\beta, \beta, \beta^*) \leq \beta^*$. From Theorem 2.3, $\beta^{**} = \beta$ because $\beta \in B(\Lambda)$. From Proposition 2.2 *iii*, $\beta \leq (\Phi(\beta, \beta, \beta^*))^*$.

v. Let $\beta \in B(\Lambda)$. For all $\delta, \theta \in \Lambda$,

$$\Phi(\beta \odot \beta^*, \delta, \theta) = (\Phi(\beta, \delta, \theta) \odot \beta^*) \vee (\beta \odot \Phi(\beta^*, \delta, \theta)$$

which implies that $\Phi(\beta, \delta, \theta) \odot \beta^* = 0$ and $\beta \odot \Phi(\beta^*, \delta, \theta) = 0$. Thus, $\Phi(\beta, \delta, \theta) \leq \beta$ and $\Phi(\beta^*, \delta, \theta) \leq \beta^*$.

□

Proposition 3.5. Let Φ be a $(\odot, \vee)$-permuting tri-derivation on Λ, φ be the trace of Φ, and $\beta, \theta \in \Lambda$ such that $\beta \leq \theta$. Then, the followings hold:

i. $\varphi(\beta \odot \theta^{^*}) = 0$

ii. $\varphi\theta^* \leq \beta^*$

iii. If $\beta \in B(\Lambda)$, then $\varphi\beta \odot \varphi\theta^* = 0$

Proof.

i. Since $\beta \leq \theta$, then $\beta \odot \theta^* \leq \theta \odot \theta^{^*} = 0$. Hence, $\beta \odot \theta^{^*} = 0$. Thus, $\varphi(\beta \odot \theta^{^*}) = 0$.

ii. Since $\beta \leq \theta$, then $\beta \odot \varphi\theta^{^*} \leq \theta \odot \varphi\theta^{^*} = 0$. Hence, $\varphi\theta^* \odot \beta = 0$. From Proposition 2.2 *vii*, $\beta \in B(\Lambda)$. Then, $\varphi\theta^* \leq \beta^*$.

iii. Let $\beta \in B(\Lambda)$. For all $\theta \in \Lambda$,

$$0 = \Phi(\beta \odot \beta^*, \theta, \theta) = (\Phi(\beta, \theta, \theta) \odot \beta^*) \vee (\beta \odot \Phi(\beta^*, \theta, \theta))$$

Hence, $\Phi(\beta, \theta, \theta) \odot \beta^* = 0$. Therefore, $\Phi(\beta, \theta, \theta) \leq \beta$. Thus, we replace θ by β in the last relation, $\varphi\beta \leq \beta$. Therefore, $\varphi\beta \odot \varphi\theta^{^*} \leq \beta \odot \varphi\theta^* = 0$.

□

Proposition 3.6. Let Φ be a $(\odot, \vee)$-permuting tri-derivation on Λ, φ be the trace of Φ, and $\beta \in B(\Lambda)$. Then,

i. $\varphi\beta \odot \varphi\beta^{^*} = 0$

ii. $\varphi\beta^* = (\varphi\beta)^{^*}$ iff φ is the identity on Λ

Proof.

i. By Proposition 3.5 *iii*, as $\beta \leq \beta$ and $\beta \in B(\Lambda)$, then $\varphi\beta \odot \varphi\beta^{^*} = 0$.

ii. $(\Rightarrow)$: Since $\beta \odot \varphi\beta^{^*} = 0$, then $\beta \odot (\varphi\beta)^{^*} = 0$. Thus, $\varphi\beta \leq \beta$ and $\beta \leq \varphi\beta$ which implies that $\varphi\beta = \beta$. Hence, φ is identity on Λ.

$(\Leftarrow)$: If φ is an identity on Λ, then $\varphi\beta^{^*} = (\varphi\beta)^{^*}$, for all $\beta \in \Lambda$.

□

Definition 3.7. Let Φ be a $(\odot, \vee)$-permuting tri-derivation on Λ. If $\beta \leq \delta$ implies $\Phi(\beta, \theta, \eta) \leq \Phi(\delta, \theta, \eta)$, for all $\beta, \theta, \eta \in \Lambda$, then Φ is called an isotone. If φ is the trace of Φ, and Φ is an isotone, then $\beta \leq \delta$ implies $\varphi\beta \leq \varphi\delta$, for all $\beta, \delta \in \Lambda$.

Example 3.8. Let Λ be a BL-algebra and Φ be a $(\odot, \vee)$-permuting tri-derivation in Example 3.3. Then, Φ is not isotone, because $\Phi(\beta, \beta, 1) \not\leq \Phi(1, \beta, 1)$.

Example 3.9. Consider $\Lambda = \{0, \beta, \theta, 1\}$ in Example 3.3. Define a map $\Phi : \Lambda \times \Lambda \times \Lambda \to \Lambda$ by

$$\Phi(x_1, x_2, x_3) = \begin{cases} \beta, & (x_1, x_2, x_3) \in \left\{ \begin{array}{c} (\beta,\beta,\beta),(\beta,\beta,\theta),(\beta,\theta,\beta),(\theta,\beta,\beta),(\beta,\beta,1),(\beta,1,\beta),(1,\beta,\beta), \\ (\beta,\theta,\theta),(\theta,\beta,\theta),(\theta,\theta,\beta),(\beta,\theta,1),(\beta,1,\theta),(\theta,\beta,1),(\theta,1,\beta), \\ (1,\beta,\theta),(1,\theta,\beta),(\beta,1,1),(1,\beta,1),(1,1,\beta) \end{array} \right\} \\ \theta, & (x_1, x_2, x_3) \in \Big\{ (\theta,\theta,\theta),(\theta,\theta,1),(\theta,1,\theta),(1,\theta,\theta),(\theta,1,1),(1,\theta,1),(1,1,\theta) \Big\} \\ 1, & (x_1, x_2, x_3) = (1,1,1) \\ 0, & \text{otherwise} \end{cases}$$

Then, Φ is an isotone $(\odot, \vee)$-permuting tri-derivation on Λ.

Proposition 3.10. Suppose that Φ is a $(\odot, \vee)$-permuting tri-derivation on Λ and φ is the trace of Φ. If $\varphi\beta^* = \varphi\beta$, for all $\beta \in \Lambda$, then the followings hold:

i. $\varphi 1 = 0$

ii. $\varphi\beta \odot \varphi\beta = 0$

iii. If Φ is an isotone on Λ, then $\varphi = 0$

Proof.

i. Replacing β by 0 in the relation $\varphi\beta^* = \varphi\beta$, since $0^* = 1$ and $\varphi 0 = 0$, then $\varphi 1 = 0$.

ii. Using hypothesis, $\varphi\beta \odot \varphi\beta = \varphi\beta \odot \varphi\beta^* = 0$, for all $\beta \in \Lambda$.

iii. Let Φ be an isotone on Λ. For $\beta \in \Lambda$, $\varphi\beta = 0$, since $\varphi\beta \leq \varphi 1 = 0$. Thus, $\varphi = 0$.

□

Definition 3.11. Let Φ be a $(\odot, \vee)$-permuting tri-derivation on Λ. If $\Phi(\beta \odot \theta, \delta, \eta) = \Phi(\beta, \delta, \eta) \odot \Phi(\theta, \delta, \eta)$, for all $\beta, \theta, \delta, \eta \in \Lambda$, then Φ is called a tri-multiplicative $(\odot, \vee)$-permuting tri-derivation on Λ.

Theorem 3.12. Suppose that Φ is a tri-multiplicative $(\odot, \vee)$-permuting tri-derivation on Λ and φ is the trace of Φ. Hence, $\varphi(B(\Lambda)) \subseteq B(\Lambda)$.

Proof.
Let $\beta \in \varphi(B(\Lambda))$. Then, $\beta = \varphi(\theta)$, for some $\theta \in B(\Lambda)$. Thus, $\beta \odot \beta = \varphi\theta \odot \varphi\theta = \Phi(\theta \odot \theta, \theta, \theta) = \varphi\theta = \beta$. Therefore, $\beta \in B(\Lambda)$. Hence, $\varphi(B(\Lambda)) \subseteq B(\Lambda)$. □

Theorem 3.13. Let Φ be a $(\odot, \vee)$-permuting tri-derivation on Λ. If there exists a $\beta \in \Lambda$ such that $\beta \odot \Phi(\theta, \delta, \eta) = 1$, for all $\theta, \delta, \eta \in \Lambda$, then $\beta = 1$.

Proof.
Assume that there exists a $\beta \in \Lambda$ such that $\Phi(\theta, \delta, \eta) \odot \beta = 1$, for all $\theta, \delta, \eta \in \Lambda$. Since Φ is a $(\odot, \vee)$-permuting tri-derivation on Λ,

$$\begin{aligned} 1 &= \Phi(\theta \odot \beta, \delta, \eta) \odot \beta \\ &= ((\Phi(\theta, \delta, \eta) \odot \beta) \vee (\theta \odot \Phi(\beta, \delta, \eta)) \odot \beta \\ &= (1 \vee (\theta \odot \Phi(\beta, \delta, \eta)) \odot \beta \\ &= 1 \odot \beta \\ &= \beta \end{aligned}$$

□

Theorem 3.14. Let Φ be a $(\odot, \vee)$-permuting tri-derivation on $B(\Lambda)$. Thus,

i. Φ is a permuting tri-derivation on a lattice, i.e.,

$$\Phi(\beta \wedge \eta, \theta, \delta) = (\Phi(\beta, \theta, \delta) \wedge \eta) \vee (\beta \wedge \Phi(\eta, \theta, \delta)), \quad \text{for all } \beta, \theta, \delta, \eta \in B(\Lambda)$$

ii. $\Phi(\beta, \theta, \delta) = \Phi(\beta, \theta, \delta) \wedge \beta$, for all $\beta, \theta, \delta \in B(\Lambda)$

Proof.

i. For all $\beta, \theta, \delta, \eta \in B(\Lambda)$,

$$\begin{aligned} \Phi(\beta \wedge \eta, \theta, \delta) &= \Phi(\beta \odot \eta, \theta, \delta) \\ &= (\Phi(\beta, \theta, \delta) \odot \eta) \vee (\beta \odot \Phi(\eta, \theta, \delta)) \\ &= (\Phi(\beta, \theta, \delta) \wedge \eta) \vee (\beta \wedge \Phi(\eta, \theta, \delta)) \end{aligned}$$

ii. For all $\beta, \theta, \delta \in B(\Lambda)$,

$$\begin{aligned} \Phi(\beta, \theta, \delta) &= \Phi(\beta \odot \beta, \theta, \delta) \\ &= (\Phi(\beta, \theta, \delta) \odot \beta) \vee (\beta \odot \Phi(\beta, \theta, \delta)) \\ &= \Phi(\beta, \theta, \delta) \odot \beta \\ &= \Phi(\beta, \theta, \delta) \wedge \beta \end{aligned}$$

□

Theorem 3.15. Suppose that Φ is a $(\odot, \vee)$-permuting tri-derivation on Gödel BL-algebra Λ, φ is the trace of Φ, and $\beta, \theta \in \Lambda$. Then, the followin conditions are valid:

i. $\varphi\beta \leq \beta$

ii. If $\beta \leq \Phi(\beta, \beta, 1)$, then $\varphi\beta = \beta$

iii. If $\beta \geq \Phi(\beta, \beta, 1)$, then $\Phi(\beta, \beta, 1) \leq \varphi\beta$

iv. If $\beta \leq \theta$, then $\varphi\beta = \beta$ or $\varphi\beta \geq \Phi(\beta, \beta, \theta)$

Proof.

i.

$$\begin{aligned} \varphi\beta &= \Phi(\beta, \beta, \beta) = \Phi(\beta \odot \beta, \beta, \beta) \\ &= (\varphi\beta \odot \beta) \vee (\beta \odot \varphi\beta) = \varphi\beta \odot \beta \\ &= \min\{\varphi\beta, \beta\} \end{aligned}$$

Thus, $\varphi\beta \leq \beta$.

ii. Let $\beta \leq \Phi(\beta, \beta, 1)$, for $\beta \in \Lambda$. Thus,

$$\begin{aligned}\varphi\beta &= \Phi(\beta, \beta, \beta)\\ &= \Phi(\beta \odot 1, \beta, \beta)\\ &= (\varphi\beta \odot 1) \vee (\beta \odot \Phi(1, \beta, \beta))\\ &= \varphi\beta \vee \min\{\beta, \Phi(1, \beta, \beta)\}\\ &= \varphi\beta \vee \beta\\ &= \beta, \text{ by } i.\end{aligned}$$

iii. Let $\beta \geq \Phi(\beta, \beta, 1)$, for $\beta \in \Lambda$. Hence,

$$\begin{aligned}\varphi\beta &= \Phi(\beta, \beta, \beta)\\ &= \Phi(\beta \odot 1, \beta, \beta)\\ &= \varphi\beta \vee \min\{\beta, \Phi(1, \beta, \beta)\}\\ &= \varphi\beta \vee \Phi(1, \beta, \beta)\end{aligned}$$

Thus, $\Phi(\beta, \beta, 1) \leq \varphi\beta$.

iv. Let $\beta \leq \theta$. From i, $\varphi\beta \leq \beta \leq \theta$. Thus, $\varphi\beta \leq \theta$. Thereby,

$$\begin{aligned}\varphi\beta &= \Phi(\beta, \beta, \beta)\\ &= \Phi(\beta \odot \theta, \beta, \beta)\\ &= (\varphi\beta \odot \theta) \vee (\beta \odot \Phi(\theta, \beta, \beta))\\ &= \varphi\beta \vee (\beta \odot \Phi(\theta, \beta, \beta))\end{aligned}$$

If $\beta \leq \Phi(\theta, \beta, \beta)$, then $\varphi\beta = \beta$ by i. If $\beta \geq \Phi(\theta, \beta, \beta)$, then $\varphi\beta = \varphi\beta \vee \Phi(\theta, \beta, \beta)$. Hence, $\varphi\beta \geq \Phi(\beta, \beta, \theta)$.

□

4. Conclusion

BL-algebras were introduced by Hajek [6] to investigate many-valued logic. One of the reasons for his motivations for introducing BL-algebras was providing an algebraic counterpart of propositional logic, called Basic Logic (BL-logic), which embodies a fragment common to some of the most important many-valued logics, namely Lukasiewicz Logic, Gödel Logic, and Product Logic. This BL-logic is proposed as "the most general" many-valued logic with truth values in $[0, 1]$. Another reason to work was to provide an algebraic mean for the study of continuous t-norms on $[0, 1]$. In this work, we introduce one type of permuting tri-derivation on BL-algebras and investigate its some properties. Moreover, we propose many of the basic properties that the trace of $(\odot, \vee)$-permuting tri-derivation provides. In the future, different permuting tri-derivations can be defined in these algebras, and generalized permuting tri-derivations can be studied in BL-algebras.

Author Contributions

The author read and approved the final version of the paper.

Conflicts of Interest

The author declares no conflict of interest.

References

[1] C. C. Chang, *Algebraic Analysis of Many-Valued Logics*, Transactions of the American Mathematical Society 88 (1958) 467–490.

[2] A. Di Nola, G. Georgescu, A. Iorgulescu, *Pseudo-BL Algebras: Part I*, Multiple Valued Logic 8 (5-6) (2002) 673–716.

[3] R. Cignoli, I. M. L. D'Ottaviano, D. Mundici, Algebraic Foundations of Many Valued Reasoning, Kluwer Academic Publication, Dordrecht, 2000.

[4] E. Turunen, S. Sessa, *Local BL-algebras*, Multiple Valued Logic 6 (1-2) (2001) 229–250.

[5] P. Hajek, L. Godo, F. Esteva, *A Complete Many-Valued Logic with Product-Conjunction*, Archive for Mathematical Logic 35 (1996) 191–208.

[6] P. Hajek, Mathematics of Fuzzy Logic, Springer Science and Business Media, Dordrecht, 1998.

[7] K. H. Kim, *On Symmetric Bi-Derivations of BL-Algebras*, Annals of Fuzzy Mathematics and Informatics 19 (2) (2020) 189–198.

[8] S. Alsatayhi, A. Moussavi, (φ, ψ)*-Derivations of BL-Algebras*, Asian-European Journal of Mathematics 11 (01) (2018) 1850016 19 pages.

[9] S. Motamed, S. Ehterami, *New Types of Derivations in BL-Algebras*, New Mathematics and Natural Computation 16 (03) (2020) 627–643.

[10] M. A. Öztürk, *Permuting Tri-Derivations in Prime and Semi-Prime Rings*, East Asian Mathematical Journal 15 (1999) 177–190.

[11] D. Yılmaz, B. Davvaz, H. Yazarlı, *Permuting Tri-Derivations in MV-Algebras*, Malaya Journal of Matematik 11 (02) (2023) 142–150.

[12] H. Yazarlı, M. A. Öztürk, Y. B. Jun, *Tri-Additive Maps and Permuting Tri-Derivations*, Communications Faculty of Sciences University of Ankara Series A1 Mathematics and Statistics 54 (01) (2005).

[13] M. A. Öztürk, H. Yazarlı, K. H. Kim, *Permuting Tri-Derivations in Lattices*, Quaestiones Mathematicae 32 (3) (2009) 415–425.

Journal of New Theory
ISSN: 2149-1402

44 (2023) 10-19
Journal of New Theory
https://dergipark.org.tr/en/pub/jnt
Open Access

New Exact Solutions of the Drinfeld-Sokolov System by the Generalized Unified Method

Tuğba Aydemir[1]

Article Info
Received: 8 May 2023
Accepted: 18 Aug 2023
Published: 30 Sep 2023
doi:10.53570/jnt.1294322
Research Article

Abstract — In this study, we apply the generalized unified method (GUM), an enhanced version of the unified method, to find novel exact solutions of the Drinfeld-Sokolov System (DSS) that models the dispersive water waves in fluid dynamics. Moreover, 3D and 2D graphs of some of the obtained exact solutions are plotted to present how various characteristic forms they have. The results show that the presented method simplifies the computation process on the computer in a highly reliable and straightforward manner while providing the solutions in more general forms. In addition, the GUM has great potential to apply to a wide range of problems, including nonlinear partial differential equations (NPDEs) and fractional partial differential equations (FPDEs) for finding exact solutions.

Keywords *Drinfeld-Sokolov system, unified method, generalized unified method, exact solution, traveling wave solutions*

Mathematics Subject Classification (2020) 35B08, 76B15

1. Introduction

Nonlinear partial differential equations (NPDEs), usually represented by an equation that describes a relationship between an unknown function and its partial derivatives, are great tools for modeling these real-world phenomena in many scientific fields. Finding solutions for NPDEs is essential because it improves our understanding of the physical phenomena these equations model, accelerates technological advances, and optimizes the production process of these technological tools. Therefore, finding numerical and exact solutions to NPDEs corresponding to the physical problems in science and engineering becomes increasingly important.

In this study, the exact solutions of the nonlinear Drinfeld-Sokolov System (DSS), considered to model for dispersive water in fluid dynamics, are investigated by using the generalized unified method (GUM). The explicit mathematical form of the system is given as follows:

$$\begin{cases} u_t(x,t) + (v^2(x,t))_x = 0 \\ v_t(x,t) - \alpha v_{xxx}(x,t) + 3\beta u_x(x,t)v(x,t) + 3\gamma u(x,t)v_x(x,t) = 0 \end{cases}$$

where α, β, and γ are real constants. This system was first proposed by Drinfeld and Sokolov [1] as an extension of the Korteweg-de Vries (KdV), which possesses Lax pairs of a special form for affine Lie algebras. The solutions of the DSS exhibit different characteristics, such as static solitons

[1]tgb.aydemir@gmail.com (Corresponding Author)
[1]Department of International Trade and Finance, Faculty of Economics and Administrative Sciences, Yalova University, Yalova, Türkiye

that interact with moving solitons without deformations [2]. Morris and Kara [3] showed that the interaction between the underlying symmetries and conservation laws of a partial differential equation system results in double reductions of a class of Drinfeld–Sokolov–Wilson equations.

Due to its significant applications in fluid dynamics and optical fiber, many researchers have developed several methods to obtain exact and numerical solutions for the Drinfeld-Sokolov family. Wazwaz [4] used the sine–cosine and tanh methods to have exact solutions for the Drinfeld-Sokolov System. Arora and Kumar [5] applied the homotopy analysis method to obtain an approximation of the analytic solution for the coupled Drinfeld's–Sokolov–Wilson. He et al. [6] obtained exact solutions for the classic Drinfeld-Sokolov-Wilson equation using the F-expansion method combined with the exp-function method. Gómez [7] studied the generalized Drinfeld-Sokolov-Wilson equation to obtain exact solutions by applying the improved tanh-coth method. Düşünceli [8] employed the improved Bernoulli sub-equation function method (IBSEFM) to have exact solutions of the Drinfeld-Sokolov equation. Zhang [9] solved the Drinfeld-Sokolov-Wilson equation using a variational approach. Günay et al. [10] derived solitary wave solutions to the DSS using the generalized exponential rational function method. Salim et al. [11] solved the Drinfeld-Sokolov-Wilson system numerically using the modified Adomian decomposition method. Alam et al. [12] established some exact solutions of the Drinfeld-Sokolov-Wilson equation with $S(\xi)$-expansion method.

Recently, fractional partial differential equations (FPDEs) have also been studied by many authors because fractional order derivatives provide a powerful and enhanced model for expressing some real-world phenomena. In particular, these fractional equations are encountered in modeling considerable complex problems in networks, optics, and fluid dynamics. Jaradat et al. [13] investigated the analytical solution of the time-fractional Drinfeld–Sokolov–Wilson system through the residual power series method. Bhatter et al. [14] considered the fractionalized homotopy analysis transform method to solve the fractional Drinfeld–Sokolov–Wilson model numerically. Gao et al. [15] found the solutions of fractional Drinfeld–Sokolov–Wilson equation using amalgamations of Laplace transform technique with q-homotopy analysis scheme, called q-homotopy analysis transform method (q-HATM) with Atangana-Baleanu derivative. Taşbozan et al. [16] applied the Sine-Gordon expansion method to obtain exact solutions and the perturbation-iteration algorithm to obtain approximate solutions for the fractional Drinfeld-Sokolov-Wilson system. Wang and Wang [17] found the numerical solution for the time-space fractional nonlinear Drinfeld–Sokolov–Wilson system using He's variational method. Noor et al. [18] used the homotopy perturbation transform method and Sumudu transform decomposition method to solve approximately the time-fractional Drinfeld–Sokolov–Wilson system.

In this paper, we have applied the GUM [19] to derive exact solutions for the DSS. The GUM is an enhanced version of the unified method [20,21] that many authors [22–36] have successfully applied to solve different types of NPDEs. Compared with other methods, the GUM requires less computational work with high reliability to solve NPDEs.

This paper is structured as follows: After describing briefly the GUM in section 2, the exact solutions of the DSS are obtained by the GUM, and graphical illustrations of some selected solutions are displayed in section 3. In section 4, the derivation of the exact solution sets obtained by some methods from the solutions obtained by the GUM is discussed. Lastly, conclusive remarks are given in section 5.

2. The Generalized Unified Method

In this section, a brief explanation of the GUM for constructing wave solutions of NPDEs is provided. In the first step, when applying the GUM, the NPDE is converted to a nonlinear ordinary differential equation (NODE) by using wave transformation $u(x,t) = U(\eta)$ such that $\eta = x - \nu t + \eta_0$. The solution

form of the obtained NODE is expressed by an ansatz statement as follows:

$$U(\eta) = a_0 + \sum_{m=1}^{M} \left[a_m \phi^m + b_m \phi^{-m}\right] \tag{1}$$

After finding the balance value M in the ansatz statement, this statement and its derivatives are substituted into NODE to obtain an algebraic polynomial system. Here, $\phi(\eta)$ is considered Riccati differential equation in the form $\phi'(\eta) = \phi^2(\eta) - \mu^2$ with $\phi' = \frac{d\phi}{d\eta}$ and $\mu = (c + id)$ where c and d are parameters. The polynomial system with powers ϕ provides to get the values of the coefficients in Equality 1. Finally, wave solutions of the NPDE are obtained in closed form with free parameters A, B, and C, using these coefficients and the solutions of the Riccati differential equation as given by:

$$\phi(\eta) = \begin{cases} \phi_1 = \frac{\mp(c+id)\sqrt{A^2+(B+iC)^2} - A(c+id)\cosh(2(c+id)(\eta+\eta_0))}{(B+iC)+A\sinh(2(c+id)(\eta+\eta_0))} \\ \phi_2 = \frac{\mp(c+id)\left(-A+e^{\mp 2(c+id)(\eta+\eta_0)}\right)}{\left(A+e^{\mp 2(c+id)(\eta+\eta_0)}\right)} \\ \phi_3 = -\frac{1}{\eta+\eta_0} \end{cases}$$

where $A \neq 0$, B, and C are real arbitrary parameters.

3. Application of The Generalized Unified Method to Drinfeld-Sokolov System

In this section, the GUM is applied to the DSS to obtain exact wave solutions by following the steps as explained in Section 2. The DSS is given by

$$\begin{cases} u_t(x,t) + (v^2(x,t))_x = 0 \\ v_t(x,t) - \alpha v_{xxx}(x,t) + 3\beta u_x(x,t)v(x,t) + 3\gamma u(x,t)v_x(x,t) = 0 \end{cases} \tag{2}$$

where α, β, and γ are real constants. Converting NPDE System 2 to ordinary differential equations (ODEs) by using the wave transformation $\eta = x - \nu t + \eta_0$ in $u(x,t)$ and $v(x,t)$ gives:

$$\begin{cases} -\nu U'(\eta) + 2V(\eta)V'(\eta) = 0 \\ -\nu V'(\eta) - \alpha V'''(\eta) + 3\beta U'(\eta)V(\eta) + 3\gamma U(\eta)V'(\eta) = 0 \end{cases} \tag{3}$$

Here, $U(\eta)$ and $V(\eta)$ denote the shape of the nonlinear wave with the wave variable $\eta = x - \nu t + \eta_0$. Integrating the first equation with respect to η yields the equality $U(\eta) = \dfrac{V^2(\eta)}{\nu}$ in ODE System 3. Substituting this equality into the second equation in ODE System 3, this second one can be rewritten in the form as follows:

$$\nu V(\eta) + \alpha V''(\eta) - \frac{6\beta + 3\gamma}{\nu} V^3(\eta) = 0 \tag{4}$$

The solutions of the DSS in Equation 2 can be written in the form with balance value $M = 1$, found from the highest order V'' and the nonlinear term V^3. Therefore, the solutions in closed form for Equation 2 are described as follows:

$$\begin{cases} V(\eta) = a_0 + a_1\phi + \frac{b_1}{\phi} \\ U(\eta) = \frac{V^2(\eta)}{\nu} \end{cases} \tag{5}$$

where a_0, a_1, and b_1 are coefficients of ϕ, determined later. Substituting the ansatz statement in Solution 5 and its derivatives into Equation 4 gives an algebraic polynomial equation system with a_0, a_1, b_1, and μ. Solving this polynomial equation system by using any symbolic computation program yields the following sets for the unknowns a_0, a_1, b_1, and μ. Substituting these values into Solution 5

with ϕ_1 and ϕ_2 gives rise to the following exact solutions to the DSS, respectively.

Case 1. For $a_0 = 0$, $a_1 = \mp\sqrt{\frac{2\alpha}{K}}$, $b_1 = 0$, and $\mu = \mp\sqrt{\frac{\nu}{2\alpha}}$ such that $K = \frac{6\beta+3\gamma}{\nu}$, the exact solutions are as follows:

$$\begin{cases} u_1(x,t) = \frac{v_1^2(x,t)}{\nu} \\ \\ v_1(x,t) = \mp\frac{\sqrt{\frac{\nu^2}{6\beta+3\gamma}}\left(\sqrt{A^2+(B+iC)^2}\mp A\cosh\left(\sqrt{\frac{2\nu}{\alpha}}(x-\nu t+\eta_0)\right)\right)}{(B+iC)\mp A\sinh\left(\sqrt{\frac{2\nu}{\alpha}}(x-\nu t+\eta_0)\right)} \end{cases}$$

and

$$\begin{cases} u_2(x,t) = \frac{v_2^2(x,t)}{\nu} \\ \\ v_2(x,y,t) = \frac{\sqrt{\frac{\nu^2}{6\beta+3\gamma}}\left(-A+e^{\mp\sqrt{\frac{2\nu}{\alpha}}(x-\nu t+\eta_0)}\right)}{\left(A+e^{\mp\sqrt{\frac{2\nu}{\alpha}}(x-\nu t+\eta_0)}\right)} \end{cases}$$

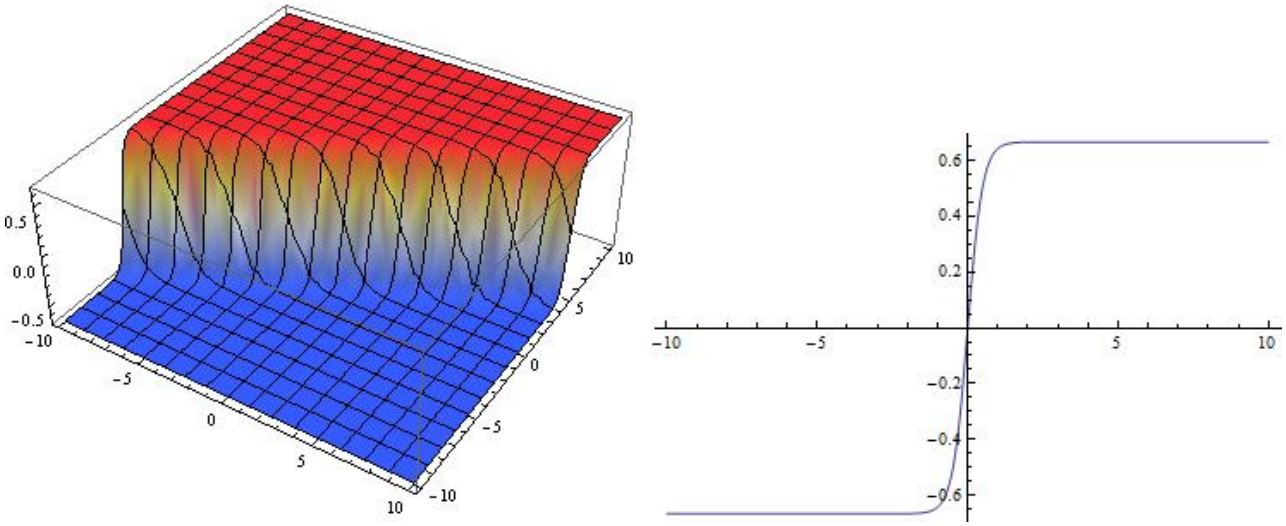

Figure 1. 3D and 2D graphs of the solution v_1 for the parameter $A = 1$, $B = 0$, and $C = 0$

Case 2. For $a_0 = 0$, $a_1 = 0$, $b_1 = \mp\nu\sqrt{\frac{1}{2K\alpha}}$, and $\mu = \mp\sqrt{\frac{\nu}{2\alpha}}$ such that $K = \frac{6\beta+3\gamma}{\nu}$,the exact solutions are as follows:

$$\begin{cases} u_3(x,t) = \frac{v_3^2(x,t)}{\nu} \\ \\ v_3(x,t) = \mp\frac{\sqrt{\frac{\nu^2}{6\beta+3\gamma}}(B+iC)\mp A\sinh\left(\sqrt{\frac{2\nu}{\alpha}}(x-\nu t+\eta_0)\right)}{\left(\sqrt{A^2+(B+iC)^2}\mp A\cosh\left(\sqrt{\frac{2\nu}{\alpha}}(x-\nu t+\eta_0)\right)\right)} \end{cases}$$

and

$$\begin{cases} u_4(x,t) = \frac{v_4^2(x,t)}{\nu} \\ \\ v_4(x,y,t) = \frac{\sqrt{\frac{\nu^2}{6\beta+3\gamma}}\left(A+e^{\mp\sqrt{\frac{2c}{\alpha}}(x-\nu t+\eta_0)}\right)}{\left(-A+e^{\mp\sqrt{\frac{2\nu}{\alpha}}(x-\nu t+\eta_0)}\right)} \end{cases}$$

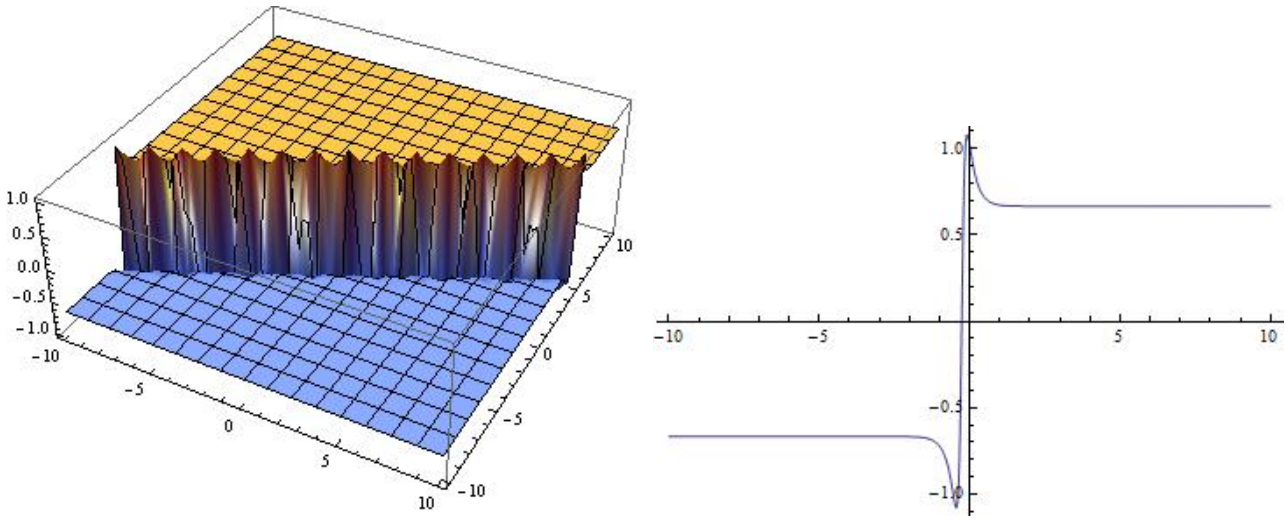

Figure 2. 3D and 2D graphs of real part for the solution v_3 for the parameter $A = 1$, $B = 1$, and $C = 1$

Case 3. For $a_0 = 0$, $a_1 = \frac{\nu}{2Kb_1}$, $b_1 = \mp\nu\sqrt{\frac{1}{8K\alpha}}$, and $\mu = \mp\frac{b_1}{\nu}\sqrt{-2\nu K}$ such that $K = \frac{6\beta+3\gamma}{\nu}$, the exact solutions are as follows:

$$\begin{cases} u_5(x,t) = \frac{v_5^2(x,t)}{\nu} \\ v_5(x,t) = \mp\sqrt{\frac{\nu^2}{-12\beta-6\gamma}}\left(\frac{(B+iC)\mp A\sinh\left(\sqrt{\frac{-\nu}{\alpha}}(x-\nu t+\eta_0)\right)}{\left(\sqrt{A^2+(B+iC)^2}\mp A\cosh\left(\sqrt{\frac{-\nu}{\alpha}}(x-\nu t+\eta_0)\right)\right)} + \frac{\left(\sqrt{A^2+(B+iC)^2}\mp A\cosh\left(\sqrt{\frac{-\nu}{\alpha}}(x-\nu t+\eta_0)\right)\right)}{(B+iC)\mp A\sinh\left(\sqrt{\frac{-\nu}{\alpha}}(x-\nu t+\eta_0)\right)}\right) \end{cases}$$

and

$$\begin{cases} u_6(x,t) = \frac{v_6^2(x,t)}{\nu} \\ v_6(x,t) = \mp\sqrt{\frac{\nu^2}{-12\beta-6\gamma}}\left(\frac{A+e^{\mp\sqrt{\frac{-\nu}{\alpha}}(x-\nu t+\eta_0)}}{-A+e^{\mp\sqrt{\frac{-\nu}{\alpha}}(x-\nu t+\eta_0)}} + \frac{-A+e^{\mp\sqrt{\frac{-\nu}{\alpha}}(x-\nu t+\eta_0)}}{A+e^{\mp\sqrt{\frac{-\nu}{\alpha}}(x-\nu t+\eta_0)}})\right) \end{cases}$$

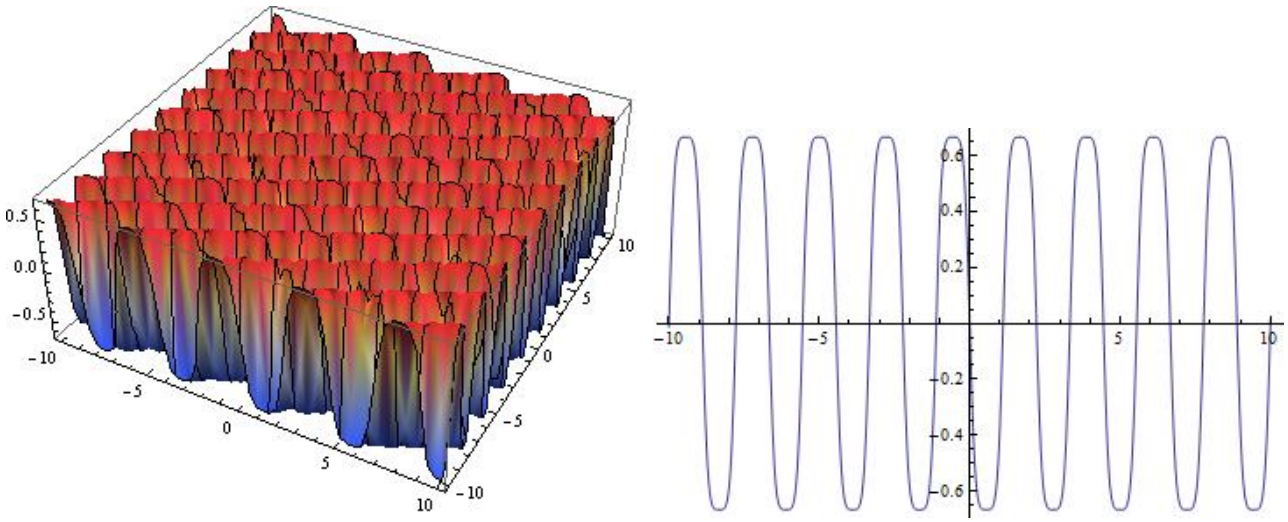

Figure 3. 3D and 2D graphs of the real part for the solution v_5 for the parameter choices $A = 1$, $B = 1$, and $C = 0$

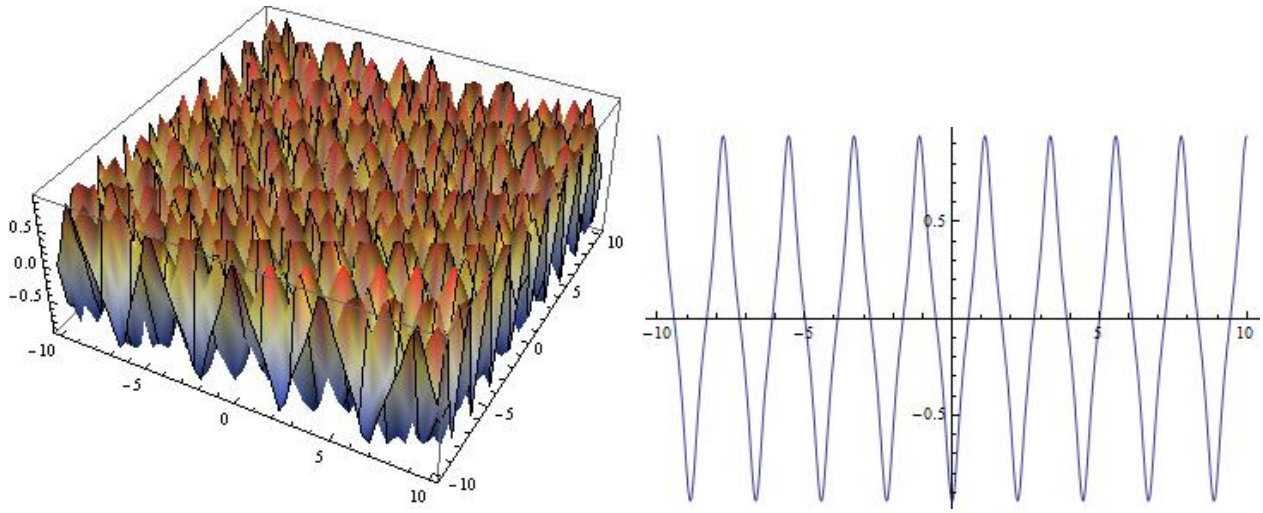

Figure 4. 3D and 2D graphs of the imaginary part for the solution v_5 for the parameter choices $A = 1$, $B = 1$, and $C = 0$

Case 4. For $a_0 = 0$, $a_1 = \frac{\nu}{4Kb_1}$, $b_1 = \mp\nu\sqrt{\frac{1}{32K\alpha}}$, and $\mu = \mp\frac{2b_1}{\nu}\sqrt{\nu K}$ such that $K = \frac{6\beta+3\gamma}{\nu}$, the exact solutions are as follows:

$$\begin{cases} u_7(x,t) = \frac{v_7^2(x,t)}{\nu} \\ v_7(x,t) = \mp\frac{\nu}{2\sqrt{6\beta+3\gamma}}\left(\frac{(B+iC)\mp A\sinh\left(\sqrt{\frac{\nu}{2\alpha}}(x-\nu t+\eta_0)\right)}{\left(\sqrt{A^2+(B+iC)^2}\mp A\cosh\left(\sqrt{\frac{\nu}{2\alpha}}(x-\nu t+\eta_0)\right)\right)} + \frac{\left(\sqrt{A^2+(B+iC)^2}\mp A\cosh\left(\sqrt{\frac{\nu}{2\alpha}}(x-\nu t+\eta_0)\right)\right)}{(B+iC)\mp A\sinh\left(\sqrt{\frac{\nu}{2\alpha}}(x-\nu t+\eta_0)\right)}\right) \end{cases}$$

and

$$\begin{cases} u_8(x,t) = \frac{v_8^2(x,t)}{\nu} \\ v_8(x,y,t) = \mp\frac{\nu}{2\sqrt{6\beta+3\gamma}}\left(\frac{A+e^{\mp\sqrt{\frac{\nu}{2\alpha}}(x-\nu t+\eta_0)}}{-A+e^{\mp\sqrt{\frac{\nu}{2\alpha}}(x-\nu t+\eta_0)}} + \frac{-A+e^{\mp\sqrt{\frac{\nu}{2\alpha}}(x-\nu t+\eta_0)}}{A+e^{\mp\sqrt{\frac{\nu}{2\alpha}}(x-\nu t+\eta_0)}})\right) \end{cases}$$

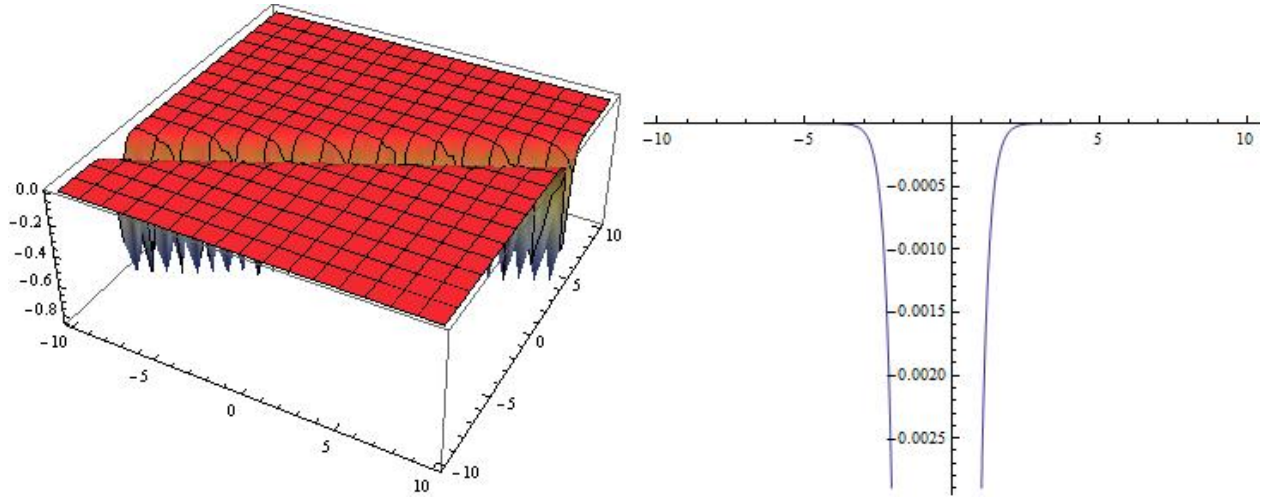

Figure 5. 3D and 2D graphs of imaginary part for the solution v_7 for the parameter choices $A = 1$, $B = 1$, and $C = 0$

The 3D and 2D graphs of the solutions v_1, v_3, v_5, and v_7 are shown as in Figures 1-5 for the parameters $\nu = 2$, $\alpha = 1$, $\beta = 1$, and $\gamma = 1$ on the intervals $-10 < x < 10$ and $-10 < t < 10$. From these figures, it is observed that the solutions obtained by the GUM display a wide variety of characteristics, represented by hyperbolic and trigonometric functions. 2D graphs of the solutions are also plotted for $x = 0$ to follow properly the characteristics of the solutions. The solutions in different shapes can be obtained by using free parameters for the corresponding physical problems.

4. Results and Discussion

We have obtained more general forms of exact solutions for the Drinfeld-Sokolov System by using the GUM in Section 3. In this section, we show more concretely how to derive solutions from some other methods from these solutions, considering some of the above solution sets.

The first group of hyperbolic and trigonometric solutions of the unified method can be obtained by taking $B = 0$ and $C = 0$, respectively, depending on the wave velocity in $\{u_1, v_1\}$ as follows:

$$\begin{cases} u_{1,1}(x,t) = \frac{v_1^2(x,t)}{\nu} \\ \\ v_{1,1}(x,t) = \mp \frac{\sqrt{\frac{\nu^2}{6\beta+3\gamma}}\left(\sqrt{A^2+B^2} \mp A\cosh\left(\sqrt{\frac{2\nu}{\alpha}}(x-\nu t+\eta_0)\right)\right)}{\left(B \mp A\sinh\left(\sqrt{\frac{2\nu}{\alpha}}(x-\nu t+\eta_0)\right)\right.} \end{cases}$$

and

$$\begin{cases} u_{1,2}(x,t) = \frac{v_1^2(x,t)}{\nu} \\ \\ v_{1,2}(x,t) = \mp \frac{\sqrt{\frac{\nu^2}{6\beta+3\gamma}}\left(\sqrt{A^2-C^2} \mp A\cosh\left(\sqrt{\frac{2\nu}{\alpha}}(x-\nu t+\eta_0)\right)\right)}{\left(iC \mp A\sinh\left(\sqrt{\frac{2\nu}{\alpha}}(x-\nu t+\eta_0)\right)\right.} \end{cases}$$

In addition, the solution sets obtained by the tanh method can be derived by taking $B = 0$ and $C = 0$ with the identities $\cosh(2x) = 2\cosh^2(x) - 1 = 2\sinh^2(x) + 1$ and $\sinh(2x) = 2\sinh(x)\cosh(x)$ as follows:

$$\begin{cases} u_{1,3}(x,t) = \frac{v_1^2(x,t)}{\nu} \\ \\ v_{1,3}(x,t) = \mp \frac{\sqrt{\frac{\nu^2}{6\beta+3\gamma}}\left(A \mp A\cosh\left(\sqrt{\frac{2\nu}{\alpha}}(x-\nu t+\eta_0)\right)\right)}{A\sinh\left(\sqrt{\frac{2\nu}{\alpha}}(x-\nu t+\eta_0)\right)} \end{cases}$$

Similarly, we can also obtain the second group of hyperbolic and trigonometric solutions of the unified method depending on the wave velocity after some simplification in $\{u_2, v_2\}$.

$$\begin{cases} u_{21}(x,t) = \frac{v_2^2(x,t)}{\nu} \\ \\ v_{21}(x,y,t) = \sqrt{\frac{\nu^2}{6\beta+3\gamma}} - \frac{2A\sqrt{\frac{\nu^2}{6\beta+3\gamma}}}{\left(A+e^{\mp\sqrt{\frac{2\nu}{\alpha}}(x-\nu t+\eta_0)}\right)} \end{cases}$$

In the studies [20, 21], it is explained that the unified method gives many more solutions than the family of the tanh method, the $\left(\frac{G'}{G}\right)$-expansion method, and the extended homogeneous balance method. Therefore, it can be concluded that the GUM gives more general solution sets than these methods.

The GUM, an enhanced version of the unified method, provides a more general solution structure for the models in mathematical physics. Considering hyperbolic-trigonometric identities and the value of μ in the case of a real number or pure imaginary number, the solutions obtained by the unified method can be derived by GUM as above while setting $B = 0$ and $C = 0$, respectively. Further, when μ is a complex number, solutions combining trigonometric-hyperbolic solution sets can also be obtained. Moreover, performing the GUM as a new expansion method on a computer contributes to a very simple, straightforward, effective, and accurate way to solve a wide range of NPDEs. Since a more general closed solution form in a compact way is obtained by the GUM with free parameters, we applied this method to solve the Drinfeld-Sokolov System.

5. Conclusion

In this study, the GUM has been successfully applied to obtain solutions for the DSS. The main contributions of this study are:

i. More general forms of exact solutions are obtained for DSS using the GUM. Some of the obtained solutions have been visualized by plotting graphs to show how diverse characteristics the solutions have.

ii. These obtained solutions can be more functional in explaining the physical characteristics of various models arising in science and engineering.

iii. We have shown that the solution sets obtained by some other exact solution methods, including the unified method, can be derived from the GUM.

iv. It is obvious that the GUM is quite simple to perform on any symbolic computation program and gives reliable and straightforward results to find exact solutions for NPDEs.

v. Moreover, the results show that the GUM can be applied in future studies for NPDEs and fractional NPDEs.

Author Contributions

The author read and approved the final version of the paper.

Conflicts of Interest

The author declares no conflict of interest.

References

[1] V. G. Drinfeld, V. V. Sokolov, *Lie Algebras and Equations of Korteweg-De Vries Type*, Journal of Soviet Mathematics 30 (1985) 1975–2036.

[2] R. Hirota, B. Grammaticos, A. Ramani, *Soliton Structure of the Drinfeld–Sokolov–Wilson Equation*, Journal of Mathematical Physics 27 (1986) 1499–1505.

[3] R. Morris, A. H. Kara, *Double Reductions/Analysis of the Drinfeld–Sokolov–Wilson Equation*, Applied Mathematics and Computation 219 (2013) 6473–6483.

[4] A. M. Wazwaz, *Exact and Explicit Traveling Wave Solutions for the Nonlinear Drinfeld–Sokolov System*, Communications in Nonlinear Science and Numerical Simulation 11 (2006) 311–325.

[5] R. Arora, A. Kumar, *Solution of the Coupled Drinfeld's-Sokolov-Wilson System by Homotopy Analysis Method*, Advanced Science Engineering and Medicine 5 (10) (2010) 1105–1111.

[6] Y. He, Y. Long, S. Li, *Exact Solutions of the Drinfel'd-Sokolov-Wilson Equation Using the F-Expansion Method Combined with Exp-Function Method*, International Mathematical Forum 5 (65) (2010) 3231–3242.

[7] C. A. Gómez, *Generalized Drinfeld-Sokolov-Wilson Equation: Exact Solutions*, Advanced Studies in Theoretical Physics 11 (4) (2017) 585–591.

[8] F. Düşünceli, *Solutions for the Drinfeld-Sokolov Equation Using an IBSEFM Method*, Mus Alparslan University Journal of Science 6 (1) (2018) 505–510.

[9] W. M. Zhang, *Solitary Solutions and Singular Periodic Solutions of the Drinfeld-Sokolov-Wilson Equation by Variational Approach*, Applied Mathematical Sciences 5 (38) (2011) 1887–1894.

[10] B. Günay, C. K. Kuo, W. X. Ma, *An Application of the Exponential Rational Function Method to Exact Solutions to the Drinfeld–Sokolov System*, Results in Physics 29 (2021) Article ID 104733 9 pages.

[11] B. J. Salim, O. A. Jasim, Z. Y. Ali, *Numerical Solution of Drinfeld-Sokolov-Wilson System by Using Modified Adomian Decomposition Method*, Indonesian Journal of Electrical Engineering and Computer Science 23 (1) (2021) 590–599.

[12] M. N. Alam, E. Bonyah, M. Fayz-Al-Asad, *Reliable Analysis for the Drinfeld-Sokolov-Wilson Equation in Mathematical Physics*, Palestine Journal of Mathematics 11 (1) (2022) 397–407.

[13] H. M. Jaradat, S. Al-Shar'a, J. A. Q. Khan, M. Alquran, K. Al-Khaled, *Analytical Solution of Time-Fractional Drinfeld-Sokolov-Wilson System Using Residual Power Series Method*, IAENG International Journal of Applied Mathematics 46 (1) (2016) 64–70.

[14] A. Bhatter, A. Mathur, D. Kumar, J. Singh, *A New Analysis of Fractional Drinfeld–Sokolov–Wilson Model with Exponential Memory*, Physica A: Statistical Mechanics and Its Applications 537 (1) (2020) Article ID 122578 13 pages.

[15] W. Gao, P. Veeresha, D. G. Prakasha, H. M. Başkonuş, G. Yel, *A Powerful Approach for Fractional Drinfeld-Sokolov-Wilson Equation with Mittag-Leffler Law*, Alexandria Engineering Journal 58 (2019) 1301–1311.

[16] O. Taşbozan, M. Şenol, A. Kurt, O. Özkan, *New Solutions of Fractional Drinfeld-Sokolov-Wilson System in Shallow Water Waves*, Ocean Engineering 161 (2018) 62–68.

[17] K. J. Wang, G. D. Wang, *He's Variational Method for the Time-Space Fractional Nonlinear Drinfeld–Sokolov–Wilson System*, Mathematical Methods in the Applied Sciences 46 (7) (2021) 1–9.

[18] S. Noor, A. S. Alshehry, H. M. Dutt, R. Nazir, A. Khan, R. Shah, *Investigating the Dynamics of Time-Fractional Drinfeld–Sokolov–Wilson System through Analytical Solutions*, Symmetry 15 (3) (2023) 703 13 pages.

[19] T. Aydemir, *Application of the Generalized Unified Method to Solve (2+1)-Dimensional Kundu–Mukherjee–Naskar Equation*, Optical and Quantum Electronics 55 (2023) Article Number 534 17 pages.

[20] Ö. F. Gözükızıl, Ş. Akçağıl, T. Aydemir, *Unification of All Hyperbolic Tangent Function Methods*, Open Physics 14 (2016) 524–541.

[21] S. Akçağıl, T. Aydemir, *A New Application of the Unified Method*, New Trends in Mathematical Sciences 6 (1) (2018) 166–180.

[22] M. S. Ullah, H. Roshid, M. S. Ali, A. Biswas, M. Ekici, S. Khan, L. Moraru, A. K. Alzahrani, M. R. Belic, *Optical Soliton Polarization With Lakshmanan–Porsezian–Daniel Model by Unified Approach*, Results in Physics 22 (2021) Article ID 103958 5 pages.

[23] M. Bilal, S. Rehman, J. Ahmad, *Analysis in Fiber Bragg Gratings with Kerr Law Nonlinearity for Diverse Optical Soliton Solutions by Reliable Analytical Techniques*, Modern Physics Letters B 36 (23) (2022) Article ID 2250122 14 pages.

[24] M. Bilal, S. Rehman, J. Ahmad, *Dynamical Nonlinear Wave Structures of the Predator-Prey Model Using Conformable Derivative and Its Stability Analysis*, Pramana Journal of Physics 96 (2022) Article ID 149 18 pages.

[25] S. Foyjonnesa, N. H. M. Shahen, M. M. Rahman, *Dispersive Solitary Wave Structures with MI Analysis to the Unidirectional DGH Equation via the Unified Method*, Partial Differential Equations in Applied Mathematics 6 (2022) Article ID 100444 11 pages.

[26] S. M. Y. Arafat, S. M. R. Islam, M. H. Bashar, *Influence of the Free Parameters and Obtained Wave Solutions from CBS Equation*, International Journal of Applied and Computational Mathematics 8 (2022) Article ID 99 17 pages.

[27] S. M. R. Islam, M. H. Bashar, S. M. Y. Arafat, H. Wang, M. M. Roshid, *Effect of the Free Parameters on the Biswas-Arshed Model with a Unified Technique*, Chinese Journal of Physics 77 (2022) 2501–2519.

[28] S. M. R. Islam, D. Kumar, E. F. Donfack, M. Inc, *Impact of Nonlinearity and Wave Dispersion Parameters on the Soliton Pulses of the (2+1)-Dimensional Kundu-Mukherjee-Naskar Equation*, Revista Mexicana de Fisica 68 (2022) 1–14.

[29] S. Uddin, S. Karim, F. S. Alshammari, H. O. Roshid, N. F. M. Noor, F. Hoque, M. Nadeem, A. Akgül, *Bifurcation Analysis of Travelling Waves and Multi-Rogue Wave Solutions for a Nonlinear Pseudo-Parabolic Model of Visco-Elastic Kelvin-Voigt Fluid*, Mathematical Problems in Engineering 2022 (2022) Article ID 8227124 16 pages.

[30] D. C. Nandi, M. S. Ullah, M. Z. Ali, *Application of the Unified Method to Solve the Ion Sound and Langmuir Waves Model*, Heliyon 8 (10) (2022) Article ID e10924 8 pages.

[31] M. S. Ullah, A. Abdeljabbar, H. Roshid, M. Z. Ali, *Application of the Unified Method to Solve the Biswas–Arshed Model*, Results in Physics 42 (2022) Article ID 105946 6 pages.

[32] D. Kumar, M. D. M. Hasan, G. C. Paul, D. Debnath, N. Mondal, O. Faruk, *Revisiting the Spatiotemporal Dynamics of a Diffusive Predator-Prey System: An Analytical Approach*, Results in Physics 44 (2023) Article ID106122 18 pages.

[33] A. Akbulut, D. Kumar, *Conservation Laws and Optical Solutions of the Complex Modified Korteweg-De Vries Equation*, Journal of Ocean Engineering and Science (in press).

[34] A. Akbulut, S. M. R. Islam, S. M. Y. Arafat, F. Tascan, *A Novel Scheme for SMCH Equation with Two Different Approaches*, Computational Methods for Differential Equations 11 (2) (2023) 263–280.

[35] S. M. Y. Arafat, K. Khan, S. M. R. Islam, M. M. Rahman, *Parametric Effects on Paraxial Nonlinear Schrödinger Equation in Kerr Media*, Chinese Journal of Physics 83 (2023) 361–378.

[36] M. Bilal, J. Ahmad, *Investigation of Diverse Genres Exact Soliton Solutions to the Nonlinear Dynamical Model via Three Mathematical Methods*, Journal of Ocean Engineering and Science (in press).

Journal of New Theory
ISSN: 2149-1402

44 (2023) 20-30
Journal of New Theory
https://dergipark.org.tr/en/pub/jnt
Open Access

An Extension of the UEHL Distribution Based on the DUS Transformation

Murat Genç[1], **Ömer Özbilen**[2]

Article Info
Received: 20 Jun 2023
Accepted: 18 Sep 2023
Published: 30 Sep 2023
doi:10.53570/jnt.1317652
Research Article

Abstract – In this study, we propose a new distribution based on the Dinesh, Umesh, and Sanjay (DUS) transformation by using the Unit Exponentiated Half-Logistic (UEHL) distribution as the baseline distribution, a member of the family of proportional hazard rate models. Moreover, we study several properties, such as moments, skewness, kurtosis, stress-strength reliability, and likelihood ratio ordering. Further, we discuss the statistical inference on the parameters of the proposed distribution by the maximum likelihood estimation (MLE) method. Besides, we conduct a simulation based on the new distribution to investigate the behavior of the maximum likelihood estimates in various conditions. Furthermore, we present a numerical example to show the performance of the distribution on a real-life data set. Finally, we discuss the need for further research.

Keywords *DUS transformation, UEHL distribution, maximum likelihood estimator, data analysis*

Mathematics Subject Classification (2020) 62E10, 60E05

1. Introduction

A variety of models exist in the literature for examining lifetime data. The Weibull distribution originated as an extension of the exponential distribution. The distribution is more flexible in shape than the exponential distribution. This property makes the Weibull distribution useful for lifetime modeling and modeling data from economics and business administration [1-3]. In reliability theory, the Weibull distribution is convenient for modeling monotonic hazard rates. However, it does not provide a reasonable parametric fit for non-monotonic failure rates [4, 5]. To improve the ability to model non-monotonic failure rates, several generalizations and modifications of the Weibull distribution have been introduced in the literature [6, 7].

As an alternative to the Weibull distribution, the omega distribution was introduced as a new probability distribution, and its applications in reliability theory were discussed [8]. Dombi et al. [8] showed that the asymptotic omega hazard rate function is the Weibull hazard rate function, which implies that the asymptotic omega distribution is just the Weibull distribution. Moreover, the omega distribution belongs to the class of proportional hazard rate models. Özbilen and Genç [9] introduced the unit exponentiated-half logistic (UEHL) distribution corresponding to the omega distribution with a special case of the parameter value of the distribution. The distribution corresponds to the exponentiated half-logistic distribution with a simple transformation, which has many applications in reliability theory [10, 11].

In statistical literature, there are various ways to generate new distributions using some baseline distributions [12, 13]. In this context, Kumar et al. [14] proposed the Dinesh, Umesh, and Sanjay (DUS) transformation to

[1]muratgenc@tarsus.edu.tr (Corresponding Author); [2]ozbilen@mersin.edu.tr
[1]Department of Management Information Systems, Faculty of Economics and Administrative Sciences, Tarsus University, Mersin, Türkiye
[2]Department of Geomatic Engineering, Faculty of Engineering, Mersin University, Mersin, Türkiye

obtain a new distribution family. Let $f(x)$ and $F(x)$ denote the probability density function (PDF) and cumulative distribution function (CDF) of the baseline distribution, respectively. Then, the PDF and CDF of the DUS family are given by

$$f_{DUS}(x) = \frac{f(x)e^{F(x)}}{e-1}, \quad x \in D \tag{1}$$

and

$$F_{DUS}(x) = \frac{e^{F(x)}-1}{e-1} \tag{2}$$

respectively. In Equation (1), D is the domain of the baseline distribution. As observed from Equations (1) and (2) that the DUS family does not contain any new parameters in addition to those used in the baseline distribution. Hence, the DUS family results in a parsimonious distribution in terms of computation and interpretation.

There exist several studies in the literature where the DUS transformation is used. Kumar et al. [14] applied the DUS transformation to an exponential CDF. Deepthi and Chacko [15] proposed the DUS-Lomax distribution, considering the Lomax distribution as the baseline distribution for the DUS transformation. Kavya and Manoharan [16] obtained the DUS-Weibull distribution with the same approach. Maurya et al. [17] proposed a generalization of the DUS transformation and studied the exponential baseline in the proposed method. Karakaya et al. [18] considered the DUS transformation with the Kumaraswamy distribution and investigated the properties of the distribution.

The performance of the UEHL distribution can be improved by applying the DUS transformation to the CDF of the UEHL distribution. In this paper, we use the DUS transformation to the UEHL distribution to enhance distribution in the scope of modeling proportional data.

The rest of the paper is organized as follows: Section 2 introduces the UEHL distribution with DUS transformation and obtains the survival and hazard rate functions. Section 3 discusses some analytical characteristics, such as the moments, quantile function, stress-strength reliability, likelihood ratio ordering, and the maximum likelihood estimation (MLE) of the method. Section 4 performs a simulation study to validate the performance of the maximum likelihood estimates of the distribution. Section 5 provides a numerical example to illustrate the performance of the proposed distribution in modeling the real data. The last section concludes the paper.

2. DUS-UEHL Distribution

Recently, the UEHL distribution [9] has been proposed as a special case of omega distribution [8], a member of the class of proportional hazard rate models. The distribution corresponds to the transformation $Z = e^{-X}$ where X has the exponentiated half-logistic distribution. The UEHL distribution has many applications in reliability theory through exponentiated half-logistic distribution [10, 19, 20]. This section applies the DUS transformation to the UEHL distribution to introduce a new class of distributions. The PDF and CDF of the UEHL distribution are given as follows, respectively:

$$f_{UEHL}(x) = 2\lambda\theta x^{\theta-1}\frac{\left(1-x^{\theta}\right)^{\lambda-1}}{(1+x^{\theta})^{\lambda+1}}, \quad 0 < x < 1 \tag{3}$$

and

$$F_{UEHL}(x) = 1 - \left(\frac{1-x^{\theta}}{1+x^{\theta}}\right)^{\lambda}, \quad 0 < x < 1 \tag{4}$$

where $\theta > 0$ and $\lambda > 0$ are the scale and shape parameters of the distribution, respectively. By applying the transformations given in Equations (1) and (2) to Equations (3) and (4), the PDF and CDF of the new distribution are obtained as follows, respectively:

$$f_{D-UEHL}(x) = \frac{1}{e-1} 2\lambda\theta x^{\theta-1} \frac{(1-x^{\theta})^{\lambda-1}}{(1+x^{\theta})^{\lambda+1}} e^{1-\left(\frac{1-x^{\theta}}{1+x^{\theta}}\right)^{\lambda}} \tag{5}$$

and

$$F_{D-UEHL}(x) = \frac{1}{e-1}\left(e^{1-\left(\frac{1-x^{\theta}}{1+x^{\theta}}\right)^{\lambda}} - 1\right) \tag{6}$$

The random variable X with the CDF in Equation (6) is said to follow the two-parameter DUS-UEHL distribution and is denoted by $D\text{-}UEHL(\theta,\lambda)$. Considering the derivative of PDF in Equation 5, we obtain

$$f'_{D-UEHL}(x) = \frac{2\lambda\theta x^{\theta-2}\left(-2\lambda\theta x^{\theta} + (\theta+1)x^{2\theta} + \theta - 1\right)\left(\frac{2}{x^{\theta}+1} - 1\right)^{\lambda}}{(x^{2\theta}-1)^2}$$

which has the critical points $x_{1,2} = \left(\frac{(\lambda\theta \pm \sqrt{\lambda^2\theta^2 - \theta^2 + 1})}{(\theta+1)}\right)^{1/\theta}$ and the extreme points 0 and 1. Given $\theta > 1$, this indicates that the $D\text{-}UEHL(\theta,\lambda)$ distribution is unimodal with the unique mode at x_1 or x_2 depending on the scale and shape parameters of the distribution. Moreover, the PDF can be an increasing, decreasing, or U-shaped function of x depending on the values of the PDF at the extreme points.

Figure 1 shows the PDF of the $D\text{-}UEHL(\theta,\lambda)$ distribution for various values of the parameters θ and λ. According to Figure 1, the $D\text{-}UEHL(\theta,\lambda)$ distribution can take different shapes, including unimodal, increasing, decreasing, and U-shaped functions.

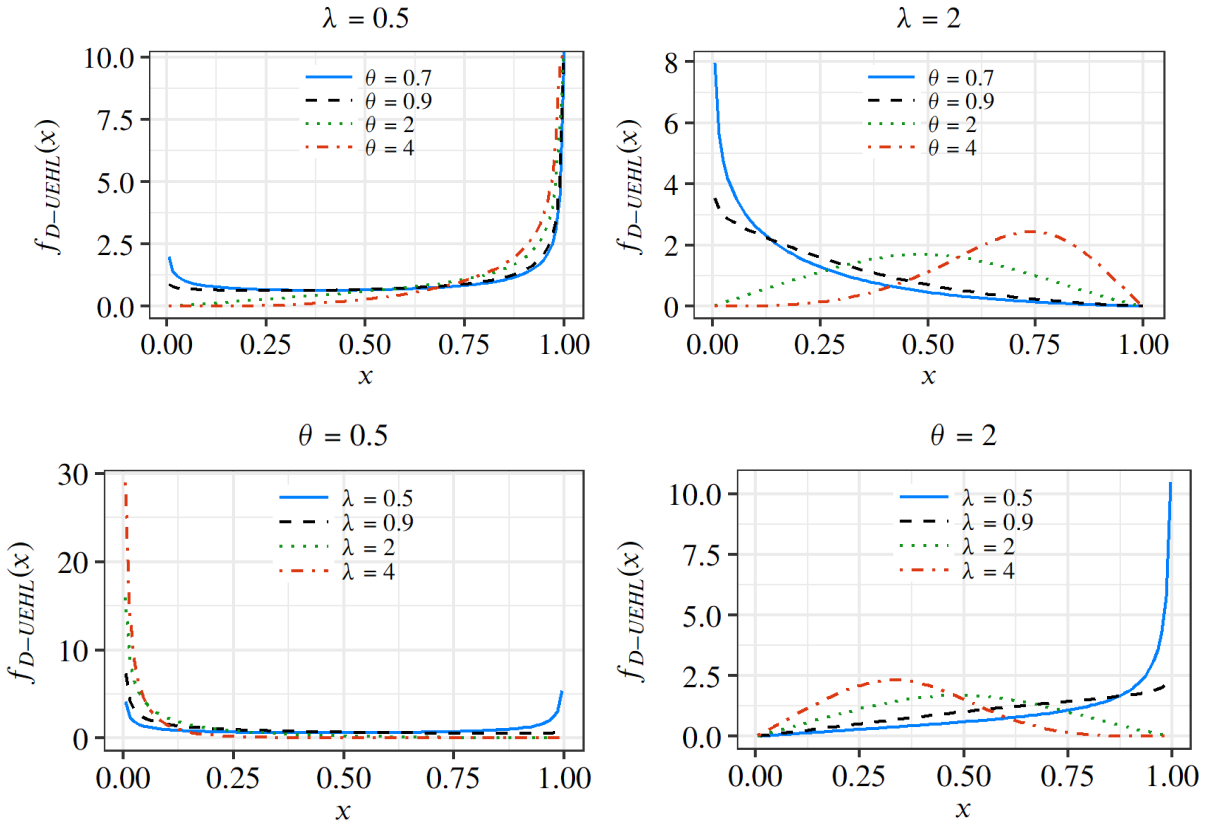

Figure 1. PDF plots of the $D\text{-}UEHL(\theta,\lambda)$ distribution for various values of the parameters θ and λ

The survival function and the hazard rate functions of the $D\text{-}UEHL$ distribution are provided as follows, respectively:

$$S_{D-UEHL}(x) = \frac{e - e^{1-\left(\frac{1-x^{\theta}}{1+x^{\theta}}\right)^{\lambda}}}{e-1} \tag{7}$$

and

$$h_{D-UEHL}(x) = \frac{2\lambda\theta x^{\theta-1}\frac{\left(1-x^{\theta}\right)^{\lambda-1}}{(1+x^{\theta})^{\lambda+1}} e^{1-\left(\frac{1-x^{\theta}}{1+x^{\theta}}\right)^{\lambda}}}{e - e^{1-\left(\frac{1-x^{\theta}}{1+x^{\theta}}\right)^{\lambda}}} \tag{8}$$

Figure 2 manifests the hazard rate function for selected values of the parameters θ and λ. According to Figure 2, the hazard function of $D\text{-}UEHL(\theta,\lambda)$ is an increasing function.

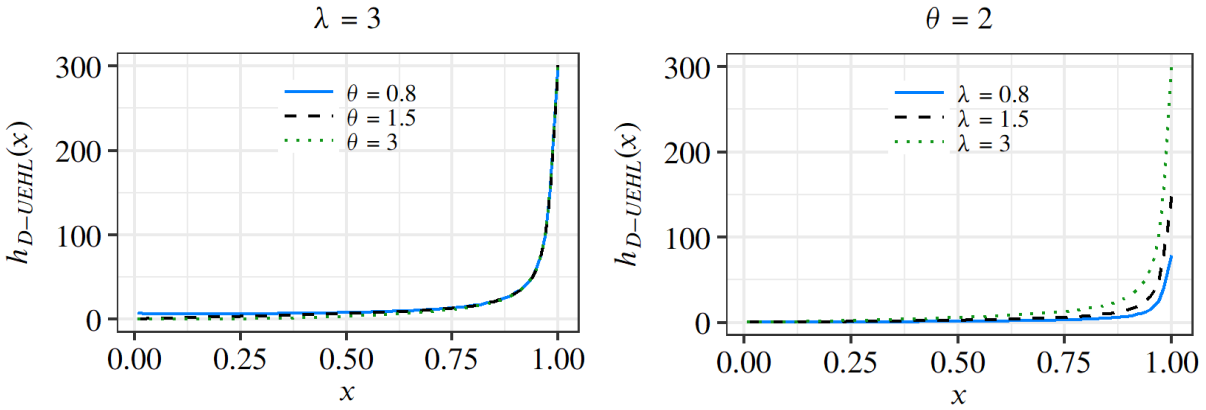

Figure 2. Hazard rate function plots of the $D\text{-}UEHL(\theta,\lambda)$ distribution for various values of the parameters θ and λ

3. Some Analytical Characteristics of the $D\text{-}UEHL(\theta,\lambda)$ Distribution

This section discusses some statistical characteristics, including the moments, quantile function, stress-strength reliability, likelihood ratio ordering, and MLE of the $D\text{-}UEHL(\theta,\lambda)$ distribution.

3.1. Moments

The moments are useful for understanding the various characteristics of a statistical distribution. In this section, we consider the moments of a $D\text{-}UEHL(\theta,\lambda)$ random variable. Let X be a $D\text{-}UEHL(\theta,\lambda)$ random variable with PDF given by Equation (5). Then, for $r \in \{1,2,3,\cdots\}$, the r-th raw moment of X is

$$E(X^r) = \frac{2\lambda e}{e-1}\int_0^1 x^r\left(\theta x^{\theta-1}\frac{\left(1-x^{\theta}\right)^{\lambda-1}}{(1+x^{\theta})^{\lambda+1}}\right)e^{1-\left(\frac{1-x^{\theta}}{1+x^{\theta}}\right)^{\lambda}}dx$$

By substituting $v = x^{\theta}$, the expectation is written as

$$E(X^r) = \frac{2\lambda e}{e-1}\int_0^1 v^{r/\theta}(1-v)^{\lambda-1}(1+v)^{-\lambda-1}e^{-\left(\frac{1-v}{1+v}\right)^{\lambda}}dv$$

By using the Taylor expansion $e^x = \sum_{j=0}^{\infty}\frac{x^j}{j!}$,

$$E(X^r) = \frac{2\lambda e}{e-1}\sum_{i=0}^{\infty}\left[\frac{(-1)^i}{i!}\int_0^1 \left(v^{r/\theta}(1-v)^{\lambda(1+i)-1}(1+v)^{-\lambda(1+i)-1}\right)dv\right]$$

Using Equation 3.197.3 provided in [21], i.e., $\int_0^1 x^{\lambda-1}(1-x)^{\mu-1}(1-\beta x)^{-\nu}dx = B(\lambda,\mu)\ {}_2F_1(\nu,\lambda;\lambda+\mu;\beta)$ such that Re $\lambda > 0$, Re $\mu > 0$, and $|\beta| < 1$, the r-th raw moment is obtained as

$$E(X^r) = \frac{2\lambda e}{e-1}\sum_{i=0}^{\infty}\frac{(-1)^i}{i!}B\left(1+\frac{r}{\theta},\lambda(1+i)\right){}_2F_1\left(\lambda(1+i)+1,1+\frac{r}{\theta};1+\frac{r}{\theta}+\lambda(1+i);-1\right)$$

where

$$B(a,b) = \int_0^1 t^{a-1}(1-t)^{b-1}\,dt \quad \text{and} \quad {}_2F_1(a,b;c;z) = \sum_{\mathrm{n}=0}^{\infty}\frac{(a)_n(b)_n}{(c)_n}\frac{z^n}{n!}$$

are the beta and Gauss hypergeometric functions, respectively, and $(a)_n = a(a+1)\cdots(a+n+1)$. Table 1 shows the mean, variance, skewness, and kurtosis of $D\text{-}UEHL(\theta,\lambda)$ distribution for selected pairs of (θ,λ). The results indicate that the $D\text{-}UEHL(\theta,\lambda)$ has various shapes depending on the values of the distribution parameters.

Table 1. Mean, variance, skewness, and kurtosis of the $D\text{-}UEHL(\theta,\lambda)$ distribution

θ	λ	Mean	Variance	Skewness	Kurtosis
0.7	0.7	0.4893	0.1057	0.0478	1.6247
	1.5	0.2600	0.0557	0.9766	3.0931
	3	0.1179	0.0168	1.8289	6.8839
1.5	0.7	0.6574	0.0725	-0.5416	2.1708
	1.5	0.4688	0.0573	0.1228	2.1052
	3	0.3153	0.0322	0.5336	2.7771
3	0.7	0.7874	0.0374	-1.0363	3.4153
	1.5	0.6571	0.0369	-0.4670	2.5985
	3	0.5355	0.0285	-0.1805	2.5863

3.2. Quantile Function

The quantile function of the $D\text{-}UEHL(\theta,\lambda)$ distribution is given by

$$Q_{D-UEHL}(u;\theta,\lambda) = F^{-1}(u;\theta,\lambda) = \left[2\left(1+\left(1-\log\left(1+u(e-1)\right)\right)^{1/\lambda}\right)^{-1}-1\right]^{1/\theta} \tag{9}$$

Based on Equation (9), the median of the $D\text{-}UEHL(\theta,\lambda)$ distribution is given by the following function, a function of the parameters θ and λ:

$$Q_{D-UEHL}(0.5;\theta,\lambda) = \left[2\left(1+(1-\log 2-\log(1+e))^{1/\lambda}\right)^{-1}-1\right]^{1/\theta} \tag{10}$$

The median values of the $D\text{-}UEHL(\theta,\lambda)$ distribution for selected parameter values are provided in Table 2.

Table 2. Median of the $D\text{-}UEHL(\theta,\lambda)$ distribution

	θ	0.1	0.5	1	2.5	5	10
	0.1	0.99874892	0.05466397	0.00033596	0.00000007	$< 10^{-8}$	$< 10^{-8}$
	0.5	0.99974966	0.55916532	0.20195643	0.03655548	0.00930982	0.00233835
λ	1	0.99987482	0.74777357	0.44939563	0.19119487	0.09648743	0.04835653
	2.5	0.99994993	0.89024193	0.72619213	0.51592966	0.39245358	0.29770219
	5	0.99997496	0.94352633	0.85216907	0.71828244	0.62646116	0.54562093
	10	0.99998748	0.97135283	0.92313004	0.84751545	0.79149299	0.73866158

3.3. Stress-Strength Reliability

Given the stress and strength random variables, Y and X, the stress-strength reliability is defined as $R = P(Y < X)$. In this section, we compute the stress-strength reliability for the model $D\text{-}UEHL(\theta, \lambda)$.

Proposition 1. Let Y and X be independent stress and strength random variables following $D\text{-}UEHL$ distribution with parameters (θ, λ_1) and (θ, λ_2), respectively. Then, the stress-strength reliability is

$$R = \frac{e^2}{(e-1)^2}\sum_{j=0}^{\infty}\frac{(-1)^j}{j!}\gamma\left(\frac{\lambda_1}{\lambda_2}j+1,1\right) - \frac{1}{e-1} \tag{11}$$

where $\lambda_1 > 0$, $\lambda_2 > 0$, and $\gamma(a,x) = \int_a^x t^{a-1}\, e^{-t}\, dt$ is the incomplete gamma function.

Proof.

By the definition, the stress-strength reliability can be written as

$$R = \int_0^1 P(Y < X \mid X = x) f_x(x) dx$$
$$= \int_0^1 \frac{1}{e-1}\left(e^{1-\left(\frac{1-x^\theta}{1+x^\theta}\right)^{\lambda_1}} - 1\right)\left(\frac{1}{e-1} 2\lambda_2\theta x^{\theta-1}\frac{\left(1-x^\theta\right)^{\lambda_2-1}}{(1+x^\theta)^{\lambda_2+1}} e^{1-\left(\frac{1-x^\theta}{1+x^\theta}\right)^{\lambda_2}}\right) dx$$

By substituting $t = \left(\frac{1-x^\theta}{1+x^\theta}\right)^{\lambda_1}$ and applying the Taylor expansion of e^x,

$$R = \frac{e}{(e-1)^2}\int_0^1 \left(e^{-t^{\lambda_1/\lambda_2+1}} - 1\right) e^{-t}\, dt$$

$$= \frac{e^2}{(e-1)^2}\int_0^1 \left(\sum_{j=0}^{\infty}\frac{(-1)^j t^{\lambda_1 j/\lambda_2}}{j!} - \frac{1}{e}\right) e^{-t}\, dt$$

$$= \frac{e^2}{(e-1)^2}\sum_{j=0}^{\infty}\left\{\frac{(-1)^j}{j!}\left(\int_0^1 t^{\lambda_1 j/\lambda_2} e^{-t}\, dt\right)\right\} - \frac{1}{e-1}$$

$$= \frac{e^2}{(e-1)^2}\sum_{j=0}^{\infty}\left\{\frac{(-1)^j}{j!}\gamma\left(\frac{\lambda_1}{\lambda_2}j+1,1\right)\right\} - \frac{1}{e-1}$$

□

3.4. Likelihood Ratio Ordering

Let X and Y be random variables with PDFs $f_X(\cdot)$ and $f_Y(\cdot)$, respectively. If $\frac{f_X(x)}{f_Y(x)}$ is non-decreasing in x, then it is said to be the random variable X is smaller than Y in likelihood ratio ordering and denoted by $X \leq_{lr} Y$. Proposition 2 gives the property of likelihood ratio ordering for the $D\text{-}UEHL$ distribution.

Proposition 2. Let $X \sim D\text{-}UEHL(\theta_1, \lambda_1)$ and $Y \sim D\text{-}UEHL(\theta_2, \lambda_2)$. If $\theta_1 = \theta_2$, then $X \leq_{lr} Y$.

PROOF.

Let $\theta_1 = \theta_2 = \theta$. The ratio of the PDFs of X and Y is given by

$$g(x) = \frac{2\lambda_1\theta x^{\theta-1}\dfrac{\left(1-x^{\theta}\right)^{\lambda_1-1}}{(1+x^{\theta})^{\lambda_1+1}}}{2\lambda_2\theta x^{\theta-1}\dfrac{(1-x^{\theta})^{\lambda_2-1}}{(1+x^{\theta})^{\lambda_2+1}}}$$

After simplifications, we obtain $g'(x) < 0$, for $0 < x < 1$ and $\theta > 0$. Hence, $g(\cdot)$ is a non-decreasing function of x, which completes the proof.

3.5. Maximum Likelihood Estimation

Let $X_1, X_2, \cdots, X_n$ be an identically independent distributed sample from $D\text{-}UEHL(\theta, \lambda)$. Then, the likelihood and log-likelihood functions are written as

$$L(\theta,\lambda) = \prod_{i=1}^{n}\left(\frac{1}{e-1}2\lambda\theta x_i^{\theta-1}\frac{\left(1-x_i^{\theta}\right)^{\lambda-1}}{\left(1+x_i^{\theta}\right)^{\lambda+1}}e^{1-\left(\frac{1-x_i^{\theta}}{1+x_i^{\theta}}\right)^{\lambda}}\right) \tag{12}$$

and

$$\begin{aligned}\ell(\theta,\lambda) = {} & -n\log(e-1) + n(1+\log 2) + n\log\lambda + n\log\theta + (\theta-1)\sum_{i=1}^{n}\log(x_i) \\ & +(\lambda-1)\sum_{i=1}^{n}\log\left(1-x_i^{\theta}\right) - (\lambda+1)\sum_{i=1}^{n}\log\left(1+x_i^{\theta}\right) - \sum_{i=1}^{n}\left(\frac{1-x_i^{\theta}}{1+x_i^{\theta}}\right)^{\lambda}\end{aligned} \tag{13}$$

respectively. Differentiating the log-likelihood function with respect to the parameters, we get the log-likelihood equations as

$$\frac{\partial\ell(\theta,\lambda)}{\partial\theta} = \frac{n}{\theta} + \sum_{i=1}^{n}\log(x_i) - (\lambda-1)\sum_{i=1}^{n}\frac{x_i^{\theta}\log x_i}{1-x_i^{\theta}} + (\lambda+1)\sum_{i=1}^{n}\frac{x_i^{\theta}\log x_i}{1+x_i^{\theta}} + 2\theta\sum_{i=1}^{n}\frac{x_i^{\theta-1}}{\left(1+x_i^{\theta}\right)^2} = 0 \tag{14}$$

and

$$\frac{\partial\ell(\theta,\lambda)}{\partial\lambda} = \frac{n}{\lambda} + \sum_{i=1}^{n}\log\left(\frac{1-x_i^{\theta}}{1+x_i^{\theta}}\right) - \sum_{i=1}^{n}\left(\frac{1-x_i^{\theta}}{1+x_i^{\theta}}\right)^{\lambda}\log\left(\frac{1-x_i^{\theta}}{1+x_i^{\theta}}\right) = 0 \tag{15}$$

Equations (14) and (15) do not have a closed-form solution. To solve these equations, some iterative methods can be employed. We apply the optim procedure in *R* to obtain the solution of the equation system.

4. Simulation Study

In this section, a simulation study is carried out to examine the properties of the MLE, which we discussed in detail in Section 3. Table 3 shows the biases and mean squared errors (MSEs) of the parameter estimates with 5000 replications for various values of the parameters (n, θ, λ). According to the results in Table 3, the MLEs are asymptotically unbiased. Moreover, the bias and MSE values of the MLEs decrease to zero as the sample size increases as desired.

Table 3. Bias and MSEs of MLE estimators for selected parameter values

			Bias		MSE	
θ	λ	n	$\hat{\theta}$	$\hat{\lambda}$	$\hat{\theta}$	$\hat{\lambda}$
2	2	50	0.06108	0.10841	0.09290	0.19997
		100	0.02521	0.04550	0.04196	0.08155
		200	0.01127	0.02281	0.01972	0.03706
		300	0.00690	0.01386	0.01311	0.02379
		500	0.00304	0.00752	0.00779	0.01394
3	1.5	50	0.09989	0.06955	0.24153	0.09187
		100	0.04119	0.02920	0.10856	0.03866
		200	0.01851	0.01493	0.05089	0.01787
		300	0.01147	0.00909	0.03392	0.01148
		500	0.00511	0.00496	0.02015	0.00676
1.5	0.8	50	0.06884	0.02793	0.09443	0.01843
		100	0.02873	0.01179	0.04116	0.00817
		200	0.01308	0.00629	0.01895	0.00389
		300	0.00834	0.00381	0.01267	0.00250
		500	0.00396	0.00216	0.00753	0.00148

5. Real Data Application

In this section, we investigate the flexibility performance of the $D\text{-}UEHL(\theta,\lambda)$ distribution with a real data application. For this purpose, we consider the reservoir data set obtained from the monthly water capacity of the Shasta Reservoir in California [22]. We compare the $D\text{-}UEHL(\theta,\lambda)$ distribution with well-known Weibull, Beta, Kumaraswamy, and UEHL distributions. The PDFs of the distributions used for comparison are given as follows:

Weibull distribution

$$f_W(x;\theta,\lambda)=\frac{\theta}{\lambda}\left(\frac{x}{\lambda}\right)^{\theta-1}e^{-(x/\lambda)^{\theta}},\quad \theta,\lambda>0$$

Beta distribution

$$f_B(x;\theta,\lambda)=\frac{1}{B(\theta,\lambda)}x^{\theta-1}(1-x)^{\lambda-1},\quad \theta,\lambda>0$$

Kumaraswamy distribution

$$f_{Kw}(x;\theta,\lambda)=\theta\lambda x^{\theta-1}\left(1-x^{\theta}\right)^{\lambda-1},\quad \theta,\lambda>0$$

We use the maximum likelihood method to estimate the unknown parameters of the considered distributions. We test the goodness of fits of the models with Kolmogorov-Smirnov test statistic (K-S (stat)) and associate p-value (K-S (p-value)). We report the Akaike information criterion (AIC) and Bayesian information criterion (BIC) to compare the proposed model with the other models. AIC and BIC are computed as

$$\text{AIC}=2k-2\ell(\theta,\lambda)\quad\text{and}\quad\text{BIC}=k\log n-2\ell(\theta,\lambda)$$

where k is the number of parameters, n is the number of observations, and ℓ is the maximum value of the likelihood function for the underlying distribution.

Table 4. Bias and MSEs of MLE estimators for selected parameter values

	θ	λ	AIC	BIC	-2ℓ	K-S (stat)	K-S (p-value)
Weibull	7.2987	0.7748	-20.5347	-18.5432	-24.5347	0.2220	0.2396
Beta	7.3157	2.9099	-21.1238	-19.1324	-25.1238	0.2359	0.1834
Kumaraswamy	6.3476	4.4894	-22.9494	-20.9580	-26.9494	0.2209	0.2447
UEHL	6.9010	2.8883	-21.2699	-19.2784	-25.2699	0.2254	0.2248
D-UEHL	6.4316	3.2682	-23.0543	-21.0629	-27.0543	0.2046	0.3267

Table 4 shows the parameter estimates, AIC values, BIC values, and -2ℓ values together with K-S (stat) and K-S (p-value) for all models fitted to the reservoir data set. The K-S test results indicate that the compared distributions are appropriate to fit the underlying data. From Table 4, it can be observed that the $D\text{-}UEHL(\theta,\lambda)$ distribution yields the lowest AIC and BIC values, followed by the Kumaraswamy distribution. Hence, we conclude that the $D\text{-}UEHL(\theta,\lambda)$ model has the best fit for the reservoir data set among the compared distributions in the study. Moreover, Figure 3 manifests the empirical and fitted curves based on the reservoir data set for illustrative purposes.

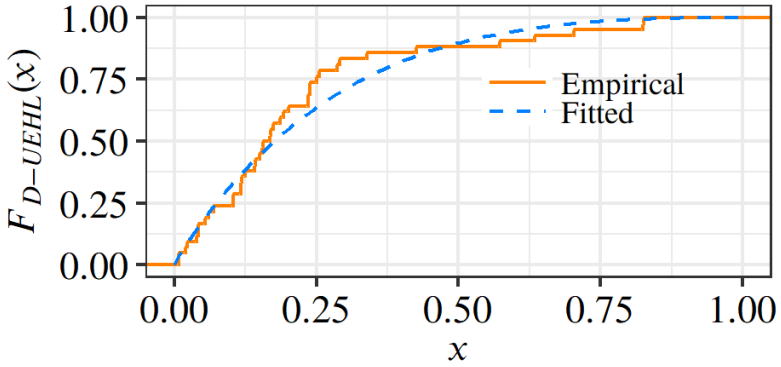

Figure 3: Empirical and fitted distribution functions based on the reservoir data set

6. Conclusion

In this study, we introduce $D\text{-}UEHL$ distribution for record data based on DUS transformation on unit exponentiated half-logistic distribution CDF. We obtain various analytical characteristics, including moments, quantile function, stress-strength reliability, and likelihood ratio ordering of the proposed distribution. We perform a simulation study that illustrates the properties of the maximum likelihood estimates of the $D\text{-}UEHL$ distribution. The real data analysis on a record data shows that the $D\text{-}UEHL$ model performs better on the data than the other well-known models in terms of AIC and BIC criteria.

The findings of this article can be extended by applying the DUS transform to the omega distribution. In this context, the effect of the extra support parameter of the omega distribution with the DUS transformation is a topic for further research.

Author Contributions

All the authors equally contributed to this work. They all read and approved the final version of the paper.

Conflict of Interest

All the authors declare no conflict of interest.

References

[1] D. P. Murthy, M. Xie, R. Jiang, Weibull Models, Wiley, New Jersey, 2004.

[2] J. I. McCool, Using the Weibull Distribution: Reliability, Modeling, and Inference, Wiley, New Jersey, 2012.

[3] M. Aslam, M. Azam, S. Balamurali, C. H. Jun, *An Economic Design of a Group Sampling Plan for a Weibull Distribution Using a Bayesian Approach*, Journal of Testing and Evaluation 43 (6) (2015) 1497–1503.

[4] S. J. Almalki, S. Nadarajah, *Modifications of the Weibull Distribution: A Review*, Reliability Engineering & System Safety 124 (1) (2014) 32–55.

[5] J. M. Carrasco, E. M. Ortega, G. M. Cordeiro, *A Generalized Modified Weibull Distribution for Lifetime Modeling*, Computational Statistics & Data Analysis 53 (2) (2008) 450–462.

[6] H. Pham, C. D. Lai, *On Recent Generalizations of the Weibull Distribution*, IEEE Transactions on Reliability 56 (2007) (3) 454–458.

[7] C. D. Lai, Generalized Weibull Distributions, Springer, Berlin, Heidelberg, 2013.

[8] J. Dombi, T. Jonas, Z. E. Toth, G. Arva, *The Omega Probability Distribution and Its Applications in Reliability Theory*, Quality and Reliability Engineering International 35 (2) (2019) 600–626.

[9] Ö. Özbilen, A. İ. Genç, *A Bivariate Extension of the Omega Distribution for Two-Dimensional Proportional Data*, Mathematica Slovaca 72 (6) (2022) 1605–1622.

[10] J. I. Seo, S. B. Kang, *Notes on the Exponentiated Half Logistic Distribution*, Applied Mathematical Modelling 39 (21) (2015) 6491–6500.

[11] W. Gui, *Exponentiated Half Logistic Distribution: Different Estimation Methods and Joint Confidence Regions*, Communications in Statistics - Simulation and Computation 46 (6) (2017) 4600–4617.

[12] R. C. Gupta, P. L. Gupta, R. D. Gupta, *Modeling Failure Time Data by Lehman Alternatives*, Communications in Statistics-Theory and Methods 27 (4) (1998) 887–904.

[13] G. M. Cordeiro, M. Castro. *A New Family of Generalized Distributions*, Journal of Statistical Computation and Simulation 81 (7) (2011) 883–898.

[14] D. Kumar, U. Singh, S. K. Singh, *A Method of Proposing New Distribution and Its Application to Bladder Cancer Patients Data*, Journal of Statistics Applications & Probability Letters 2 (3) (2015) 235–245.

[15] K. S. Deepthi, V. M. Chacko, *An Upside-Down Bathtub-Shaped Failure Rate Model Using a DUS Transformation of Lomax Distribution*, in: L. Cui, I. B. Frenkel, A. Lisnianski (Eds.), Stochastic Models in Reliability Engineering, CRC Press, Boca Raton, 2020, Ch. 6, pp. 81–100.

[16] P. Kavya, M. Manoharan, *On a Generalized Lifetime Model Using DUS Transformation*, in: V. C. Joshua, S. R. S. Varadhan, V. M. Vishnevsky (Eds.), Applied Probability and Stochastic Processes, Springer, Singapore, 2020, pp. 281–291.

[17] S. Maurya, A. Kaushik, S. Singh, U. Singh, *A New Class of Distribution Having Decreasing, Increasing, and Bathtub-Shaped Failure Rate*, Communications in Statistics-Theory and Methods 46 (20) (2017) 10359–10372.

[18] K. Karakaya, İ. Kınacı, K. Coşkun, Y. Akdoğan, *On the DUS-Kumaraswamy Distribution*, Istatistik Journal of the Turkish Statistical Association 13 (1) (2021) 29–38.

[19] S. B. Kang, J. I. Seo, *Estimation in an Exponentiated Half Logistic Distribution under Progressively Type-2 Censoring*, Communications for Statistical Applications and Methods 18 (5) (2011) 657–666.

[20] M. K. Rastogi, Y. M. Tripathi, *Parameter and Reliability Estimation for an Exponentiated Half-Logistic Distribution Under Progressive Type-II Censoring*, Journal of Statistical Computation and Simulation 84 (8) (2014) 1711–1727.

[21] I. S. Gradshteyn, I. M. Ryzhik, Table of Integrals, Series, and Products, 7th edition, Academic Press, San Diego, 2007.

[22] M. Nadar, A. Papadopoulos, F. Kızılaslan, *Statistical Analysis for Kumaraswamy's Distribution Based on Record Data*, Statistical Papers 54 (2013) 355–369.

Journal of New Theory
ISSN: 2149-1402

44 (2023) 31-42
Journal of New Theory
https://dergipark.org.tr/en/pub/jnt
Open Access

On Dual Quaternions with $k-$Generalized Leonardo Components

Çiğdem Zeynep Yılmaz[1], **Gülsüm Yeliz Saçlı**[2]

Article Info
Received: 17 Jul 2023
Accepted: 21 Sep 2023
Published: 30 Sep 2023
doi:10.53570/jnt.1328605
Research Article

Abstract — In this paper, we define a one-parameter generalization of Leonardo dual quaternions, namely $k-$generalized Leonardo-like dual quaternions. We introduce the properties of k-generalized Leonardo-like dual quaternions, including relations with Leonardo, Fibonacci, and Lucas dual quaternions. We investigate their characteristic relations, involving the Binet-like formula, the generating function, the summation formula, Catalan-like, Cassini-like, d'Ocagne-like, Tagiuri-like, and Hornsberger-like identities. The crucial part of the present paper is that one can reduce the calculations of Leonardo-like dual quaternions by considering k. For $k = 1$, these results are generalizations of the ones for ordered Leonardo quadruple numbers. Finally, we discuss the need for further research.

Keywords *Leonardo sequence, recurrence relations, dual quaternions*

Mathematics Subject Classification (2020) 11B37, 11B39

1. Introduction

The well-known Fibonacci sequence $\{F_n\}_{n\geq 2}$ and the Lucas sequence $\{L_n\}_{n\geq 2}$ are defined recursively by $F_n = F_{n-1} + F_{n-2}$, and $L_n = L_{n-1} + L_{n-2}$ with initial conditions $F_0 = 0$, $F_1 = 1$, and $L_0 = 2$, $L_1 = 1$, respectively [1]. The Binet's formulas of the Fibonacci and Lucas sequences are as follows, respectively:

$$F_n = \frac{\alpha^n - \beta^n}{\alpha - \beta} \tag{1}$$

and

$$L_n = \alpha^n + \beta^n$$

where $\alpha = \frac{1+\sqrt{5}}{2}$ and $\beta = \frac{1-\sqrt{5}}{2}$ are roots of characteristic equation $x^2 - x - 1 = 0$ [1]. Many generalizations of the Fibonacci and Lucas sequences have been studied by several researchers. In this study, we consider the Leonardo sequence. The Leonardo sequence $\{Le_n\}_{n\geq 2}$ is defined non-homogeneous recursively by

$$Le_n = Le_{n-1} + Le_{n-2} + 1$$

or

$$Le_{n+1} = 2Le_n - Le_{n-2}$$

[1]cigdem.yilmaz@std.yildiz.edu.tr; [2]yeliz.sacli@yildiz.edu.tr (Corresponding Author)
[1,2]Department of Mathematics, Faculty of Arts and Sciences, Yildiz Technical University, İstanbul, Türkiye

with initial conditions $Le_0 = Le_1 = 1$ and $Le_2 = 3$ [2]. The Binet-like formula of the Leonardo sequence is

$$Le_n = 2\left(\frac{\alpha^{n+1} - \beta^{n+1}}{\alpha - \beta}\right) - 1$$

There exist many identities between Fibonacci, Lucas, and Leonardo numbers. For $n \geq 0$, the fundamental relationships between the Fibonacci, Lucas, and Leonardo sequences are [2]:

$$Le_n = 2F_{n+1} - 1$$

$$Le_n = 2\left(\frac{L_n + L_{n+2}}{5}\right) - 1$$

$$Le_{n+3} = \frac{L_{n+1} + L_{n+7}}{5} - 1$$

and

$$Le_n = L_{n+2} - F_{n+2} - 1$$

Although the Fibonacci, Lucas, and Leonardo sequences are closely related, they exhibit distinct characteristic properties. Several different properties and generalizations of the Leonardo sequence were previously studied by various researchers [3–15]. Recently, a one-parameter generalized Leonardo sequence has been defined as non-homogeneous recursively by

$$\mathsf{Le}_n^{(k)} = \mathsf{Le}_{n-1}^{(k)} + \mathsf{Le}_{n-2}^{(k)} + k, \quad n \geq 2 \tag{2}$$

with the initial conditions $\mathsf{Le}_0^{(k)} = \mathsf{Le}_1^{(k)} = 1$. Here, k is a fixed positive integer [4]. The Binet-like formula of the $k-$generalized Leonardo sequence is

$$\mathsf{Le}_n^{(k)} = (k+1)\left(\frac{\alpha^{n+1} - \beta^{n+1}}{\alpha - \beta}\right) - k$$

The $k-$generalized Leonardo sequence is related to the Fibonacci and Lucas sequences. For $n \geq 0$, the fundamental relationships between Fibonacci, Lucas, and the $k-$generalized Leonardo sequences are [4]:

$$\mathsf{Le}_n^{(k)} = (k+1)F_{n+1} - k \tag{3}$$

and

$$\mathsf{Le}_n^{(k)} = (k+1)\left(L_n - F_{n-1}\right) - k$$

The summation formulas of the $k-$generalized Leonardo numbers are [4]:

$$\sum_{s=0}^{n} \mathsf{Le}_s^{(k)} = \mathsf{Le}_{n+2}^{(k)} - k\,(n+1) - 1 \tag{4}$$

$$\sum_{s=0}^{n} \mathsf{Le}_{2s}^{(k)} = \mathsf{Le}_{2n+1}^{(k)} - kn \tag{5}$$

and

$$\sum_{s=0}^{n} \mathsf{Le}_{2s+1}^{(k)} = \mathsf{Le}_{2n+2}^{(k)} - k(n+2) \tag{6}$$

The $k-$generalized Leonardo sequence is the key concept of the present paper. For $k = 1$, this sequence is the classical Leonardo sequence, i.e., $\mathsf{Le}_n^{(1)} = Le_n$. In this case, we may omit the superscript (1) in the notation.

There are several ways to define new special sequences but the most popular method is to define a

sequence with different hypercomplex number components. Horadam [16] defined the real quaternions with the classic Fibonacci sequence $\{QF_n\}_{n\geq 2}$ and the classic Lucas sequence $\{QL_n\}_{n\geq 2}$ recursively by

$$QF_n = F_n + F_{n+1}e_1 + F_{n+2}e_2 + F_{n+3}e_3$$

and

$$QL_n = L_n + L_{n+1}e_1 + L_{n+2}e_2 + L_{n+3}e_3$$

where F_n and L_n are the n-th classic Fibonacci and Lucas numbers, respectively. Here, the quaternionic units $\{e_1, e_2, e_3\}$ satisfy the following multiplication rules:

$$e_1{}^2 = e_2{}^2 = e_3{}^2 = -1, \quad e_1e_2 = -e_2e_1 = e_3, \quad e_2e_3 = -e_3e_2 = e_1, \quad \text{and} \quad e_3e_1 = -e_1e_3 = e_2$$

In general, a real quaternion q is of the form $q = a+e_1b+e_2c+e_3d$ where $a, b, c, d \in \mathbb{R}$. The quaternions form a four-dimensional associative and non-commutative algebra over the real numbers. For a deeper discussion of the quaternions, see [17–19]. Changing conditions in the multiplication rules produces different type of quaternions. In this study, we consider the dual quaternions. The dual quaternionic units obey the following multiplication rules:

$$e_1{}^2 = e_2{}^2 = e_3{}^2 = 0 \quad \text{and} \quad e_1e_2 = -e_2e_1 = e_2e_3 = -e_3e_2 = e_3e_1 = -e_1e_3 = 0 \tag{7}$$

Yüce et al. [20] defined the dual quaternions with the Fibonacci sequence $\{\hat{\mathcal{F}}_n\}_{n\geq 2}$ and the Lucas sequence $\{\hat{\mathcal{L}}_n\}_{n\geq 2}$ recursively by

$$\hat{\mathcal{F}}_n = F_n + F_{n+1}e_1 + F_{n+2}e_2 + F_{n+3}e_3$$

and

$$\hat{\mathcal{L}}_n = L_n + L_{n+1}e_1 + L_{n+2}e_2 + L_{n+3}e_3$$

where F_n and L_n are the n-th classic Fibonacci and Lucas numbers, respectively. Here, the non-real dual quaternionic units $\{e_1, e_2, e_3\}$ satisfy Equation 7. For a deeper discussion of the dual quaternions, see [21–27]. Nurkan et al. [13] defined the dual quaternions with the classic Leonardo sequence $\{\hat{\mathcal{L}}e_n\}_{n\geq 2}$ recursively by

$$\hat{\mathcal{L}}e_n = Le_n + Le_{n+1}e_1 + Le_{n+2}e_2 + Le_{n+3}e_3$$

where Le_n is the n-th classic Leonardo number.

Considering all these details, a natural question is whether the paper [13] can be generalized. In this study, we aim to determine the dual quaternions with the $k-$generalized Leonardo sequence. We consider the coefficients of the dual quaternions as the $k-$generalized Leonardo sequence.

2. The $k-$Generalized Leonardo-like Dual Quaternion Sequence

This section introduces the dual quaternions with one parameter generalized Leonardo sequence and investigates their characteristic properties.

Definition 2.1. The n-th $k-$generalized Leonardo-like dual quaternion is defined by

$$\hat{\mathsf{Le}}_n^{(k)} = \mathsf{Le}_n^{(k)} + \mathsf{Le}_{n+1}^{(k)}\, e_1 + \mathsf{Le}_{n+2}^{(k)}\, e_2 + \mathsf{Le}_{n+3}^{(k)}\, e_3 \tag{8}$$

where $\mathsf{Le}_n^{(k)}$ is the n-th $k-$generalized Leonardo number, k is a fixed positive integer, and $\{e_1, e_2, e_3\}$ are the set of all the dual quaternionic units. The $k-$generalized Leonardo-like dual quaternion sequence is denoted by $\left\{\hat{\mathsf{Le}}_n^{(k)}\right\}_{n\geq 2}$.

Note that, if $k = 1$, the generalized Leonardo-like dual quaternion sequence $\left\{\hat{\mathsf{Le}}_n^{(k)}\right\}_{n\geq 2}$ is the Leonardo

quadruple sequence. In this case, we may omit the superscript (1) in the notation.

Let $\hat{\mathsf{Le}}_n^{(k)}$ and $\hat{\mathsf{Le}}_m^{(k)}$ be two $k-$generalized Leonardo-like dual quaternions. The $k-$generalized Leonardo number $\mathsf{Le}_n^{(k)}$ is called scalar (real) part of $\hat{\mathsf{Le}}_n^{(k)}$ and denoted by $\mathcal{S}_{\hat{\mathsf{Le}}_n^{(k)}}$ and the vector

$$\mathsf{Le}_{n+1}^{(k)}\, e_1 + \mathsf{Le}_{n+2}^{(k)}\, e_2 + \mathsf{Le}_{n+3}^{(k)}\, e_3$$

is called the pure part of $\hat{\mathsf{Le}}_n^{(k)}$ and denoted by $\mathcal{V}_{\hat{\mathsf{Le}}_n^{(k)}}$. The addition is defined component-wise as

$$\hat{\mathsf{Le}}_n^{(k)} \pm \hat{\mathsf{Le}}_m^{(k)} = \left(\mathsf{Le}_n^{(k)} \pm \mathsf{Le}_m^{(k)}\right) + \left(\mathsf{Le}_{n+1}^{(k)} \pm \mathsf{Le}_{m+1}^{(k)}\right) e_1 + \left(\mathsf{Le}_{n+2}^{(k)} \pm \mathsf{Le}_{m+2}^{(k)}\right) e_2 + \left(\mathsf{Le}_{n+3}^{(k)} \pm \mathsf{Le}_{m+3}^{(k)}\right) e_3$$

whereas multiplication is defined by

$$\begin{aligned}\hat{\mathsf{Le}}_n^{(k)}\hat{\mathsf{Le}}_m^{(k)} = &\left(\mathsf{Le}_n^{(k)}\mathsf{Le}_m^{(k)}\right) + \left(\hat{\mathsf{Le}}_n^{(k)}\hat{\mathsf{Le}}_{m+1}^{(k)} + \hat{\mathsf{Le}}_m^{(k)}\hat{\mathsf{Le}}_{n+1}^{(k)}\right) e_1 + \left(\hat{\mathsf{Le}}_n^{(k)}\hat{\mathsf{Le}}_{m+2}^{(k)} + \hat{\mathsf{Le}}_m^{(k)}\hat{\mathsf{Le}}_{n+2}^{(k)}\right) e_2 \\ &+ \left(\hat{\mathsf{Le}}_n^{(k)}\hat{\mathsf{Le}}_{m+3}^{(k)} + \hat{\mathsf{Le}}_m^{(k)}\hat{\mathsf{Le}}_{n+3}^{(k)}\right) e_3\end{aligned}$$

or

$$\hat{\mathsf{Le}}_n^{(k)}\hat{\mathsf{Le}}_m^{(k)} = \mathcal{S}_{\hat{\mathsf{Le}}_n^{(k)}}\mathcal{S}_{\hat{\mathsf{Le}}_m^{(k)}} + \mathcal{S}_{\hat{\mathsf{Le}}_n^{(k)}}\mathcal{V}_{\hat{\mathsf{Le}}_m^{(k)}} + \mathcal{S}_{\hat{\mathsf{Le}}_m^{(k)}}\mathcal{V}_{\hat{\mathsf{Le}}_n^{(k)}}$$

The conjugate and norm of any $k-$generalized Leonardo-like dual quaternion $\hat{\mathsf{Le}}_n^{(k)}$ is given by

$$\overline{\hat{\mathsf{Le}}_n^{(k)}} = \mathcal{S}_{\hat{\mathsf{Le}}_n^{(k)}} - \mathcal{V}_{\hat{\mathsf{Le}}_n^{(k)}} = \hat{\mathsf{Le}}_n^{(k)} - \hat{\mathsf{Le}}_{n+1}^{(k)} e_1 - \hat{\mathsf{Le}}_{n+2}^{(k)}\, e_2 - \hat{\mathsf{Le}}_{n+3}^{(k)} e_3$$

and

$$||\hat{\mathsf{Le}}_n^{(k)}|| = \hat{\mathsf{Le}}_n^{(k)}\, \overline{\hat{\mathsf{Le}}_n^{(k)}} = \left(\hat{\mathsf{Le}}_n^{(k)}\right)^2 \in \mathbb{R}$$

respectively.

Theorem 2.2. The recurrence relation of the $k-$generalized Leonardo-like dual quaternion sequence is

$$\hat{\mathsf{Le}}_n^{(k)} = \hat{\mathsf{Le}}_{n-1}^{(k)} + \hat{\mathsf{Le}}_{n-2}^{(k)} + \hat{\mathcal{K}}, \quad n \geq 2$$

where $\hat{\mathcal{K}} = k\,(1 + e_1 + e_2 + e_3)$ with initial conditions $\hat{\mathsf{Le}}_0^{(k)} = 1 + e_1 + (2+k)\, e_2 + (3+2k)\, e_3$ and $\hat{\mathsf{Le}}_1^{(k)} = 1 + (2+k)\, e_1 + (3+2k)\, e_2 + (5+4k)\, e_3$.

Proof.
From Definition 2.1, it follows that

$$\begin{aligned}\hat{\mathsf{Le}}_{n-1}^{(k)} + \hat{\mathsf{Le}}_{n-2}^{(k)} + \hat{\mathcal{K}} = &\left(\mathsf{Le}_{n-1}^{(k)} + \mathsf{Le}_{n-2}^{(k)} + k\right) + \left(\mathsf{Le}_n^{(k)} + \mathsf{Le}_{n-1}^{(k)} + k\right) e_1 + \left(\mathsf{Le}_{n+1}^{(k)} + \mathsf{Le}_n^{(k)} + k\right) e_2 \\ &+ \left(\mathsf{Le}_{n+2}^{(k)} + \mathsf{Le}_{n+1}^{(k)} + k\right) e_3\end{aligned}$$

By applying Equation 2, we complete the proof. □

Throughout this paper, let $\hat{\mathcal{K}} = k\,(1 + e_1 + e_2 + e_3)$.

Theorem 2.3. The other recurrence relation of $\left\{\hat{\mathsf{Le}}_n^{(k)}\right\}_{n\geq 2}$ is

$$\hat{\mathsf{Le}}_{n+1}^{(k)} = 2\hat{\mathsf{Le}}_n^{(k)} - \hat{\mathsf{Le}}_{n-2}^{(k)}$$

Proof.
By Theorem 2.2, the proof is straightforward. □

Afterward, we state the Binet-like formula for the $k-$generalized Leonardo-like dual quaternion $\hat{\mathsf{Le}}_n^{(k)}$. Thus, we derive some well-known mathematical properties.

Theorem 2.4. The Binet-like formula of the $k-$generalized Leonardo-like dual quaternion $\hat{\mathsf{Le}}_n^{(k)}$ is

$$\hat{\mathsf{Le}}_n^{(k)} = (k+1)\left(\frac{\alpha^*\alpha^{n+1} - \beta^*\beta^{n+1}}{\alpha-\beta}\right) - \hat{\mathcal{K}} \tag{9}$$

where $\alpha^* = 1 + \alpha e_1 + \alpha^2 e_2 + \alpha^3 e_3$ and $\beta^* = 1 + \beta e_1 + \beta^2 e_2 + \beta^3 e_3$.

Proof.
By using Definition 2.1 and Equation 3,

$$\begin{aligned}\hat{\mathsf{Le}}_n^{(k)} &= \mathsf{Le}_n^{(k)} + \mathsf{Le}_{n+1}^{(k)}\, e_1 + \mathsf{Le}_{n+2}^{(k)}\, e_2 + \mathsf{Le}_{n+3}^{(k)}\, e_3 \\ &= (k+1)\,(F_{n+1} + F_{n+2}\, e_1 + F_{n+3}\, e_2 + F_{n+4}\, e_3) - k\,(1 + e_1 + e_2 + e_3)\end{aligned}$$

Applying the Binet's formula of the Fibonacci sequence in Equation 1 and then taking $\alpha^* = 1+\alpha e_1 + \alpha^2 e_2 + \alpha^3 e_3$, $\beta^* = 1 + \beta e_1 + \beta^2 e_2 + \beta^3 e_3$, and $\hat{\mathcal{K}} = k\,(1 + e_1 + e_2 + e_3)$,

$$\begin{aligned}\hat{\mathsf{Le}}_n^{(k)} &= (k+1)\left(\frac{\alpha^{n+1}\,(1+\alpha e_1+\alpha^2 e_2+\alpha^3 e_3) - \beta^{n+1}\,(1+\beta e_1+\beta^2 e_2+\beta^3 e_3)}{\alpha-\beta}\right) - \hat{\mathcal{K}} \\ &= (k+1)\left(\frac{\alpha^*\alpha^{n+1} - \beta^*\beta^{n+1}}{\alpha-\beta}\right) - \hat{\mathcal{K}}\end{aligned}$$

is obtained. □

Here, we state some relations between $k-$generalized Leonardo-like dual quaternions, Fibonacci dual quaternions, Lucas dual quaternions, and Fibonacci and Lucas numbers.

Theorem 2.5. Let $\hat{\mathsf{Le}}_n^{(k)}$ be the n-th $k-$generalized Leonardo-like dual quaternion, $\hat{\mathcal{F}}_n$ be the n-th Fibonacci dual quaternion, and $\hat{\mathcal{L}}_n$ be the n-th Lucas dual quaternion. For positive integers n, m, r, and t with $n \geq r$ and $n \geq m$, the following relations hold:

i. $\hat{\mathsf{Le}}_n^{(k)} = (k+1)\hat{\mathcal{F}}_{n+1} - \hat{\mathcal{K}}$

ii. $\hat{\mathsf{Le}}_n^{(k)} = (k+1)(\hat{\mathcal{L}}_n - \hat{\mathcal{F}}_{n-1}) - \hat{\mathcal{K}}$

iii. $\hat{\mathsf{Le}}_{n+r}^{(k)} + \hat{\mathsf{Le}}_{n-r}^{(k)} = (k+1)\begin{cases} L_r\hat{\mathcal{F}}_{n+1} - 2\hat{\mathcal{K}}, & r = 2t \\ F_r\hat{\mathcal{L}}_{n+1} - 2\hat{\mathcal{K}}, & r = 2t+1 \end{cases}$

iv. $\hat{\mathsf{Le}}_{n+r}^{(k)} - \hat{\mathsf{Le}}_{n-r}^{(k)} = (k+1)\begin{cases} F_r\hat{\mathcal{L}}_{n+1}, & r = 2t \\ L_r\hat{\mathcal{F}}_{n+1}, & r = 2t+1 \end{cases}$

v. $\hat{\mathsf{Le}}_{n+m}^{(k)} + (-1)^m\hat{\mathsf{Le}}_{n-m}^{(k)} = L_m\hat{\mathsf{Le}}_n^{(k)} + \hat{\mathcal{K}}(L_m - (-1)^m - 1)$

vi. $\hat{\mathsf{Le}}_{n+m}^{(k)} - (-1)^m\hat{\mathsf{Le}}_{n-m}^{(k)} = (k+1)\,F_m\hat{\mathcal{L}}_{n+1} - \hat{\mathcal{K}}\,(1 - (-1)^m)$

Proof.
Let $\hat{\mathsf{Le}}_n^{(k)}$ be the n-th $k-$generalized Leonardo-like dual quaternion, $\hat{\mathcal{F}}_n$ be the n-th Fibonacci dual quaternion, and $\hat{\mathcal{L}}_n$ be the n-th Lucas dual quaternion.

i. According to Equation 3,

$$\begin{aligned}\hat{\mathsf{Le}}_n^{(k)} &= ((k+1)\,F_{n+1} - k) + ((k+1)\,F_{n+2} - k)\,e_1 + ((k+1)\,F_{n+3} - k)\,e_2 + ((k+1)\,F_{n+4} - k)\,e_3 \\ &= (k+1)\,\hat{\mathcal{F}}_{n+1} - \hat{\mathcal{K}}\end{aligned}$$

iii.

$$\hat{\mathsf{Le}}_{n+r}^{(k)} + \hat{\mathsf{Le}}_{n-r}^{(k)} = \left(\mathsf{Le}_{n+r}^{(k)} + \mathsf{Le}_{n-r}^{(k)}\right) + \left(\mathsf{Le}_{n+1+r}^{(k)} + \mathsf{Le}_{n+1-r}^{(k)}\right) e_1 + \left(\mathsf{Le}_{n+2+r}^{(k)} + \mathsf{Le}_{n+2-r}^{(k)}\right) e_2 + \left(\mathsf{Le}_{n+3+r}^{(k)} + \mathsf{Le}_{n+3-r}^{(k)}\right) e_3$$

Considering Equation 3,

$$\hat{\mathsf{Le}}_{n+r}^{(k)} + \hat{\mathsf{Le}}_{n-r}^{(k)} = (k+1)\left(\left(F_{n+1+r} + F_{n+1-r}\right) + \left(F_{n+2+r} + F_{n+2-r}\right) e_1 + \left(F_{n+3+r} + F_{n+3-r}\right) e_2 + \left(F_{n+4+r} + F_{n+4-r}\right) e_3\right) - 2\hat{\mathcal{K}}$$

By using the definition of Fibonacci dual quaternion and the following relation of Fibonacci numbers (see [1])

$$F_{n+r} + F_{n-r} = \begin{cases} F_n L_r, & r = 2t \\ F_r L_n, & r = 2t+1 \end{cases}$$

we complete the proof.

v. From Theorem 2.5(i) and the Binet's formulas of Fibonacci and Lucas numbers,

$$\begin{aligned} \hat{\mathsf{Le}}_{n+m}^{(k)} + (-1)^m \hat{\mathsf{Le}}_{n-m}^{(k)} &= \left((k+1)\hat{\mathcal{F}}_{n+m+1} - \hat{\mathcal{K}}\right) + (-1)^m \left((k+1)\hat{\mathcal{F}}_{n-m+1} - \hat{\mathcal{K}}\right) \\ &= (k+1)\hat{\mathcal{F}}_{n+1} L_m + \hat{\mathcal{K}}\left(-1 - (-1)^m\right) \\ &= \left((k+1)\hat{\mathcal{F}}_{n+1} - \hat{\mathcal{K}}\right) L_m + \hat{\mathcal{K}}(L_m - (-1)^m - 1) \\ &= L_m \hat{\mathsf{Le}}_n^{(k)} + \hat{\mathcal{K}}(L_m - (-1)^m - 1) \end{aligned}$$

□

Corollary 2.6. Using the identities *iii* and *iv* presented in Theorem 2.5, the following basic identities are obtained:

i. $\hat{\mathsf{Le}}_{n+1}^{(k)} + \hat{\mathsf{Le}}_{n-1}^{(k)} = (k+1)\hat{\mathcal{L}}_{n+1} - 2\hat{\mathcal{K}}$

ii. $\hat{\mathsf{Le}}_{n+1}^{(k)} - \hat{\mathsf{Le}}_{n-1}^{(k)} = (k+1)\hat{\mathcal{F}}_{n+1}$

iii. $\hat{\mathsf{Le}}_{n+2}^{(k)} + \hat{\mathsf{Le}}_{n-2}^{(k)} = 3(k+1)\hat{\mathcal{F}}_{n+1} - 2\hat{\mathcal{K}}$

iv. $\hat{\mathsf{Le}}_{n+2}^{(k)} - \hat{\mathsf{Le}}_{n-2}^{(k)} = (k+1)\hat{\mathcal{L}}_{n+1}$

Theorem 2.7. Let $\hat{\mathsf{Le}}_n^{(k)}$ be the n-th $k-$generalized Leonardo-like dual quaternion. Then, the following relations hold:

i. $\hat{\mathsf{Le}}_n^{(k)} - \hat{\mathsf{Le}}_{n+1}^{(k)} e_1 - \hat{\mathsf{Le}}_{n+2}^{(k)} e_2 - \hat{\mathsf{Le}}_{n+3}^{(k)} e_3 = \mathsf{Le}_n^{(k)}$

ii. $\hat{\mathsf{Le}}_n^{(k)} + \overline{\hat{\mathsf{Le}}_n^{(k)}} = 2\mathsf{Le}_n^{(k)}$

iii. $\left(\hat{\mathsf{Le}}_n^{(k)}\right)^2 = 2\mathsf{Le}_n^{(k)} \hat{\mathsf{Le}}_n^{(k)} - \left(\mathsf{Le}_n^{(k)}\right)^2$

iv. $\hat{\mathsf{Le}}_n^{(k)} \overline{\hat{\mathsf{Le}}_n^{(k)}} + \hat{\mathsf{Le}}_{n+1}^{(k)} \overline{\hat{\mathsf{Le}}_{n+1}^{(k)}} = (k+1)\,\mathsf{Le}_{2n+2}^{(k)} - 2k\,\mathsf{Le}_{n+2}^{(k)} + k\,(k+1)$

v. $\hat{\mathsf{Le}}_{n+1}^{(k)} \overline{\hat{\mathsf{Le}}_{n+1}^{(k)}} - \hat{\mathsf{Le}}_{n-1}^{(k)} \overline{\hat{\mathsf{Le}}_{n-1}^{(k)}} = (k+1)\,\mathsf{Le}_{2n+1}^{(k)} - 2k\,\mathsf{Le}_n^{(k)} - k\,(k-1)$

Proof.
Let $\hat{\mathsf{Le}}_n^{(k)}$ be the n-th $k-$generalized Leonardo-like dual quaternion.

iv. Using Equation 3 and the Binet's formula of the Fibonacci sequence in Equation 1,

$$\begin{aligned}\hat{\mathsf{Le}}_n^{(k)}\overline{\hat{\mathsf{Le}}_n^{(k)}}+\hat{\mathsf{Le}}_{n+1}^{(k)}\overline{\hat{\mathsf{Le}}_{n+1}^{(k)}} &= \left(\mathsf{Le}_n^{(k)}\right)^2+\left(\mathsf{Le}_{n+1}^{(k)}\right)^2\\ &= \left((k+1)F_{n+1}-k\right)^2+\left((k+1)F_{n+2}-k\right)^2\\ &= (k+1)^2\left(F_{n+1}^2+F_{n+2}^2\right)-2k(k+1)\left(F_{n+1}+F_{n+2}\right)+2k^2\\ &= (k+1)^2F_{2n+3}-2k(k+1)F_{n+3}+2k^2\\ &= (k+1)\left((k+1)F_{2n+3}-k\right)+k(k+1)-2k\left((k+1)F_{n+3}-k\right)\\ &= (k+1)\,\mathsf{Le}_{2n+2}^{(k)}-2k\,\mathsf{Le}_{n+2}^{(k)}+k(k+1)\end{aligned}$$

is obtained.

v. Applying Equation 3 and the Binet's formula of the Fibonacci sequence in Equation 1,

$$\begin{aligned}\hat{\mathsf{Le}}_{n+1}^{(k)}\overline{\hat{\mathsf{Le}}_{n+1}^{(k)}}-\hat{\mathsf{Le}}_{n-1}^{(k)}\overline{\hat{\mathsf{Le}}_{n-1}^{(k)}} &= \left(\mathsf{Le}_{n+1}^{(k)}\right)^2-\left(\mathsf{Le}_{n-1}^{(k)}\right)^2\\ &= \left((k+1)F_{n+2}-k\right)^2-\left((k+1)F_n-k\right)^2\\ &= (k+1)^2\left(F_{n+2}^2-F_n^2\right)+2k(k+1)\left(F_n-F_{n+2}\right)\\ &= (k+1)\left((k+1)F_{2n+2}-k\right)+k(k+1)-2k\left((k+1)F_{n+1}-k\right)-2k^2\\ &= (k+1)\,\mathsf{Le}_{2n+1}^{(k)}-2k\,\mathsf{Le}_n^{(k)}-k(k-1)\end{aligned}$$

is obtained.

□

Theorem 2.8. Let $\hat{\mathsf{Le}}_n^{(k)}$ be the n-th $k-$generalized Leonardo-like dual quaternion. For $n\geq 2$, the generating function $\mathsf{G}(x)=\sum_{n=0}^{\infty}\hat{\mathsf{Le}}_n^{(k)}$ is as follows:

$$\begin{aligned}\mathsf{G}(x) &= \frac{\hat{\mathsf{Le}}_0^{(k)}+\left(\hat{\mathsf{Le}}_1^{(k)}-2\hat{\mathsf{Le}}_0^{(k)}\right)x+\left(\hat{\mathsf{Le}}_2^{(k)}-2\hat{\mathsf{Le}}_1^{(k)}\right)x^2}{1-2x+x^3}\\ &= \frac{\left(1-x+kx^2\right)+\left(1+kx-x^2\right)e_1+\left(2+k-x+x^2\right)e_2+\left(3+2k-x+\left(-2-k\right)x^2\right)\,e_3}{1-2x+x^3}\end{aligned}$$

where $1-2x+x^3\neq 0$.

Proof.
The proof is similar to the proof of the generating function of the Leonardo sequence in [2]. □

Theorem 2.9. For $n\geq 0$, the following summation formulas are satisfied:

i. $\sum_{s=0}^{n}\hat{\mathsf{Le}}_s^{(k)}=\hat{\mathsf{Le}}_{n+2}^{(k)}-\hat{\mathcal{K}}(n+2)+(k-1)-2e_1+(-k-3)e_2+(-5-3k)e_3$

ii. $\sum_{s=0}^{n}\hat{\mathsf{Le}}_{2s}^{(k)}=\hat{\mathsf{Le}}_{2n+1}^{(k)}-\hat{\mathcal{K}}n-(2k)e_1+(-k-1)e_2+(-3k-1)e_3$

iii. $\sum_{s=0}^{n}\hat{\mathsf{Le}}_{2s+1}^{(k)}=\hat{\mathsf{Le}}_{2n+2}^{(k)}-\hat{\mathcal{K}}n-(2k)+(-k-1)e_1+(-3k-1)e_2+(-3k-3)e_3$

Proof.
Let $n\geq 0$.

i. Using Equations 4 and 8,

$$\begin{aligned}\sum_{s=0}^{n}\hat{\mathsf{Le}}_s^{(k)} &= \sum_{s=0}^{n}\mathsf{Le}_s^{(k)} + \left(\sum_{s=0}^{n}\mathsf{Le}_{s+1}^{(k)}\right)e_1 + \left(\sum_{s=0}^{n}\mathsf{Le}_{s+2}^{(k)}\right)e_2 + \left(\sum_{s=0}^{n}\mathsf{Le}_{s+3}^{(k)}\right)e_3\\ &= \left(\mathsf{Le}_{n+2}^{(k)} - k(n+1) - 1\right) + \left(\sum_{s=0}^{n+1}\mathsf{Le}_s^{(k)} - \mathsf{Le}_0^{(k)}\right)e_1 + \left(\sum_{s=0}^{n+2}\mathsf{Le}_s^{(k)} - \mathsf{Le}_0^{(k)} - \mathsf{Le}_1^{(k)}\right)e_2\\ &\quad + \left(\sum_{s=0}^{n+3}\mathsf{Le}_s^{(k)} - \mathsf{Le}_0^{(k)} - \mathsf{Le}_1^{(k)} - \mathsf{Le}_2^{(k)}\right)e_3\\ &= \left(\mathsf{Le}_{n+2}^{(k)} - k(n+1) - 1\right) + \left(\mathsf{Le}_{n+3}^{(k)} - k(n+2) - 1 - 1\right)e_1\\ &\quad + \left(\mathsf{Le}_{n+4}^{(k)} - k(n+3) - 1 - 1 - 1\right)e_2 + \left(\mathsf{Le}_{n+5}^{(k)} - k(n+4) - 1 - 1 - 1 - (2+k)\right)e_3\\ &= \hat{\mathsf{Le}}_{n+2}^{(k)} - \hat{\mathcal{K}}(n+2) + (k-1) - 2e_1 + (-k-3)e_2 + (-5-3k)e_3\end{aligned}$$

ii. Using Equations 5, 6, and 8,

$$\begin{aligned}\sum_{s=0}^{n}\hat{\mathsf{Le}}_{2s}^{(k)} &= \sum_{s=0}^{n}\mathsf{Le}_{2s}^{(k)} + \left(\sum_{s=0}^{n}\mathsf{Le}_{2s+1}^{(k)}\right)e_1 + \left(\sum_{s=0}^{n}\mathsf{Le}_{2s+2}^{(k)}\right)e_2 + \left(\sum_{s=0}^{n}\mathsf{Le}_{2s+3}^{(k)}\right)e_3\\ &= \left(\mathsf{Le}_{2n+1}^{(k)} - kn\right) + \left(\mathsf{Le}_{2n+2}^{(k)} - k(n+2)\right)e_1 + \left(\sum_{s=0}^{n+1}\mathsf{Le}_{2s}^{(k)} - \mathsf{Le}_0^{(k)}\right)e_2 + \left(\sum_{s=0}^{n+1}\mathsf{Le}_{2s+1}^{(k)} - \mathsf{Le}_1^{(k)}\right)e_3\\ &= \left(\mathsf{Le}_{2n+1}^{(k)} - kn\right) + \left(\mathsf{Le}_{2n+2}^{(k)} - k(n+2)\right)e_1 + \left(\mathsf{Le}_{2n+3}^{(k)} - k(n+1) - 1\right)e_2\\ &\quad + \left(\mathsf{Le}_{2n+4}^{(k)} - k(n+3) - 1\right)e_3\\ &= \hat{\mathsf{Le}}_{2n+1}^{(k)} - \hat{\mathcal{K}}n + (-2k)e_1 + (-k-1)e_2 + (-3k-1)e_3\end{aligned}$$

□

Theorem 2.10 (The Honsberger-like identity)**.** Let $\hat{\mathsf{Le}}_n^{(k)}$ be the n-th $k-$generalized Leonardo-like dual quaternion. For positive integers n and m,

$$\begin{aligned}\hat{\mathsf{Le}}_n^{(k)}\hat{\mathsf{Le}}_m^{(k)} + \hat{\mathsf{Le}}_{n+1}^{(k)}\hat{\mathsf{Le}}_{m+1}^{(k)} &= (k+1)\left(2\hat{\mathsf{Le}}_{n+m+2}^{(k)} + k\right) - k\,\hat{\mathsf{Le}}_{n+2}^{(k)} - k\,\hat{\mathsf{Le}}_{m+2}^{(k)} - (k+1)\,\mathsf{Le}_{n+m+2}^{(k)}\\ &\quad - (e_1+e_2+e_3)\left(k\,\mathsf{Le}_{n+2}^{(k)} + k\,\mathsf{Le}_{m+2}^{(k)} - 2k(k+1)\right)\end{aligned}$$

where $\mathsf{Le}_n^{(k)}$ is the n-th $k-$generalized Leonardo number.

Proof.
Let $\hat{\mathsf{Le}}_n^{(k)}$ be the n-th $k-$generalized Leonardo-like dual quaternion and n and m be positive integers. Then,

$$\begin{aligned}\hat{\mathsf{Le}}_n^{(k)}\hat{\mathsf{Le}}_m^{(k)} + \hat{\mathsf{Le}}_{n+1}^{(k)}\hat{\mathsf{Le}}_{m+1}^{(k)} &= \left(\mathsf{Le}_n^{(k)}\,\mathsf{Le}_m^{(k)} + \mathsf{Le}_{n+1}^{(k)}\,\mathsf{Le}_{m+1}^{(k)}\right)\\ &\quad + \left(\left(\mathsf{Le}_n^{(k)}\,\mathsf{Le}_{m+1}^{(k)} + \mathsf{Le}_{n+1}^{(k)}\,\mathsf{Le}_{m+2}^{(k)}\right) + \left(\mathsf{Le}_{n+1}^{(k)}\,\mathsf{Le}_m^{(k)} + \mathsf{Le}_{n+2}^{(k)}\,\mathsf{Le}_{m+1}^{(k)}\right)\right)e_1\\ &\quad + \left(\left(\mathsf{Le}_n^{(k)}\,\mathsf{Le}_{m+2}^{(k)} + \mathsf{Le}_{n+1}^{(k)}\,\mathsf{Le}_{m+3}^{(k)}\right) + \left(\mathsf{Le}_{n+2}^{(k)}\,\mathsf{Le}_m^{(k)} + \mathsf{Le}_{n+3}^{(k)}\,\mathsf{Le}_{m+1}^{(k)}\right)\right)e_2\\ &\quad + \left(\left(\mathsf{Le}_n^{(k)}\,\mathsf{Le}_{m+3}^{(k)} + \mathsf{Le}_{n+1}^{(k)}\,\mathsf{Le}_{m+4}^{(k)}\right) + \left(\mathsf{Le}_{n+3}^{(k)}\,\mathsf{Le}_m^{(k)} + \mathsf{Le}_{n+4}^{(k)}\,\mathsf{Le}_{m+1}^{(k)}\right)\right)e_3\end{aligned}$$

We conclude from Equation 3 and $F_nF_m + F_{n+1}F_{m+1} = F_{n+m+1}$ [1] that

$$\hat{\mathsf{Le}}_n^{(k)}\hat{\mathsf{Le}}_m^{(k)} + \hat{\mathsf{Le}}_{n+1}^{(k)}\hat{\mathsf{Le}}_{m+1}^{(k)} = (k+1)^2\left(2\hat{\mathcal{F}}_{n+m+3} - F_{n+m+3}\right) - k(k+1)(F_{n+3}+F_{m+3})(e_1+e_2+e_3)$$
$$-k(k+1)\left(\hat{\mathcal{F}}_{m+3}+\hat{\mathcal{F}}_{n+3}\right) + 4k^2(1+e_1+e_2+e_3) - 2k^2$$

Then, applying Theorem 2.5(i),

$$\hat{\mathsf{Le}}_n^{(k)}\hat{\mathsf{Le}}_m^{(k)} + \hat{\mathsf{Le}}_{n+1}^{(k)}\hat{\mathsf{Le}}_{m+1}^{(k)} = (k+1)\left(2\hat{\mathsf{Le}}_{n+m+2}^{(k)} + k\right) - k\,\hat{\mathsf{Le}}_{n+2}^{(k)} - k\,\hat{\mathsf{Le}}_{m+2}^{(k)} - (k+1)\,\mathsf{Le}_{n+m+2}^{(k)}$$
$$-(e_1+e_2+e_3)\left(k\,\mathsf{Le}_{n+2}^{(k)} + k\,\mathsf{Le}_{m+2}^{(k)} - 2k(k+1)\right)$$

is obtained. □

Across this study, let $\alpha^*\beta^* = 1 + e_1 + 3e_2 + 4e_3$.

Theorem 2.11 (The Catalan-like identity)**.** Let $\hat{\mathsf{Le}}_n^{(k)}$ be the n-th $k-$generalized Leonardo-like dual quaternion. For positive integers n and r with $n \geq r$,

$$\left(\hat{\mathsf{Le}}_n^{(k)}\right)^2 - \hat{\mathsf{Le}}_{n+r}^{(k)}\hat{\mathsf{Le}}_{n-r}^{(k)} = (k+1)^2\,\alpha^*\beta^*\,(-1)^{n-r+1}\,(F_r)^2 - \hat{\mathcal{K}}\left(2\hat{\mathsf{Le}}_n^{(k)} - \hat{\mathsf{Le}}_{n+r}^{(k)} - \hat{\mathsf{Le}}_{n-r}^{(k)}\right)$$

where F_n is the n-th Fibonacci number.

Proof.
By using the Binet-like formula in Equation 9,

$$\left(\hat{\mathsf{Le}}_n^{(k)}\right)^2 - \hat{\mathsf{Le}}_{n+r}^{(k)}\hat{\mathsf{Le}}_{n-r}^{(k)} = \left((k+1)\left(\frac{\alpha^*\alpha^{n+1} - \beta^*\beta^{n+1}}{\alpha-\beta}\right) - \hat{\mathcal{K}}\right)^2$$
$$-\left((k+1)\left(\frac{\alpha^*\alpha^{n+r+1} - \beta^*\beta^{n+r+1}}{\alpha-\beta}\right) - \hat{\mathcal{K}}\right)\left((k+1)\left(\frac{\alpha^*\alpha^{n-r+1} - \beta^*\beta^{n-r+1}}{\alpha-\beta}\right) - \hat{\mathcal{K}}\right)$$
$$= \frac{(k+1)^2}{5}\,\alpha^*\beta^*\left(\alpha^{n-r+1}\beta^{n-r+1}\right)\left(\alpha^{2r} + \beta^{2r} - 2\alpha^r\beta^r\right)$$
$$-\hat{\mathcal{K}}\left(2\left(\hat{\mathsf{Le}}_n^{(k)} + \hat{\mathcal{K}}\right) - \left(\hat{\mathsf{Le}}_{n+r}^{(k)} + \hat{\mathcal{K}}\right) - \left(\hat{\mathsf{Le}}_{n-r}^{(k)} + \hat{\mathcal{K}}\right)\right)$$
$$= (k+1)^2\,\alpha^*\beta^*\,(-1)^{n-r+1}\,(F_r)^2 - \hat{\mathcal{K}}\left(2\hat{\mathsf{Le}}_n^{(k)} - \hat{\mathsf{Le}}_{n+r}^{(k)} - \hat{\mathsf{Le}}_{n-r}^{(k)}\right)$$

□

Theorem 2.12 (The Cassini-like identity)**.** Let $\hat{\mathsf{Le}}_n^{(k)}$ be the n-th $k-$generalized Leonardo-like dual quaternion. For positive integer n with $n \geq 3$,

$$\hat{\mathsf{Le}}_{n-1}^{(k)}\hat{\mathsf{Le}}_{n+1}^{(k)} - \left(\hat{\mathsf{Le}}_n^{(k)}\right)^2 = (k+1)^2\,(-1)^{n+1}\,\alpha^*\beta^* - \hat{\mathcal{K}}\,\hat{\mathsf{Le}}_{n-3}^{(k)} - \hat{\mathcal{K}}^2$$

Proof.
From the Cassini identity and the recurrence relation of the Fibonacci dual quaternion sequence (see [20]),

$$\hat{\mathsf{Le}}_{n-1}^{(k)}\hat{\mathsf{Le}}_{n+1}^{(k)} - \left(\hat{\mathsf{Le}}_n^{(k)}\right)^2 = \left((k+1)\,\hat{\mathcal{F}}_n - \hat{\mathcal{K}}\right)\left((k+1)\,\hat{\mathcal{F}}_{n+2} - \hat{\mathcal{K}}\right) - \left((k+1)\,\hat{\mathcal{F}}_{n+1} - \hat{\mathcal{K}}\right)^2$$
$$= ((k+1))^2\left(\hat{\mathcal{F}}_n\,\hat{\mathcal{F}}_{n+2} - \left(\hat{\mathcal{F}}_{n+1}\right)^2\right) - \hat{\mathcal{K}}\,(k+1)\left(\hat{\mathcal{F}}_n + \hat{\mathcal{F}}_{n+2} - 2\hat{\mathcal{F}}_{n+1}\right)$$
$$= (k+1)^2\,(-1)^{n+1}\,(1+e_1+3e_2+4e_3) - \hat{\mathcal{K}}\,(k+1)\left(\left(\hat{\mathcal{F}}_{n+2} - \hat{\mathcal{F}}_{n+1}\right) - \left(\hat{\mathcal{F}}_{n+1} - \hat{\mathcal{F}}_n\right)\right)$$
$$= (k+1)^2\,(-1)^{n+1}\,(1+e_1+3e_2+4e_3) - \hat{\mathcal{K}}\left((k+1)\,\hat{\mathcal{F}}_{n-2} - \hat{\mathcal{K}}\right) - \hat{\mathcal{K}}^2$$
$$= (k+1)^2\,(-1)^{n+1}\,(1+e_1+3e_2+4e_3) - \hat{\mathcal{K}}\,\hat{\mathsf{Le}}_{n-3}^{(k)} - \hat{\mathcal{K}}^2$$

□

Theorem 2.13 (The d'Ocagne-like identity)**.** Let $\hat{\mathsf{Le}}_n^{(k)}$ be the n-th $k-$generalized Leonardo-like dual quaternion. For positive integers m and n,

$$\hat{\mathsf{Le}}_m^{(k)}\hat{\mathsf{Le}}_{n+1}^{(k)} - \hat{\mathsf{Le}}_{m+1}^{(k)}\hat{\mathsf{Le}}_n^{(k)} = (k+1)^2\,\alpha^*\beta^*\,(-1)^{n+1}\,F_{m-n} + \hat{\mathcal{K}}\left(\hat{\mathsf{Le}}_{m-1}^{(k)} - \hat{\mathsf{Le}}_{n-1}^{(k)}\right)$$

where F_n is the n-th Fibonacci number.

Proof.
Applying the Binet-like formula in Equation 9,

$$\begin{aligned}
\hat{\mathsf{Le}}_m^{(k)}\hat{\mathsf{Le}}_{n+1}^{(k)} - \hat{\mathsf{Le}}_{m+1}^{(k)}\hat{\mathsf{Le}}_n^{(k)} &= \left((k+1)\left(\frac{\alpha^*\alpha^{m+1} - \beta^*\beta^{m+1}}{\alpha-\beta}\right) - \hat{\mathcal{K}}\right)\left((k+1)\left(\frac{\alpha^*\alpha^{n+2} - \beta^*\beta^{n+2}}{\alpha-\beta}\right) - \hat{\mathcal{K}}\right) \\
&\quad - \left((k+1)\left(\frac{\alpha^*\alpha^{m+2} - \beta^*\beta^{m+2}}{\alpha-\beta}\right) - \hat{\mathcal{K}}\right)\left((k+1)\left(\frac{\alpha^*\alpha^{n+1} - \beta^*\beta^{n+1}}{\alpha-\beta}\right) - \hat{\mathcal{K}}\right) \\
&= \frac{(k+1)^2}{\alpha-\beta}\,\alpha^*\beta^*\left(\alpha^{m+1}\beta^{n+1} - \alpha^{n+1}\beta^{m+1}\right) \\
&\quad -\hat{\mathcal{K}}\left(\left(\hat{\mathsf{Le}}_m^{(k)} + \hat{\mathcal{K}}\right) + \left(\hat{\mathsf{Le}}_{n+1}^{(k)} + \hat{\mathcal{K}}\right) - \left(\hat{\mathsf{Le}}_{m+1}^{(k)} + \hat{\mathcal{K}}\right) - \left(\hat{\mathsf{Le}}_n^{(k)} + \hat{\mathcal{K}}\right)\right) \\
&= (k+1)^2\,\alpha^*\beta^*\alpha^{n+1}\beta^{n+1}\frac{(\alpha^{m-n} - \beta^{m-n})}{\alpha-\beta} + \hat{\mathcal{K}}\left(\left(\hat{\mathsf{Le}}_{m+1}^{(k)} - \hat{\mathsf{Le}}_m^{(k)}\right) - \left(\hat{\mathsf{Le}}_{n+1}^{(k)} - \hat{\mathsf{Le}}_n^{(k)}\right)\right) \\
&= (k+1)^2\,\alpha^*\beta^*\,(-1)^{n+1}\,F_{m-n} + \hat{\mathcal{K}}\left(\hat{\mathsf{Le}}_{m-1}^{(k)} - \hat{\mathsf{Le}}_{n-1}^{(k)}\right)
\end{aligned}$$

□

Theorem 2.14 (The Tagiuri-like identity)**.** Let $\hat{\mathsf{Le}}_n^{(k)}$ be the n-th $k-$generalized Leonardo-like dual quaternion. For positive integers $n, n+r$ and $n+s$,

$$\hat{\mathsf{Le}}_{n+r}^{(k)}\hat{\mathsf{Le}}_{n+s}^{(k)} - \hat{\mathsf{Le}}_n^{(k)}\hat{\mathsf{Le}}_{n+r+s}^{(k)} = \frac{(k+1)^2}{5}\alpha^*\beta^*(-1)^{n+1}(L_{r+s} - (-1)^s L_{r-s}) + \hat{\mathcal{K}}(\hat{\mathsf{Le}}_n^{(k)} + \hat{\mathsf{Le}}_{n+r+s}^{(k)} - \hat{\mathsf{Le}}_{n+r}^{(k)} - \hat{\mathsf{Le}}_{n+s}^{(k)})$$

where L_n is the n-th Lucas number.

Proof.
The proof is straightforward from applying the Binet-like formula in Equation 9. □

Note that the d'Ocagne-like, Catalan-like, and Cassini-like identities are the special cases of the Tagiuri-like identity.

3. Conclusion

Taking $k = 1$ gives the analogous relations for the Leonardo sequence with the dual-quaternions coefficients. Hence, we can say that our main results presented here generalize the paper [13]. These results can trigger further research on the subjects of the Leonardo sequence and the dual quaternions. Additionally, this study opens the door for future research on sequences; for instance, one may define non-commutative quaternions (real, split, semi-split, etc.) with the $k-$generalized Leonardo sequence.

Author Contributions

All the authors equally contributed to this work. They all read and approved the final version of the paper.

Conflicts of Interest

All the authors declare no conflict of interest.

References

[1] T. Koshy, Fibonacci and Lucas Numbers with Applications, John Wiley & Sons, New York, 2001.

[2] P. Catarino, A. Borges, *On Leonardo Numbers*, Acta Mathematica Universitatis Comenianae 89 (1) (2020) 75–86.

[3] E. W. Dijkstra, *Fibonacci Numbers and Leonardo Numbers* (1981), https://www.cs.utexas.edu/users/EWD/transcriptions/EWD07xx/EWD797.html, Accessed 10 July 2023.

[4] K. Kuhapatanakul, J. Chobsorn, *On the Generalized Leonardo Numbers*, Integers (22) (2022) Article ID A48 7 pages.

[5] P. Catarino, A. Borges, *A Note on Incomplete Leonardo Numbers*, Integers (20) (2020) Article ID A43 7 pages.

[6] Y. Alp, E. G. Koçer, *Hybrid Leonardo Numbers*, Chaos, Solitons & Fractals (150) (2021) Article ID 111128 5 pages.

[7] Y. Alp, E. G. Koçer, *Some Properties of Leonardo Numbers*, Konuralp Journal of Mathematics 9 (1) (2021) 183–189.

[8] A. Shannon, Ö. Deveci, *A Note on Generalized and Extended Leonardo Sequences*, Notes on Number Theory and Discrete Mathematics 28 (1) (2022) 109–114.

[9] A. Karataş, *On Complex Leonardo Numbers*, Notes on Number Theory and Discrete Mathematics 28 (3) (2022) 458–465.

[10] S. Ö. Karakuş, S. K. Nurkan, M. Turan, *Hyper-Dual Leonardo Numbers*, Konuralp Journal of Mathematics 10 (2) (2022) 269–275.

[11] M. Shattuck, *Combinatorial Proofs of Identities for the Generalized Leonardo Numbers*, Notes on Number Theory and Discrete Mathematics 28 (4) (2022) 778–790.

[12] Y. Soykan, *Special Cases of Generalized Leonardo Numbers: Modified p-Leonardo, p-Leonardo-Lucas and p-Leonardo Numbers*, Earthline Journal of Mathematical Sciences 11 (2) (2023) 317–342.

[13] S. K. Nurkan, İ. A. Güven, *Ordered Leonardo Quadruple Numbers*, Symmetry 15 (1) (2023) Article ID 149 15 pages.

[14] E. Tan, H. H. Leung, *On Leonardo p-Numbers*, Integers (23) (2023) Article ID A7 11 pages.

[15] O. Dişkaya, H. Menken, P. M. M. C. Catarino, *On the Hyperbolic Leonardo and Hyperbolic Francois Quaternions*, Journal of New Theory (42) (2023) 74–85.

[16] A. F. Horadam, *Complex Fibonacci Numbers and Fibonacci Quaternions*, American Mathematical Monthly (70) (1963) 289–291.

[17] W. R. Hamilton, Elements of Quaternions, Chelsea Publishing Company, New York, 1969.

[18] W. R. Hamilton, Lectures on Quaternions, Hodges and Smith, Dublin, 1853.

[19] W. R. Hamilton, *On Quaternions; or On a New System of Imaginaries in Algebra*, The London, Edinburgh and Dublin Philosophical Magazine and Journal of Science (3rd Series), xxv-xxxvi, (1844–1850), https://www.emis.de/classics/Hamilton/OnQuat.pdf, Accessed 10 July 2023.

[20] S. Yüce, F. T. Aydın, *A New Aspect of Dual Fibonacci Quaternions*, Advances in Applied Clifford Algebras (26) (2016) 873–884.

[21] W. K. Clifford, *Preliminary Sketch of Bi-Quaternions*, Proceedings of the London Mathematical Society s1–4 (1) (1873) 381–395.

[22] J. D. Jr. Edmonds, Relativistic Reality: A Modern View, World Scientific, Singapore, 1997.

[23] Z. Ercan, S. Yüce, *On Properties of the Dual Quaternions*, European Journal of Pure and Applied Mathematics 4 (2) (2011) 142–146.

[24] V. Majernik, *Quaternion Formulation of the Galilean Space-Time Transformation*, Acta Physica Slovaca 56 (1) (2006) 9–14.

[25] V. Majernik, M. Nagy, *Quaternionic Form of Maxwell's Equations with Sources*, Lettere al Nuovo Cimento (16) (1976) 165–169.

[26] V. Majernik, *Galilean Transformation Expressed by the Dual Four-Component Numbers*, Acta Physica Polonica A (87) (1995) 919–923.

[27] Y. Yaylı, E. E. Tutuncu, *Generalized Galilean Transformations and Dual Quaternions*, Scientia Magna 5 (1) (2009) 94–100.

Journal of New Theory
ISSN: 2149-1402

44 (2023) 43-51
Journal of New Theory
https://dergipark.org.tr/en/pub/jnt
Open Access

Inverse Problems for a Conformable Fractional Diffusion Operator

Yaşar Çakmak[1]

Article Info
Received: 1 Aug 2023
Accepted: 25 Sep 2023
Published: 30 Sep 2023
doi:10.53570/jnt.1335702
Research Article

Abstract — In this paper, we consider a diffusion operator with discrete boundary conditions, which include the conformable fractional derivatives of order α such that $0 < \alpha \leq 1$ instead of the ordinary derivatives in the classical diffusion operator. We prove that the coefficients of the given operator are uniquely determined by the Weyl function and spectral data, which consist of a spectrum and normalizing numbers. Moreover, using the well-known Hadamard's factorization theorem, we prove that the characteristic function $\Delta_\alpha(\rho)$ is determined by the specification of its zeros for each fixed α. The obtained results in this paper can be regarded as partial α-generalizations of similar findings obtained for the classical diffusion operator.

Keywords *Inverse problem, diffusion operator, conformable fractional derivative, Weyl function, spectral data*

Mathematics Subject Classification (2020) 34A55, 26A33

1. Introduction

Inverse spectral problems aim to reconstruct the coefficients of an operator from given data such as the Weyl function, nodal points, and spectral data (two spectra or a spectrum and normalizing numbers). For the last century, these kinds of problems for various classical Sturm-Liouville, diffusion, and Dirac operators have been extensively investigated; for more details, see [1–7].

The beginning of the fractional derivative dates back to 1695, and many fractional derivative concepts have been proposed until today, such as the Riemann-Liouville fractional derivative, the Caputo fractional derivative, and the Atangana fractional derivative. In 2014, Khalil et al. [8] introduced the conformable fractional derivative. Then, many researchers identified important and fundamental properties of this derivative in [9–14]. In 2017, Jarad et al. [15] showed that this derivative is necessary and useful for generating new types of fractional operators. In recent years, numerous significant studies [16–20] have been conducted on inverse problems related to various conformable fractional operators, including the diffusion operator.

We consider a conformable fractional diffusion operator with discrete boundary conditions, denoted as $L_\alpha = L_\alpha(p(x), q(x), h, H)$. The form of this operator is as follows:

$$\ell_\alpha y := -T_x^\alpha T_x^\alpha y + [2\rho p(x) + q(x)]\, y = \rho^2 y, \quad 0 < x < \pi \tag{1}$$

$$U_\alpha(y) := T_x^\alpha y(0) - h y(0) = 0$$

[1]ycakmak@cumhuriyet.edu.tr(Corresponding Author)
[1]Department of Mathematics, Faculty of Science, Sivas Cumhuriyet University, Sivas, Türkiye

and

$$V_\alpha(y) := T_x^\alpha y(\pi) + Hy(\pi) = 0$$

where ρ is the spectral parameter, $h, H \in \mathbb{R}$, $q(x) \in W_{2,\alpha}^1[0,\pi]$ and $p(x) \in W_{2,\alpha}^2[0,\pi]$ are real-valued functions such that $p(x) \neq const$, $T_x^\alpha y$ is a conformable fractional derivative of order $\alpha \in (0,1]$ of y at x,

$$T_x^\alpha y(x) = \lim_{h\to 0} \frac{y(x + hx^{1-\alpha}) - y(x)}{h}, \quad \text{for all } x > 0$$

$$W_{2,\alpha}^1[0,\pi] = \{f(x) \mid f(x) \text{ is absolutely continuous on } [0,\pi] \text{ and } T_x^\alpha f(x) \in L_{2,\alpha}(0,\pi)\}$$

$$W_{2,\alpha}^2[0,\pi] = \{f(x) \mid f(x) \text{ and } T_x^\alpha f(x) \text{ are absolutely continuous on } [0,\pi] \text{ and } T_x^\alpha T_x^\alpha f(x) \in L_{2,\alpha}(0,\pi)\}$$

and the space $L_{2,\alpha}(0,\pi)$ consists of all the functions $f : [0,\pi] \to \mathbb{R}$ satisfying the condition

$$\left(\int_0^\pi |f(x)|^2 \, d_\alpha x\right)^{1/2} = \left(\int_0^\pi |f(x)|^2 \, x^{\alpha-1} dx\right)^{1/2} < \infty$$

This operator is referred to as the Conformable Fractional Diffusion Operator (CFDO).

In this paper, we have proved that the coefficients of the given operator can be uniquely determined by the Weyl function and spectral data, which consist of a spectrum and normalizing numbers.

2. Preliminaries

This section provides some basic notions to be needed in the following sections. Let the functions $\varphi = \varphi(x,\rho;\alpha)$, $\psi = \psi(x,\rho;\alpha)$, and $S = S(x,\rho;\alpha)$ be the solutions of Equation 1 satisfying the following initial conditions

$$\varphi(0,\rho;\alpha) = 1 \quad \text{and} \quad T_x^\alpha \varphi(0,\rho;\alpha) = h \tag{2}$$

$$\psi(\pi,\rho;\alpha) = 1 \quad \text{and} \quad T_x^\alpha \psi(\pi,\rho;\alpha) = -H \tag{3}$$

$$S(0,\rho;\alpha) = 0 \quad \text{and} \quad T_x^\alpha S(0,\rho;\alpha) = 1 \tag{4}$$

respectively. From [19, 21, 22], these solutions satisfy the following asymptotic formulas, for $|\rho| \to \infty$ and each fixed α,

$$\varphi = \cos\left(\frac{\rho x^\alpha}{\alpha} - \theta(x)\right) + O\left(\frac{1}{|\rho|}\exp\left(\frac{|\mathrm{Im}\rho|\, x^\alpha}{\alpha}\right)\right) \tag{5}$$

$$T_x^\alpha \varphi = -\rho \sin\left(\frac{\rho x^\alpha}{\alpha} - \theta(x)\right) + O\left(\exp\left(\frac{|\mathrm{Im}\rho|\, x^\alpha}{\alpha}\right)\right) \tag{6}$$

$$\psi = \cos\left(\frac{\rho(\pi^\alpha - x^\alpha)}{\alpha} - \theta(\pi) + \theta(x)\right) + O\left(\frac{1}{|\rho|}\exp\left(\frac{|\mathrm{Im}\rho|(\pi^\alpha - x^\alpha)}{\alpha}\right)\right) \tag{7}$$

$$T_x^\alpha \psi = \rho \sin\left(\frac{\rho(\pi^\alpha - x^\alpha)}{\alpha} - \theta(\pi) + \theta(x)\right) + O\left(\exp\left(\frac{|\mathrm{Im}\rho|(\pi^\alpha - x^\alpha)}{\alpha}\right)\right) \tag{8}$$

$$S = \frac{1}{\rho}\sin\left(\frac{\rho x^\alpha}{\alpha} - \theta(x)\right) + O\left(\frac{1}{\rho^2}\exp\left(\frac{|\mathrm{Im}\rho|\, x^\alpha}{\alpha}\right)\right) \tag{9}$$

$$T_x^\alpha S = \cos\left(\frac{\rho x^\alpha}{\alpha} - \theta(x)\right) + O\left(\frac{1}{\rho}\exp\left(\frac{|\mathrm{Im}\rho|\, x^\alpha}{\alpha}\right)\right) \tag{10}$$

where

$$\theta(x) = \int_0^x p(t)\, d_\alpha t$$

We denote

$$\Delta_\alpha(\rho) = W_\alpha[\psi,\varphi] = \begin{vmatrix} \psi & \varphi \\ T_x^\alpha\psi & T_x^\alpha\varphi \end{vmatrix} = \psi T_x^\alpha\varphi - \varphi T_x^\alpha\psi \tag{11}$$

where $W_\alpha[\psi,\varphi]$ is the fractional Wronskian of the functions ψ and φ. Furthermore, the $\Delta_\alpha(\rho)$ is called as the characteristic function of the operator L_α and is entire function in ρ for each fixed α.

Lemma 2.1. [23] For each fixed α, $\Delta_\alpha(\rho)$ does not depend on x and can be written as

$$\Delta_\alpha(\rho) = V_\alpha(\varphi) = -U_\alpha(\psi) \tag{12}$$

Lemma 2.2. [23] The zeros $\{\rho_n\}$ of the function $\Delta_\alpha(\rho)$ are coincide with the eigenvalues of the operator L_α, and for eigenfunctions $\psi(x,\rho_n;\alpha)$ and $\varphi(x,\rho_n;\alpha)$, there exists a sequence $\{\beta_n\}$ such that

$$\psi(x,\rho_n;\alpha) = \beta_n\varphi(x,\rho_n;\alpha) \quad \text{and} \quad \beta_n \neq 0 \tag{13}$$

are satisfied for each fixed α.

It is clear from Equations 2, 3, and 13 that $\beta_n = \psi(0,\rho_n;\alpha) = \frac{1}{\varphi(\pi,\rho_n;\alpha)}$.

Lemma 2.3. [23] The equality $\dot{\Delta}_\alpha(\rho_n) = -2\rho_n\beta_n\alpha_n$ is valid where $\dot{\Delta}_\alpha(\rho) = \dfrac{d\Delta_\alpha(\rho)}{d\rho}$ and the normalizing numbers are

$$\alpha_n = \int_0^\pi \varphi^2(x,\rho_n;\alpha)\,d_\alpha x - \frac{1}{\rho_n}\int_0^\pi p(x)\,\varphi^2(x,\rho_n;\alpha)\,d_\alpha x$$

Definition 2.4. The data $\{\rho_n,\alpha_n\}_{n\geq 1}$ are called the spectral data of the operator L_α.

Let $\{\rho_n\}$ be the eigenvalues set of the operator L_α. From [23], the numbers ρ_n hold the following estimate:

$$\rho_n = \frac{n\alpha}{\pi^{\alpha-1}} + c_{\alpha,0} + \frac{c_{\alpha,1}}{n} + o\left(\frac{1}{n}\right), \quad n\to\infty$$

where

$$c_{\alpha,0} = \frac{\alpha}{\pi^\alpha}\int_0^\pi p(x)d_\alpha x$$

and

$$c_{\alpha,1} = \frac{1}{\pi}\left[h + H + \frac{1}{2}\int_0^\pi \left(q(x) + p^2(x)\right)d_\alpha x\right]$$

Let $G_\delta = \left\{\rho \mid \left|\rho - \frac{n\alpha}{\pi^{\alpha-1}}\right| \geq \delta,\ n\in\{1,2,\ldots\}\right\}$ where δ is a sufficiently small positive number. It is obvious from Equations 5, 6, and 12 that the function $\Delta_\alpha(\rho)$ satisfies the inequality

$$|\Delta_\alpha(\rho)| \geq c_\delta|\rho|\exp\left(\frac{|\mathrm{Im}\rho|}{\alpha}\pi^\alpha\right), \quad \rho\in G_\delta \tag{14}$$

3. Main Results

This section proves uniqueness theorems for the solution of inverse problems according to the Weyl function and spectral data, which consist of a spectrum and normalizing numbers. Together with L_α, we consider a second operator $\widetilde{L}_\alpha = \widetilde{L}_\alpha(p(x),\widetilde{q}(x),\widetilde{h},\widetilde{H})$ of the following form

$$\widetilde{\ell}_\alpha y := -T_x^\alpha T_x^\alpha y + [2\rho p(x) + \widetilde{q}(x)]\,y = \rho^2 y, \quad 0<x<\pi$$

$$\widetilde{U}_\alpha(y) := T_x^\alpha y(0) - \widetilde{h}y(0) = 0$$

and

$$\widetilde{V}_\alpha(y) := T_x^\alpha y(\pi) + \widetilde{H} y(\pi) = 0$$

We note that if a certain symbol σ denotes an object related to L_α, then $\widetilde{\sigma}$ will denote an analogous object related to $\widetilde{L}_\alpha$.

It can be observed that $W_\alpha[\varphi, S]|_{x=0} = 1 \neq 0$. Thus, the functions φ and S are linearly independent, and the function ψ can be written as

$$\psi(x,\rho;\alpha) = c_1(\rho;\alpha)\,\varphi(x,\rho;\alpha) + c_2(\rho;\alpha)\,S(x,\rho;\alpha) \tag{15}$$

where $c_1(\rho;\alpha)$ and $c_2(\rho;\alpha)$ are arbitrary constant for each fixed α. It is clear from Equation 15 that

$$\psi(0,\rho;\alpha) = c_1(\rho;\alpha)\,\varphi(0,\rho;\alpha) + c_2(\rho;\alpha)\,S(0,\rho;\alpha)$$

and

$$T_x^\alpha \psi(0,\rho;\alpha) = c_1(\rho;\alpha)\,T_x^\alpha \varphi(0,\rho;\alpha) + c_2(\rho;\alpha)\,T_x^\alpha S(0,\rho;\alpha)$$

From Equations 2, 4, and 12,

$$c_1(\rho;\alpha) = \psi(0,\rho;\alpha)$$

and

$$c_2(\rho;\alpha) = T_x^\alpha \psi(0,\rho;\alpha) - h\psi(0,\rho;\alpha) = -\Delta_\alpha(\rho)$$

Consequently, Equation 15 is rewritten as

$$\psi(x,\rho;\alpha) = \psi(0,\rho;\alpha)\,\varphi(x,\rho;\alpha) - \Delta_\alpha(\rho)\,S(x,\rho;\alpha)$$

or

$$-\frac{\psi(x,\rho;\alpha)}{\Delta_\alpha(\rho)} = -\frac{\psi(0,\rho;\alpha)}{\Delta_\alpha(\rho)}\varphi(x,\rho;\alpha) + S(x,\rho;\alpha) \tag{16}$$

If we denote

$$\Phi(x,\rho;\alpha) := -\frac{\psi(x,\rho;\alpha)}{\Delta_\alpha(\rho)} \quad \text{and} \quad M_\alpha(\rho) := \Phi(0,\rho;\alpha) = -\frac{\psi(0,\rho;\alpha)}{\Delta_\alpha(\rho)} \tag{17}$$

then, from Equation 16,

$$\Phi(x,\rho;\alpha) = S(x,\rho;\alpha) + M_\alpha(\rho)\,\varphi(x,\rho;\alpha) \tag{18}$$

The functions $\Phi(x,\rho;\alpha)$ and $M_\alpha(\rho)$ are called as the Weyl solution and the Weyl function of the operator L_α, respectively. It is obvious that $\Phi(x,\rho;\alpha)$ is the solution of Equation 1 under the conditions $U_\alpha(\Phi) = 1$, $V_\alpha(\Phi) = 0$, and $M_\alpha(\rho)$ is a meromorphic function with poles in $\{\rho_n\}$.

Theorem 3.1. If $M_\alpha(\rho) = \widetilde{M}_\alpha(\rho)$ for each fixed α, then $q(x) = \widetilde{q}(x)$, almost everywhere in $[0,\pi]$, $h = \widetilde{h}$, and $H = \widetilde{H}$. Thus, the Weyl function uniquely determines the operator L_α.

Proof.
Consider the functions $P_1(x,\rho;\alpha)$ and $P_2(x,\rho;\alpha)$ defined by

$$P_1(x,\rho;\alpha) = \varphi(x,\rho;\alpha)\,T_x^\alpha \widetilde{\Phi}(x,\rho;\alpha) - \Phi(x,\rho;\alpha)\,T_x^\alpha \widetilde{\varphi}(x,\rho;\alpha) \tag{19}$$

and

$$P_2(x,\rho;\alpha) = \Phi(x,\rho;\alpha)\,\widetilde{\varphi}(x,\rho;\alpha) - \varphi(x,\rho;\alpha)\,\widetilde{\Phi}(x,\rho;\alpha) \tag{20}$$

From Equation 18,

$$P_1(x,\rho;\alpha) = \varphi(x,\rho;\alpha)\,T_x^\alpha \widetilde{S}(x,\rho;\alpha) - S(x,\rho;\alpha)\,T_x^\alpha \widetilde{\varphi}(x,\rho;\alpha) + \left[\widetilde{M}_\alpha(\rho) - M_\alpha(\rho)\right]\varphi(x,\rho;\alpha)\,T_x^\alpha \widetilde{\varphi}(x,\rho;\alpha)$$

and

$$P_2(x,\rho;\alpha) = S(x,\rho;\alpha)\,\widetilde{\varphi}(x,\rho;\alpha) - \varphi(x,\rho;\alpha)\,\widetilde{S}(x,\rho;\alpha) + \left[M_\alpha(\rho) - \widetilde{M}_\alpha(\rho)\right]\varphi(x,\rho;\alpha)\,\widetilde{\varphi}(x,\rho;\alpha)$$

Since $M_\alpha(\rho) = \widetilde{M}_\alpha(\rho)$, the functions $P_1(x,\rho;\alpha)$ and $P_2(x,\rho;\alpha)$ are entire in ρ, for each fixed α. Moreover, from Equations 11 and 17,

$$W_\alpha\left[\varphi(x,\rho;\alpha), \Phi(x,\rho;\alpha)\right] = -\frac{W_\alpha\left[\varphi(x,\rho;\alpha), \psi(x,\rho;\alpha)\right]}{\Delta_\alpha(\rho)} = 1$$

and similarly,

$$W_\alpha\left[\widetilde{\varphi}(x,\rho;\alpha), \widetilde{\Phi}(x,\rho;\alpha)\right] = 1$$

Thus, Equation 19 can be rewritten as

$$P_1(x,\rho;\alpha) = 1 + \varphi(x,\rho;\alpha)\left[T_x^\alpha\widetilde{\Phi}(x,\rho;\alpha) - T_x^\alpha\Phi(x,\rho;\alpha)\right] + \Phi(x,\rho;\alpha)\left[T_x^\alpha\varphi(x,\rho;\alpha) - T_x^\alpha\widetilde{\varphi}(x,\rho;\alpha)\right]$$

It follows from the asymptotic formulas of Equations 5-10 and Equality 14 that

$$|P_1(x,\rho;\alpha) - 1| \le \frac{C_\delta}{|\rho|} \quad \text{and} \quad |P_2(x,\rho;\alpha)| \le \frac{C_\delta}{|\rho|}, \quad x \in [0,\pi], \ \ |\rho| \in G_\delta$$

Therefore, since $\lim\limits_{|\rho|\to\infty} |P_1(x,\rho;\alpha) - 1| = \lim\limits_{|\rho|\to\infty} |P_2(x,\rho;\alpha)| = 0$ by the well-known Liouville's theorem, we obtain for $x \in [0,\pi]$ and each fixed α that

$$P_1(x,\rho;\alpha) = 1 \quad \text{and} \quad P_2(x,\rho;\alpha) = 0 \tag{21}$$

Hence, by using Equations 19-21, we get the following system

$$\begin{cases} \varphi(x,\rho;\alpha)\,T_x^\alpha\widetilde{\Phi}(x,\rho;\alpha) - \Phi(x,\rho;\alpha)\,T_x^\alpha\widetilde{\varphi}(x,\rho;\alpha) = 1 \\ \Phi(x,\rho;\alpha)\,\widetilde{\varphi}(x,\rho;\alpha) - \varphi(x,\rho;\alpha)\,\widetilde{\Phi}(x,\rho;\alpha) = 0 \end{cases} \tag{22}$$

If System 22 is solved according to functions $\varphi(x,\rho;\alpha)$ and $\Phi(x,\rho;\alpha)$, then

$$\varphi(x,\rho;\alpha) = \widetilde{\varphi}(x,\rho;\alpha)$$

and

$$\Phi(x,\rho;\alpha) = \widetilde{\Phi}(x,\rho;\alpha)$$

is obtained, for all x and ρ and each fixed α. Thus, $q(x) = \widetilde{q}(x)$, almost everywhere in $[0,\pi]$, $h = \widetilde{h}$, and $H = \widetilde{H}$. Consequently, $L_\alpha = \widetilde{L}_\alpha$. □

Lemma 3.2. For each fixed α, the characteristic function $\Delta_\alpha(\rho)$ is determined by the specification of its zeros as:

$$\Delta_\alpha(\rho) = C\rho\exp(C_1\rho)\prod_{n=1}^{\infty}\left(1 - \frac{\rho}{\rho_n}\right)\exp\left(\frac{\rho}{\rho_n}\right)$$

where

$$C = \sin\theta(\pi)\prod_{n=1}^{\infty}\frac{\rho}{\rho_n^0}, \quad C_1 = -\frac{\pi^\alpha}{\alpha}\cot\theta(\pi) + \sum_{n=1}^{\infty}\left(\frac{1}{\rho_n^0} - \frac{1}{\rho_n}\right), \quad \rho_n^0 = \left(n + \frac{\theta(\pi)}{\pi}\right)\frac{\alpha}{\pi^{\alpha-1}}, \quad n \in \{1,2,\cdots\}$$

Proof.

It is clear from Equations 5, 6, and 12 that the characteristic function $\Delta_\alpha(\rho)$ holds the following asymptotic representation:

$$\Delta_\alpha(\rho) = -\rho\sin\left(\frac{\rho\pi^\alpha}{\alpha} - \theta(\pi)\right) + O\left(\exp\left(\frac{|\mathrm{Im}\rho|}{\alpha}\pi^\alpha\right)\right) \tag{23}$$

Consider the function

$$\Delta_\alpha^0(\rho) = -\rho \sin\left(\frac{\rho\pi^\alpha}{\alpha} - \theta(\pi)\right) \tag{24}$$

The zeros of the function $\Delta_\alpha^0(\rho)$ are $\rho = 0$ and $\rho_n^0 = \left(n + \frac{\theta(\pi)}{\pi}\right)\frac{\alpha}{\pi^{\alpha-1}}$ such that $n \in \{1, 2, 3, \cdots\}$. Since $\Delta_\alpha^0(\rho)$ is an entire function, according to the Hadamard's factorization theorem,

$$\Delta_\alpha^0(\rho) = -\rho^m \exp(g(\rho)) \prod_{n=1}^{\infty} E_p\left(\frac{\rho}{\rho_n^0}\right) \tag{25}$$

where $m \geq 0$ is the multiplicity of the zero eigenvalue, $g(\rho)$ is a polynomial with $\deg(g(\rho)) = p$, and

$$E_p(\xi) = \begin{cases} (1-\xi), & n = 0 \\ (1-\xi)\exp\left(\frac{\xi}{1} + \frac{\xi^2}{2} + \ldots + \frac{\xi^n}{n}\right), & \text{otherwise} \end{cases}$$

Since the multiplicity of the zero is 1, $m = 1$. Besides, for every $r > 0$ and for $p = 1$, the series $\sum_{n=1}^{\infty} \frac{r^{1+p}}{|\rho_n^0|^{1+p}}$ converges. Therefore, Equation 25 can rewrite as

$$\Delta_\alpha^0(\rho) = -\rho \exp(a\rho + b)) \prod_{n=1}^{\infty} \left(1 - \frac{\rho}{\rho_n^0}\right) \exp\left(\frac{\rho}{\rho_n^0}\right)$$

If we consider the following equalities to find the constants a and b,

$$\lim_{\rho\to 0} \sin\left(\frac{\rho\pi^\alpha}{\alpha} - \theta(\pi)\right) = \lim_{\rho\to 0} \exp(a\rho + b)) \prod_{n=1}^{\infty} \left(1 - \frac{\rho}{\rho_n^0}\right) \exp\left(\frac{\rho}{\rho_n^0}\right)$$

and

$$\lim_{\rho\to 0} \frac{d}{d\rho} \ln\left[\sin\left(\frac{\rho\pi^\alpha}{\alpha} - \theta(\pi)\right)\right] = \lim_{\rho\to 0} \frac{d}{d\rho} \ln\left[C^0 \exp(a\rho)) \prod_{n=1}^{\infty} \left(1 - \frac{\rho}{\rho_n^0}\right) \exp\left(\frac{\rho}{\rho_n^0}\right)\right]$$

then

$$C^0 = \exp(b) = -\sin\theta(\pi)$$

and

$$C_1^0 = a = -\frac{\pi^\alpha}{\alpha}\cot\theta(\pi)$$

respectively. Thus,

$$\Delta_\alpha^0(\rho) = -\rho C^0 \exp\left(C_1^0\rho)\right) \prod_{n=1}^{\infty} \left(1 - \frac{\rho}{\rho_n^0}\right) \exp\left(\frac{\rho}{\rho_n^0}\right) \tag{26}$$

Moreover,

$$\Delta_\alpha(\rho) = C \exp(C_1\rho)) \rho^m \prod_{n=1}^{\infty} \left(1 - \frac{\rho}{\rho_n}\right) \exp\left(\frac{\rho}{\rho_n}\right) \tag{27}$$

where C and C_1 are constants and $m \geq 0$. According to Equations 23 and 24,

$$\frac{\Delta_\alpha(\rho)}{\Delta_\alpha^0(\rho)} = 1 + O\left(\frac{1}{\rho}\right), \quad |\rho| \to \infty$$

Then, together with Equations 26 and 27,

$$\frac{\Delta_\alpha(\rho)}{\Delta_\alpha^0(\rho)} = -\frac{C}{C^0}\rho^{m-1} \prod_{n=1}^{\infty} \frac{\rho_n^0}{\rho_n} \prod_{n=1}^{\infty} \left(1 + \frac{\rho_n - \rho_n^0 - \rho}{\rho_n^0 - \rho}\right) \exp\left(\sum_{n=1}^{\infty} \frac{\rho_n^0 - \rho_n}{\rho_n\rho_n^0} + C_1 - C_1^0\right)\rho$$

Consequently,

$$m = 1, \quad C = -C^0 \prod_{n=1}^{\infty} \frac{\rho_n}{\rho_n^0}, \quad \text{and} \quad C_1 = C_1^0 + \sum_{n=1}^{\infty} \left(\frac{1}{\rho_n^0} - \frac{1}{\rho_n}\right)$$

□

Theorem 3.3. If $\{\rho_n, \alpha_n\}_{n\geq 1} = \{\widetilde{\rho}_n, \widetilde{\alpha}_n\}_{n\geq 1}$ for each fixed α, then $q(x) = \widetilde{q}(x)$, almost everywhere in $[0, \pi]$, $h = \widetilde{h}$, and $H = \widetilde{H}$. Thus, the spectral data $\{\rho_n, \alpha_n\}_{n\geq 1}$ uniquely determines the operator L_α.

Proof.
Since $\rho_n = \widetilde{\rho}_n$, according to Lemma 3.2, $\Delta_\alpha(\rho) = \widetilde{\Delta}_\alpha(\rho)$. Using Lemma 2.3 and $\alpha_n = \widetilde{\alpha}_n$, $\beta_n = \widetilde{\beta}_n$ and thus $\psi(0, \rho_n; \alpha) = \widetilde{\psi}(0, \rho_n; \alpha)$. For each fixed α, let

$$H_\alpha(\rho) := \frac{\psi(0, \rho; \alpha) - \widetilde{\psi}(0, \rho; \alpha)}{\Delta_\alpha(\rho)}$$

It is clear that $H_\alpha(\rho)$ is entire on ρ. Moreover, by using Equations 7 and 14,

$$H_\alpha(\rho) := O\left(\frac{1}{\rho^2}\right), \quad |\rho| \to \infty$$

Hence, $H_\alpha(\rho) \equiv 0$ and $\psi(0, \rho; \alpha) = \widetilde{\psi}(0, \rho; \alpha)$. Consequently, from Equation 17, $M_\alpha(\rho) \equiv \widetilde{M}_\alpha(\rho)$. Thus, the proof is completed by Theorem 3.1. □

4. Conclusion

The Weyl function and spectral data are very natural and useful spectral characteristics in inverse problem theory. Until today, by using these concepts, many inverse problems have been studied for various classes of operators, such as regular or singular Sturm-Liouville operators, diffusion operators, and Dirac operators, including the classical derivatives. In [18], some inverse problems for the Sturm-Liouville operator, including conformable fractional derivatives, are investigated.

In this study, the diffusion operator, which includes conformable fractional derivatives, is considered, and the inverse problems are investigated for this operator for the first time according to both the Weyl function and spectral data. This study can be considered as a partial α-generalization of similar findings for the classical diffusion operator.

Considering this study's results, some inverse problems can be investigated in the future for various conformable operators with jump conditions, parameter-dependent boundary conditions, or non-local boundary conditions.

Author Contributions

The author read and approved the final version of the paper.

Conflicts of Interest

The author declares no conflict of interest.

References

[1] V. A. Ambartsumyan, *Über Eine Frage Der Eigenwerttheorie*, Zeitschrift für Physik 53 (1929) 690–695.

[2] G. Borg, *Eine Umkehrung der Sturm-Liouvilleschen Eigenwertaufgabe: Bestimmung der Differentialgleichung durch die Eigenwerte*, Acta Mathematica 78 (1946) 1–96.

[3] N. Levinson, *The Inverse Sturm-Liouville Problem*, Matematisk Tidsskrift B 25 (1949) 25–30.

[4] V. A. Marchenko, *Concerning the Theory of a Differential Operator of the Second Order*, Doklady Akademii Nauk SSSR 72 (1950) 457–460.

[5] E. L. Isaacson, E. Trubowitz, *The Inverse Sturm-Liouville Problem I*, Communications on Pure and Applied Mathematics 36 (1983) 767–783.

[6] M. G. Gasymov, G. Sh. Guseinov, *Determining of the Diffusion Operator from Spectral Data*, Doklady Akademii Nauk Azerbaijan SSR 37 (2) (1981) 19–23.

[7] G. Freiling, V.A. Yurko, Inverse Sturm-Liouville Problems and Their Applications, Nova Science Publishers, New York, 2001.

[8] R. Khalil , M. Al Horani, A. Yousef, M. Sababheh, *A New Definition of Fractional Derivative*, Journal of Computational and Applied Mathematics 264 (2014) 65–70.

[9] T. Abdeljawad, *On Conformable Fractional Calculus*, Journal of Computational and Applied Mathematics 279 (2015) 57–66.

[10] A. Atangana, D. Baleanu, A. Alsaedi, *New Properties of Conformable Derivative*, Open Mathematics 13 (2015) 889–898.

[11] M. Abu Hammad, R.Khalil, *Abel's Formula and Wronskian for Conformable Fractional Differential Equations*, International Journal of Differential Equations and Applications 13 (3) (2014) 177–183.

[12] O. T. Birgani, S. Chandok, N. Dedovic, S. Radenoviç, *A Note on Some Recent Results of the Conformable Derivative*, Advances in the Theory of Nonlinear Analysis and its Applications 3 (1) (2019) 11–17.

[13] D. Zhao, M. Luo, *General Conformable Fractional Derivative and its Physical Interpretation*, Calcolo 54 (2017) 903–917.

[14] Y. Wang, J. Zhou, Y. Li, *Fractional Sobolev's Spaces on Time Scales via Conformable Fractional Calculus and Their Application to a Fractional Differential Equation on Time Scales*, Advances in Mathematical Physics 2016 (2016) Article ID 963649121 21 pages.

[15] F. Jarad, E. Uğurlu, T. Abdeljawad, D. Baleanu, *On a New Class of Fractional Operators*, Advances in Difference Equations 2017 (2017) Article Number 247 16 pages.

[16] H. Mortazaasl, A. Jodayree Akbarfam, *Trace Formula and Inverse Nodal Problem for a Conformable Fractional Sturm-Liouville Problem*, Inverse Problems in Science and Engineering 28 (4) (2020) 524–555.

[17] B. Keskin, *Inverse Problems for One Dimentional Conformable Fractional Dirac Type Integro Differential System*, Inverse Problems 36 (6) (2020) 065001 10 pages.

[18] İ. Adalar, A. S. Özkan, *Inverse Problems for a Conformable Fractional Sturm-Liouville Operators*, Journal of Inverse and Ill-posed Problems 28 (6) (2020) 775–782.

[19] Y. Çakmak, *Inverse Nodal Problem for a Conformable Fractional Diffusion Operator*, Inverse Problems in Science and Engineering 29 (9) (2021) 1308–1322.

[20] Y. Çakmak, *Inverse Nodal Problem for a Conformable Fractional Diffusion Operator with Parameter-Dependent Nonlocal Boundary Condition*, Cumhuriyet Science Journal 44 (2) (2023) 356–363

[21] Y. Çakmak, *Trace Formulae for a Conformable Fractional Diffusion Operator*, Filomat 36 (14) (2022) 4665–4674.

[22] S. A. Buterin, *On Half Inverse Problem for Differential Pencils with the Spectral Parameter in the Boundary Conditions*, Tamkang Journal of Mathematics 42 (3) (2011) 355–364.

[23] E. Koç, Y. Çakmak, *α-Integral Representation of the Solution for a Conformable Fractional Diffusion Operator and Basic Properties of the Operator*, Cumhuriyet Science Journal 44 (1) (2023) 170–180.

Journal of New Theory
ISSN: 2149-1402

44 (2023) 52-61
Journal of New Theory
https://dergipark.org.tr/en/pub/jnt
Open Access

Results of Paired-Domination of Some Special Graph Families on Transformation Graphs: G^{xy+} and G^{xy-}

Hande Tunçel Gölpek[1]

Article Info
Received: 4 Aug 2023
Accepted: 22 Sep 2023
Published: 30 Sep 2023
doi:10.53570/jnt.1337633
Research Article

Abstract – In this study, transformation graphs obtained from the concept of the total graph and the result of its paired domination number for some special graph families are discussed. If a subset S of the vertex set of the graph G dominates and the induced subgraph $\langle S \rangle$ has a perfect matching that covers every vertex of the graph, then S is called a paired-dominating set of G. A paired dominating set with the smallest cardinality is denoted by γ_{pr}-set. Haynes and Slater introduced paired domination parameters. The present study commences with assessing outcomes stemming from eight permutations within the realm of path graphs. Subsequently, building upon this foundational structure, the results are extrapolated from the realm of cycle transformation graph structures based on findings from path transformation graphs.

Keywords *Graph theory, graph vulnerability, paired domination number, transformation graphs*

Mathematics Subject Classification (2020) 05C69, 05C76

1. Introduction

In graph theory, the investigation of domination numbers and their various forms has garnered significant attention, leading to a continual expansion of knowledge in this domain. Let G be a graph with the vertex set $V(G)$ (or simply V) and the edge set $E(G)$ (or simply E). Then, $S \subseteq V$ is called the dominating set of G if every vertex in $V - S$ is adjacent to any vertex in S, and the domination number of G is denoted by $\gamma(G)$. The domination number is the minimum cardinality of a dominating set.

Furthermore, the discourse extends to exploring the total domination number, a parameter that has drawn extensive discussion. A total dominating set S of G, denoted by TD-set, is a dominating set with no isolated vertex and total domination number, which is the minimum cardinality of a total dominating set abbreviated by $\gamma_t(G)$. Total domination was introduced by Cockayne et al. [1].

This paper delves into another alteration of the domination parameter, termed paired domination. Let $S \subseteq V$. Then, S is called a paired-dominating set of G and is denoted PD-set, if it dominates, and the induced subgraph $\langle S \rangle$ has a perfect matching that covers every vertex of the graph. A paired dominating set with the smallest cardinality is denoted by γ_{pr}-set. This concept was pioneered by Haynes and Slater [2]. To explain the meaning of these three domination parameters in terms of application, consider each $s \in S$ as a protector that can guard each vertex where s dominates then every protector guards itself. Regarding total domination, every protector must be guarded by another protector. As for paired domination, the guards' positions must be chosen as pairs of adjacent vertices so that each guard is assigned to each other and exists as substitutes for each other. There

[1]hande.tuncel@deu.edu.tr (Corresponding Author)
[1]Department of Maritime Education, Maritime Faculty, Dokuz Eylül University, İzmir, Türkiye

are many domination parameters in different categories, and the paired domination parameters discussed in this paper are considered under the category with restricted forms based on $\langle S \rangle$. We can present the reader with references to some significant studies, particularly in this work, that address the behavior of the paired domination number under various graph operations, as [3-11] in the literature. In addition, regarding the domination parameter, the three new books, which provide even more comprehensive coverage of current studies on domination parameters, can be offered to the reader as references [12-14].

In this paper, we consider simple graphs and refer to the book [15] for notation and terminology. The open neighborhood of any vertex in $V(G)$, denoted by $N(v) = \{u \in V(G) \mid (uv) \in E(G)\}$. The degree of a vertex v is the number of edges that are incident to it and is denoted by $\deg(v)$. Moreover, a vertex whose degree is one is called a pendant vertex. Furthermore, the maximum degree of G, denoted by $\Delta(G)$, is the degree of the vertex with the maximum number of edges incident to it. Similarly, the minimum degree of G, abbreviated by $\delta(G)$, is the degree of a vertex with the minimum number of edges incident to it. The distance between two vertices u and v is the shortest path between them and is denoted by the notation $d(u, v)$.

In this study, transformation graphs G^{xy-} and G^{xy+} are considered, and values of their paired-domination number for some special graph families are obtained. Transformation graph definitions are bottomed on the total graph [16]. Let $V(G) \cup E(G)$ be the vertex set of a total graph where two vertices are adjacent if and only if the vertices and edges are adjacent or incident in G. The transformation graphs introduced by Wu and Meng can be provided, denoted by G^{xyz}. Their paper considers its eight structure cases and generalizations of the total graph concept [17]. Before defining transformation graphs, we must explain some fundamental graph constructions such as complement and line graphs. The complement graph of G, denoted by the notation $\overline{G}$, is based on the same vertex set $V(G)$ but a different edge set completes the graph G to complement the graph. The line graph $L(G)$ of G is the graph that takes the edge set $E(G)$ as its vertex set. Two vertices are adjacent in the line graph $L(G)$ if and only if corresponding edges are adjacent in graph G [18]. Thus, the concept of the transformation graph represented by G^{xyz} can now be addressed, where x, y, and z can take values $+$ or $-$. The transformation graph G^{xyz} of G is a simple graph having as the vertex set $V(G) \cup E(G)$, and for $\alpha, \beta \in V(G) \cup E(G)$ and their relationships in G^{xyz} can be explained as follows:

i. Let $\alpha, \beta \in V(G)$. Then, α and β are adjacent in G^{xyz} if $x = +$; otherwise $x = -$.
ii. Let $\alpha, \beta \in E(G)$. Then, α and β are adjacent in G^{xyz} if $y = +$; otherwise $y = -$.
iii. Let $\alpha \in V(G)$ and $\beta \in E(G)$. Then, α and β are incidents in G^{xyz} if $z = +$; otherwise $z = -$.

There are eight distinct constructions from three signature permutations $\{+, -\}$. Then, it may be obtained transformation graphs where G^{+++} is the total graph of G, and G^{---} is the complement of it. Moreover, G^{-+-}, G^{--+}, and G^{-++} are the complements of G^{+-+}, G^{++-}, and G^{+--}, respectively. Moreover, the transformation graph can be expressed as a relationship between G (or $\overline{G}$) and its line graph $L(G)$ (or $\overline{L(G)}$) depending on the sign of x, y, and z. If $x = +$, then the transformation graph includes G as a subgraph, otherwise includes $\overline{G}$ as a subgraph, and if $y = +$, then the transformation graph includes $L(G)$ as a subgraph, otherwise includes $\overline{L(G)}$ as a subgraph alike. Thus, depending on the sign of z, the relationship between G (or $\overline{G}$) and $L(G)$ (or $\overline{L(G)}$) has been structured based on the aforesaid situation *(iii)*. Let $V(G) \cup V\big(L(G)\big)$ be the vertex set of the transformation graph where $V(G) = \{1,2, \cdots, n\}$ and $V\big(L(G)\big) = \{(ij) : (ij) \in E(G)\}$. The vertex set will be expressed in this form unless otherwise stated. We direct readers' attention to select papers that offer comprehensive insights into the outcomes concerning specific domination parameters in transformation graphs. These referenced works provide detailed and in-depth information that can facilitate a deeper understanding of the subject matter of transformation graphs [19- 26].

2. Preliminaries

This section presents pivotal outcomes from scholarly literature concerning the paired domination number.

Proposition 2.1. [2] If u is adjacent to an end vertex of G, then u is in every paired dominating set. Furthermore, for certain specific families of graphs, $\gamma_{pr}(K_n) = \gamma_{pr}(K_{r,s}) = \gamma_{pr}(W_n) = 2$ and $\gamma_{pr}(P_n) = \gamma_{pr}(C_n) = 2\left\lceil \frac{n}{4} \right\rceil$.

Here, the notation $\lceil . \rceil$ represents the ceiling function.

Theorem 2.2. [2] For any graph G, $\gamma_{pr}(\overline{G}) \geq 4$ if and only if $\mathrm{diam}(G) = 2$.

Theorem 2.3. [2] If a graph G has no isolated vertices, then $2 \leq \gamma_{pr}(G) \leq n$.

Proposition 2.4. [2] If a graph G has no isolated vertices, then $\gamma(G) \leq \gamma_t(G) \leq \gamma_{pr}(G)$, and $\gamma_{pr}(G)$ is even.

3. Results

This section presents the results of the eight different permutations of path and cycle transformation graphs for the paired domination parameter.

3.1. Paired Domination of Transformation Path Graphs

In this designated section, we intend to acquire and elucidate the outcomes of the paired domination of transformation graphs across all permutations. We shall commence our exposition by focusing on the specific P_n^{+++} form of permutations.

Theorem 3.1. Let $n > 6$ and P_n be a path graph. Then,

$$\gamma_{pr}(P_n^{+++}) = \begin{cases} \left\lceil \frac{4n-2}{7} \right\rceil, & n \equiv 0,3,4,6 \pmod 7 \\ \left\lceil \frac{4n-2}{7} \right\rceil + 1, & \text{otherwise} \end{cases}$$

Proof.

The vertices of the graph P_n^{+++} can be partitioned into two parts, such as $V = V_1 \cup V_2$. To alleviate the burden of complex notation, the vertex sets can be labeled as $V_1 = \{1,2,\cdots,n\}$ and $V_2 = \{n+1, n+2, \cdots, 2n\}$. Let D be a PD-set of P_n^{+++}. To begin, we establish an upper bound for $\gamma_{pr}(P_n^{+++})$ as follows: Let $S = S_1 \cup S_2$ be a set where S_1 includes the vertices of $V(P_n^{+++})$, and S_2 includes the vertices of $V\left(L(P_n^{+++})\right)$ as follows:

$$S_1 = \bigcup_{i=0}^{\left\lceil \frac{n-2}{7} \right\rceil - 1} \{(7i+2, 7i+3)\}$$

and

$$S_2 = \bigcup_{i=0}^{\left\lceil \frac{n-6}{7} \right\rceil - 1} \{(n+7i+5, n+7i+6)\}$$

Here, the cardinality of S is $|S| = 2\left\lceil \frac{n-2}{7} \right\rceil + 2\left\lceil \frac{n-6}{7} \right\rceil$.

i. If $n \equiv 0,3,4 \pmod 7$, then $D = S$.

ii. If $n \equiv 1,2 \pmod 7$, then $D = S \cup \{n, n-1\}$.

iii. If $n \equiv 5,6 \pmod 7$, then $D = S \cup \{2n-2, 2n-1\}$.

Therefore, $|D| = \left\lceil \frac{4n-2}{7} \right\rceil$, for $n \equiv 0,3,4 \pmod 7$, otherwise $|D| = \left\lceil \frac{4n-2}{7} \right\rceil + 1$. Thus,

$$\gamma_{pr}(P_n^{+++}) \leq \begin{cases} \left\lceil \frac{4n-2}{7} \right\rceil, & n \equiv 0,3,4 \pmod 7 \\ \left\lceil \frac{4n-2}{7} \right\rceil + 1, & \text{otherwise} \end{cases}$$

In order to prove the necessary condition, assume that the set $T = \{a_1, a_2, \cdots, a_t\}$ is γ_{pr}-set of P_n^{+++}. Assume that the elements of T are ordered as $a_1 < a_2 < \cdots < a_i < \cdots < a_m < a_{m+1} < \cdots < a_j < \cdots < a_t$. Here, a_i and a_j are positive integers, $1 \leq a_i \leq n$, for all $i \in \{1, \cdots, m\}$, and $n+1 \leq a_j \leq 2n-1$, for all $j \in \{m+1, \cdots, t\}$. Define a function such as $f_x = a_{x+2} - a_x$ where $x \in \{1,2, \cdots, t-2\}$ such that $x \neq m$ and $x \neq m-1$. It is needed to prove that $f_x \leq 7$. Assume that a value of f_x is greater than or equal to 8. Without loss of generality, choose $f_1 = 8$. Therefore, for $n \geq 14$, we can create a set

$$S' = \{2,3, n+5, n+6, n+7, n+8\} \cup \left(\bigcup_{i=0}^{\left\lceil \frac{n-10}{7} \right\rceil - 1} \{7i+10, 7i+11\} \right) \cup \left(\bigcup_{i=0}^{\left\lceil \frac{n-10}{7} \right\rceil - 1} \{n+7i+13, n+7i+14\} \right)$$

For $n \equiv 3 \pmod 7$, $T = S' \cup \{n, n-1\}$. Thus,

$$|T| = |S'| + 2 = 8 + 2\left(\frac{n-10}{7}\right) + 2\left(\frac{n-10}{7}\right) = \frac{4n+16}{7}$$

However, it contradicts the obtained upper bound $\left\lceil \frac{4n-2}{7} \right\rceil$. Hence, f_x should be less than or equal to 7. Then, the upper bound for the total value of f_x can be gotten as follows:

$$\sum_{x_1=1}^{m-2} f_{x_1} + \sum_{x_2=m+1}^{t-2} f_{x_2} \leq 7(t-4)$$

In order to construct a relationship between the values of t and n, the total value of f_x can be evaluated as

$$\sum_{x_1=1}^{m-2} f_{x_1} + \sum_{x_2=m+1}^{t-2} f_{x_2} = a_m + a_{m-1} + a_t + a_{t-1} - (2n+16)$$

where $a_1 = 2$, $a_2 = 3$, $a_{m+1} = n+5$, and $a_{m+2} = n+6$.

If $n \equiv 0 \pmod 7$, then

$$\sum_{x_1=1}^{m-2} f_{x_1} + \sum_{x_2=m+1}^{t-2} f_{x_2} = 4n - 28 \leq 7(t-4)$$

It is obtained that $t \geq \frac{4n}{7}$ where $a_m = n-4$, $a_{m-1} = n-5$, $a_t = 2n-1$, and $a_{t-1} = 2n-2$. Therefore,

$$|T| = t \geq \frac{4n}{7} = \left\lceil \frac{4n-2}{7} \right\rceil$$

Thus, it requires that $\gamma_{pr}({P_n}^{+++}) \geq \left\lceil \frac{4n-2}{7} \right\rceil$, for $n \equiv 0 \pmod 7$.

If $n \equiv 1 \pmod 7$, then

$$\sum_{x_1=1}^{m-2} f_{x_1} + \sum_{x_2=m+1}^{t-2} f_{x_2} = 4n - 22 \leq 7(t-4)$$

It is obtained that $t \geq \frac{4n+6}{7}$ where $a_m = n$, $a_{m-1} = n-1$, $a_t = 2n-2$, and $a_{t-1} = 2n-3$. Therefore,

$$|T| = t \geq \frac{4n+6}{7} = \left\lceil \frac{4n-2}{7} \right\rceil + 1$$

Thus, $\gamma_{pr}(P_n^{+++}) \geq \left\lceil \frac{4n-2}{7} \right\rceil + 1$, for $n \equiv 1 \pmod 7$.

If $n \equiv 2 \pmod 7$, then

$$\sum_{x_1=1}^{m-2} f_{x_1} + \sum_{x_2=m+1}^{t-2} f_{x_2} = 4n - 24 \leq 7(t-4)$$

It is obtained that $t \geq \frac{4n+4}{7}$ where $a_m = n$, $a_{m-1} = n-1$, $a_t = 2n-3$, and $a_{t-1} = 2n-4$. Therefore,

$$|T| = t \geq \frac{4n+4}{7} = \left\lceil \frac{4n-2}{7} \right\rceil + 1$$

Thus, $\gamma_{pr}(P_n^{+++}) \geq \left\lceil \frac{4n-2}{7} \right\rceil + 1$, for $n \equiv 2 \pmod 7$.

If $n \equiv 3 \pmod 7$, then

$$\sum_{x_1=1}^{m-2} f_{x_1} + \sum_{x_2=m+1}^{t-2} f_{x_2} = 4n - 26 \leq 7(t-4)$$

It is obtained that $t \geq \frac{4n+2}{7}$ where $a_m = n$, $a_{m-1} = n-1$, $a_t = 2n-4$, and $a_{t-1} = 2n-5$. Therefore,

$$|T| = t \geq \frac{4n+2}{7} = \left\lceil \frac{4n-2}{7} \right\rceil$$

Thus, $\gamma_{pr}(P_n^{+++}) \geq \left\lceil \frac{4n-2}{7} \right\rceil$, for $n \equiv 3 \pmod 7$.

If $n \equiv 4 \pmod 7$, then

$$\sum_{x_1=1}^{m-2} f_{x_1} + \sum_{x_2=m+1}^{t-2} f_{x_2} = 4n - 30 \leq 7(t-4)$$

It is obtained that $t \geq \frac{4n-2}{7}$ where $a_m = n-1$, $a_{m-1} = n-2$, $a_t = 2n-5$, and $a_{t-1} = 2n-6$. Therefore,

$$|T| = t \geq \frac{4n-2}{7} = \left\lceil \frac{4n-2}{7} \right\rceil$$

Thus, $\gamma_{pr}(P_n^{+++}) \geq \left\lceil \frac{4n-2}{7} \right\rceil$, for $n \equiv 4 \pmod 7$.

If $n \equiv 5 \pmod 7$, then

$$\sum_{x_1=1}^{m-2} f_{x_1} + \sum_{x_2=m+1}^{t-2} f_{x_2} = 4n - 24 \leq 7(t-4)$$

It is obtained that $t \geq \frac{4n+4}{7}$ where $a_m = n-2$, $a_{m-1} = n-3$, $a_t = 2n-1$, and $a_{t-1} = 2n-2$. Therefore,

$$|T| = t \geq \frac{4n+4}{7} = \left\lceil \frac{4n-2}{7} \right\rceil + 1$$

Thus, $\gamma_{pr}(P_n^{+++}) \geq \left\lceil \frac{4n-2}{7} \right\rceil + 1$, for $n \equiv 5 \pmod 7$.

If $n \equiv 6 \pmod 7$, then

$$\sum_{x_1=1}^{m-2} f_{x_1} + \sum_{x_2=m+1}^{t-2} f_{x_2} = 4n - 26 \leq 7(t-4)$$

It is obtained that $t \geq \frac{4n+2}{7}$ where $a_m = n-3$, $a_{m-1} = n-4$, $a_t = 2n-1$, and $a_{t-1} = 2n-2$. Therefore,

$$|T| = t \geq \frac{4n+2}{7} = \left\lceil \frac{4n-2}{7} \right\rceil$$

Thus, $\gamma_{pr}(P_n^{+++}) \geq \left\lceil \frac{4n-2}{7} \right\rceil + 1$ for $n \equiv 6 \pmod 7$.

Hence, from the necessary and sufficient conditions, we obtain the result as

$$\gamma_{pr}(P_n^{+++}) = \begin{cases} \left\lceil \frac{4n-2}{7} \right\rceil, & n \equiv 0,3,4,6 \pmod 7 \\ \left\lceil \frac{4n-2}{7} \right\rceil + 1, & \text{otherwise} \end{cases}$$

Theorem 3.2. Let $n > 5$ and P_n be a path graph. Then, $\gamma_{pr}(P_n^{++-}) = 4$.

Proof.

Consider the set of vertices $\{1,2,\cdots,n\}$ as the vertex set of P_n. Let S be paired dominating set of P_n^{++-} and $S = S_1 \cup S_2$ where $S_1 = \{u \mid u \in V(P_n)\}$ and $S_2 = \{e \mid e \in V(L(P_n))\}$. If the vertex 1 is part of S_1 then all the vertices in $L(P_n)$ except for $(12) \in V(L(P_n))$ are dominated. To achieve perfect matching and ensure the domination of the vertex (12) and the remaining vertices $\{3,4,\cdots,n\} \in V(P_n)$, it is needed to add a vertex $e = (uv)$ to S_2, which is adjacent to 1, and v and $v+1$ to S_1. Therefore, $\{1,(uv),v,v+1\}$ is a paired dominating set for P_n^{++-} and $|S| \leq 4$. However, it is impossible to dominate all the vertices with two pairs of vertices. Then, $|S| > 2$. Moreover, since the paired domination number must be an even number according to Proposition 2.4. Then,

$$\gamma_{pr}(P_n^{++-}) = 4$$

□

Theorem 3.3. Let $n \geq 6$ and P_n be a path graph. Then, $\gamma_{pr}(P_n^{+-+}) = 2 + \gamma_{pr}(P_{n-4})$.

Proof.

Consider the set of vertices $\{1,2,\cdots,n\}$ as the vertex set of P_n. Let S be the minimum paired dominating set of P_n^{+-+}. It is known that $|S| \geq 2$ from Theorem 2.3. If the vertices (12) and $\big((n-1)(n)\big)$ with the maximum degree in P_n^{+-+} are added to S, then all the vertices in $V\overline{(L(P_n))}$ are dominated. However, there are some non-dominated vertices such as $\{3,4,\cdots,(n-2)\} \in V(P_n^{+-+})$. These non-dominated $(n-4)$ vertices construct a P_{n-4} structure. As a result, the size of S can be expressed as $2 + \gamma_{pr}(P_{n-4})$. □

Theorem 3.4. Let P_n be a path graph. Then, $\gamma_{pr}(P_n^{+--}) = 2$.

Proof.

Let $\{1,2,\cdots,n\}$ be the vertex set of P_n. Let S be a paired dominating set of P_n^{+--}. It is clear that all the vertices in P_n^{+--} dominated pairedly by $\{(12),\big((n-1)n\big)\}$. This insight leads to the conclusion that $|S| \leq 2$. By Theorem 2.3, it is established that S must have a size of at least 2. Consequently, combining these observations, we can affirm that $|S| = 2$. □

Theorem 3.5. Let P_n be a path graph. Then, $\gamma_{pr}(P_n^{---}) = 2$.

PROOF.

Let $\{1,2,\cdots,n\}$ be the vertex set of P_n. Let S be a paired dominating set of P_n^{---}. As in the proof of P_n^{+--}, all the vertices in P_n^{---} dominated pairedly by $\{(12),((n-1)n)\}$. Therefore, $|S| \leq 2$. It is known that $|S| \geq 2$ from Theorem 2.3. Consequently, $|S| = 2$. □

Theorem 3.6. Let P_n be a path graph. Then, $\gamma_{pr}(P_n^{--+}) = 4$.

PROOF.

Let $\{1,2,\cdots,n\}$ be the vertex set of P_n. Consider that S be paired dominating set of P_n^{--+} and $S = S_1 \cup S_2$ where $S_1 = \{u \mid u \in V(P_n)\}$ and $S_2 = \{e \mid e \in V(L(P_n))\}$. If $1 \in S_1$, then all the vertices in P_n^{--+} except for $2 \in V(P_n)$ and the vertex $(12) \in V(L(P_n))$ are dominated. In order to get perfect matching and dominate $2 \in V(P_n)$, it is needed to add a vertex (12) to S_2, which is adjacent to 1. However, the vertex (23) is the only non-dominated vertex in the graph. Therefore, a pair should be added to the set as $\{1,(12),v,v+1\}$, a paired dominating set for P_n^{--+}. Hence, $|S| \leq 4$. Furthermore, it is not feasible to achieve domination over all the vertices using only two pairs of vertices, leading to the conclusion that $|S| > 2$. Considering Proposition 2.4 stating the paired domination number must be an even value, $\gamma_{pr}(P_n^{++-}) = 4$. □

Theorem 3.7. Let P_n be a path graph. Then, $\gamma_{pr}(P_n^{-+-}) = 2$.

PROOF.

Consider the set of vertices $\{1,2,\cdots,n\}$ as the vertex set of P_n. Let S represent the paired dominating set of P_n^{-+-}. All the vertices in P_n^{-+-} are dominated pairedly by $\{1,n\}$. As a direct consequence, we deduce that $|S| \leq 2$. It is established in Theorem 2.3 that $|S|$ must have a minimum size of 2. Hence, combining these results, $|S| = 2$. □

Theorem 3.8. Let P_n be a path graph. Then, $\gamma_{pr}(P_n^{-++}) = 2 + \gamma_{pr}(P_{n-5})$.

PROOF.

Let $\{1,2,\cdots,n\}$ be the vertex set of P_n, and S be the minimum paired dominating set of P_n^{-++}. It is known that $|S| \geq 2$ from Theorem 2.3. Upon introducing the vertices (2) and $((n-1))$, which possess the highest degree in G, are added to the set S, then all the vertices in $V(\overline{P_n})$ are dominated. Nevertheless, there are some non-dominated vertices, such as $\{(34),(45),\ldots,((n-3)(n-2))\}$ in $V(L(G))$. These non-dominated $(n-5)$ vertices construct a P_{n-5} structure. Therefore, it is obtained that $S = 2 + \gamma_{pr}(P_{n-5})$. □

3.2. Paired Domination of Transformation Cycle Graphs

Given the particular structure of the cycle graph, it is noteworthy that the line graph of C_n exhibits isomorphism to itself. This observation leads to deduce the subsequent results:

Theorem 3.9. Let C_n be a cycle graph. Then, $\gamma_{pr}(C_n^{++-}) = 4$.

PROOF.

Let $\{1,2,3,\cdots,n\}$ be the vertex set of C_n, and S be the paired dominating set of C_n^{++-}. If S contains the vertex 1 and the vertex (12), then it ensures the domination of all the vertices within the graph. Nevertheless, these two vertices are not adjacent according to the form of the graph. In order to get perfect matching, it is needed to add two more vertex. It holds that the size of set S exceeds 2. Consequently, we can deduce that the parameter $\gamma_{pr}(C_n^{++-})$ is equal to 4. □

Theorem 3.10. Let C_n be a cycle graph and $n \geq 9$. Then, $\gamma_{pr}(C_n^{-++}) = \gamma_{pr}(C_n^{+-+}) = 4 + 2\left\lceil\frac{n-8}{4}\right\rceil$.

PROOF.

Let $\{1,2,3,\cdots,n\}$ be the vertex set of C_n and S be the paired dominating set of C_n^{-++}. If S includes the vertices (12), $(1n)$, 4, and $(n-2)$, then all the vertices of $\overline{C}_n$ and the vertices labeled by (12), (23), (34), (45), $\big((n-3)(n-2)\big)$, $\big((n-2)(n-1)\big)$, $\big((n-1)(n)\big)$, and $(n1)$ in $L(C_n)$ are dominated pairedly. However, the non-dominated P_{n-8} the structure remains. Consequently, from [2]

$$\gamma_{pr}(C_n^{-++}) = \gamma_{pr}(C_n^{+-+}) = 4 + \gamma_{pr}(P_{n-8}) = 4 + 2\left\lceil\frac{n-8}{4}\right\rceil$$

□

Theorem 3.11. Let C_n be a cycle graph and $n \geq 6$. Then, $\gamma_{pr}(C_n^{-+-}) = \gamma_{pr}(C_n^{+--}) = 2$.

PROOF.

Consider the vertex set $\{1,2,3,\cdots,n\}$ as the vertex set of C_n, and let S denote a paired dominating set of C_n^{+--}. If S includes (12) and (45) from $V\big(L(C_n)\big)$, then all the vertices in C_n^{+--} are dominated pairedly. Consequently, it follows that $\gamma_{pr}(C_n^{-+-}) = \gamma_{pr}(C_n^{+--}) = 2$, establishing the paired domination number for C_n^{-+-} and C_n^{+--}. □

Theorem 3.12. Let C_n be a cycle graph and $n \geq 6$. Then, $\gamma_{pr}(C_n^{--+}) = 4$.

PROOF.

Given the graph C_n^{--+}, the complete graph of C_n^{++-}, it can be deduced from Theorem 2.2 that its diameter is 2. Consequently, this implies that $\gamma_{pr}(C_n^{--+}) \geq 4$. Considering the vertex set $\{1,2,3,\cdots,n\}$ as the vertex set of C_n, and let S be paired dominating set of C_n^{--+}. If S is included (1) and (3) from $V\big(\overline{C_n}\big)$ and (12) and (34) from $V\left(\overline{L(C_n)}\right)$, then all the vertices in C_n^{--+} are dominated. This observation leads to the conclusion that $|S| = \gamma_{pr}(C_n^{--+}) \leq 4$. Hence, $\gamma_{pr}(C_n^{--+}) = 4$. □

Theorem 3.13. Let C_n be a cycle graph. Then, $\gamma_{pr}(C_n^{---}) = 2$.

PROOF.

Consider the vertex set $\{1,2,3,\cdots,n\}$ of the C_n, and let S be a paired dominating set of C_n^{---}. If S contains the vertices 1 and 4, then it ensures that S dominates $\overline{C_n}$ and $\overline{L(C_n)}$. Additionally, $\langle S\rangle$ forms a graph with perfect matching. □

Theorem 3.14. Let C_n be a cycle graph. Then,

$$\gamma_{pr}(C_n^{+++}) = \begin{cases} \gamma_{pr}(P_n^{+++}) + 2, & n \equiv 4 \pmod 7 \\ \gamma_{pr}(P_n^{+++}), & \text{otherwise} \end{cases}$$

PROOF.

Let S be the γ_{pr}-set of P_n^{+++}. Considered similar to the proof of the P_n^{+++}, S is also the γ_{pr}-set of C_n^{+++} when $n \not\equiv 4 \pmod 7$. If the vertex set of $L(C_n)$ labeled as in the proof of P_n^{+++}, the vertex $(n1)$ corresponds to the vertex $2n$. However, the vertex $(2n) \in V\big(L(C_n^{+++})\big)$ cannot be dominated by S when $n \equiv 4 \pmod 7$. In such cases, the addition of two extra vertices becomes necessary to ensure paired domination. Hence,

$$\gamma_{pr}(C_n^{+++}) = \gamma_{pr}(P_n^{+++}) + 2$$

when $n \equiv 4 \pmod 7$. Henceforth, it is deduced that

$$\gamma_{pr}(C_n^{+++}) = \begin{cases} \gamma_{pr}(P_n^{+++}) + 2, & n \equiv 4 \pmod 7 \\ \gamma_{pr}(P_n^{+++}), & \text{otherwise} \end{cases}$$

□

4. Conclusion

We have implemented the discussed paired domination parameter from this research on path and cycle structures, two significant classes within the realm of graphs. We have derived outcomes for the transformation graphs encompassing all eight permutations in both these structural contexts. The outcome $\gamma_{pr}(P_n^{+++})$ is then applied to derive the $\gamma_{pr}(C_n^{+++})$ result for the cycle structure.

In upcoming research endeavors related to the topic, paired domination values of transformation graphs can be investigated for a general G graph. Furthermore, an attempt can be made to establish associations with other graph parameters to derive lower or upper-bound values. Since the concept of domination holds a significant position in graph theory, researchers interested in the subject might also explore the influence of transformation graphs on other domination parameters.

Author Contributions

The author read and approved the final version of the paper.

Conflict of Interest

The author declares no conflict of interest.

References

[1] E. J. Cockayne, R. M. Dawes, S. T. Hedetniemi, *Total Domination in Graphs*, Networks 10 (3) (1980) 211-219.

[2] T. W. Haynes, P. J. Slater, *Paired-Domination in Graphs*, Networks 32 (3) (1998) 199-206.

[3] W. J. Desormeaux, M. A. Henning, *Paired Domination in Graphs: A Survey and Recent Results*, Utilitas Mathematica 94 (2014) 101–166.

[4] M. Chellali, T. W. Haynes, *Total and Paired-Domination Numbers of a Tree*, AKCE International Journal of Graphs and Combinatorics 1 (2) (2004) 69–75.

[5] A. D. Gray, M. A. Henning, *Paired-Domination Game Played on Cycles*, Discrete Applied Mathematics *336* (2023) 132–140.

[6] P. Eakawinrujee, N. Trakultraipruk, *Total and Paired Domination Numbers of Windmill Graphs*, Asian-European Journal of Mathematics 16 (7) (2023) 2350123.

[7] P. Dorbec, S. Gravier, M. A. Henning, *Paired-Domination in Generalized Claw-Free Graphs*, Journal of Combinatorial Optimization 14 (2007) 1–7.

[8] T. W. Haynes, P. J. Slater, *Paired-Domination and the Paired-Domatic Number*, Congressus Numerantium 109 (1995) 65–72.

[9] S. Fitzpatrick, B. Hartnel, *Paired-Domination*, Discussiones Mathematicae Graph Theory 18 (1998) 63–72.

[10] B. Bresar, M. A. Henning, D. F. Rall, *Paired-Domination of Cartesian Products of Graphs*, Utilitas Mathematica 22 (1) (2005) 233–237.

[11] M. Dettlaff, D. Gözüpek, J. Raczek, *Paired Domination Versus Domination and Packing Number in Graphs*, Journal of Combinatorial Optimization 44 (2022) 921–933.

[12] T. W. Haynes, S. T. Hedetniemi, M. A. Henning, Domination in Graphs: Core Concepts, Springer, Cham, 2022.

[13] T. W. Haynes, S. T. Hedetniemi, M. A. Henning, Topics in Domination in Graphs, Springer, Cham, 2020.

[14] T. W. Haynes, S. T. Hedetniemi, M. A. Henning, Structures of Domination in Graphs, Springer, Cham, 2021.

[15] G. Chartrand, L. Lesniak, P. Zhang, Graphs & Digraphs, 6th Edition, Chapman and Hall/CRC, New York, 2015.

[16] M. Behzad, *A Criterion for the Planarity of a Total Graph*, Mathematical Proceedings of Cambridge Philosophy Society 63 (1967) 679–681.

[17] B. Wu, J. Meng, *Basic Properties of Total Transformation Graphs*, Journal of Mathematical Study 34 (2) (2001) 109–116.

[18] J. W. Moon, *On the Line-Graph of the Complete Bigraph*, The Annals of Mathematical Statistics 34 (1963) 664–667.

[19] V. Aytac, T. Turaci, *Analysis of Vulnerability of Some Transformation Networks*, International Journal of Foundations of Computer Science 34 (1) (2023) 11–24.

[20] A. Aytac, T. Turaci, *Vulnerability Measures of Transformation Graph* G^{xy+}, International Journal of Foundations of Computer Science 26 (6) (2015) 667–675.

[21] A. Aytac, T. Turaci, *Bondage and Strong-Weak Bondage Numbers of Transformation Graphs* G^{xyz}, International Journal of Pure and Applied Mathematics 106 (2) (2016) 689–698.

[22] A. Aytac, T. Turaci, *On the Domination, Strong and Weak Domination in Transformation Graph* G^{xy-}, Utilitas Mathematica 113 (2019) 181–189.

[23] M. K. A. Jebitha, J. P. Joseph, *Domination in Transformation Graph*, International Journal of Mathematical Combinatorics 1 (2012) 58–73.

[24] X. Lan, W. Baoyindureng, *Transformation Graph*, Discrete Mathematics 308 (2008) 5144–5148.

[25] L. Yi, B. Wu, *The Transformation Graph* G^{++-}, The Australasian Journal of Combinatorics 44 (2009) 37–42.

[26] W. Baoyindureng, L. Zhang, Z. Zhang, *The Transformation Graph* G^{xyz} *when* $xyz = -++$, Discrete Mathematics 296 (2005) 263–270.

Journal of New Theory
ISSN: 2149-1402

44 (2023) 62-78
Journal of New Theory
https://dergipark.org.tr/en/pub/jnt
Open Access

A New Form of Smooth Cubic Surfaces with 9 Lines

Fatma Karaoğlu[1]

Article Info
Received: 11 Aug 2023
Accepted: 27 Sep 2023
Published: 30 Sep 2023
doi:10.53570/jnt.1341754
Research Article

Abstract — A smooth cubic surface has at most 27 lines, with equality if and only if the underlying field is algebraically closed. Only a few cases are possible regarding the number of lines over fields that are not algebraically closed. The next two cases of interest are smooth cubic surfaces with 15 or 9 lines. The author has recently settled the case of 15 lines. In this paper, we address the case of smooth cubic surfaces with 9 lines. We describe a way to create some cubic surfaces with 9 or more lines based on a set of six field elements. Conditions on the six parameters are given under which the surface has exactly 9, 15, or 27 lines. However, the problem of generating all cubic surfaces with 9 lines remains open.

Keywords *Cubic surface, parametrization, non-algebraically closed fields*

Mathematics Subject Classification (2020) 14G27, 68W30

1. Introduction

It is well known that a smooth cubic surface over an algebraically closed field has exactly 27 lines [1]. However, the number of lines over a non-algebraically closed field varies. Naturally, the following question arises: How many lines can a smooth cubic surface have over a non-algebraically closed field? The problem of determining these numbers over the fields of $\mathbb{R}$, $\mathbb{Q}$, $\mathbb{F}_q$ where q is odd, and $\mathbb{F}_2$ has been considered by several authors [2–5]. In [6], the author gives the possible number of lines of smooth cubic surfaces over $\mathbb{F}_q$ where q is even. The number of lines of a smooth cubic surface is one of 27, 15, 9, 7, 5, 3, 2, 1, or 0 [3]. The results on cubic surfaces with 15 or 27 lines over a given field are found in [7–11], as well as using alternative methods in papers [12–14]. All the classification results agree with an enumerative formula recently found by Das [15].

In this paper, we focus on smooth surfaces with at least 9 lines over various fields, characteristic 0 or p. In [2], Schlafli described 27 lines of the cubic surface, explaining the line intersection properties. Each line intersects ten others and skews to 16. He defined the term "double-six", which has 12 lines with some special properties, and another 15 can be produced by these 12. To give the intersection properties of the lines for 9, we use the same idea of the double-six but for double-three. Smooth cubic surfaces may only have less than 27 lines if the field is nonalgebraically closed. However, over the algebraic closure of that field, the surface will have 27 lines. Therefore, we can use Schlafli labeling to notate 9 lines. We will then prove that the line intersection graph of the smooth cubic surfaces with 9 lines is unique.

[1]fkaraoglu@gtu.edu.tr (Corresponding Author)
[1]Department of Mathematics, Faculty of Natural Sciences, Gebze Technical University, Kocaeli, Türkiye

We go back to the original proof by Cayley and Salmon that the surface has 27 lines over the algebraically closed fields as we did in [11]. We see that there is a discriminant condition certain polynomial of degree 5, which can have irreducible factors of degree 3 over the field $\mathbb{F}$, which is not algebraically closed. When this happens, we end up with cubic surfaces with 9 lines. Considering the rational lines over a given field $\mathbb{F}$, we formulate the conditions that the surface has 9 lines over the given field. We describe smooth cubic surfaces with at least 9 lines using six parameters. Our approach is experimental. We study some examples of smooth cubic surfaces with 9 lines that we obtain using the computer algebra system Orbiter [16]. Once we observe the pattern, we make the computer free proof. The proof is based on the symmetry of the projective group. We use the computer algebra system Maple for the symbolic computations. When we extend the field over the algebraic closure $\overline{\mathbb{F}}$, the surface is complete to 27 lines since these surfaces are smooth. Using our model, we will show examples of cubic surfaces over a field of characteristic zero and p. These examples would have 9, 15, or 27 lines depending on whether the special polynomial is irreducible or reducible into two irreducible polynomials or splits completely over the base field.

We give the rational parameterization of points of our new form. To do this, we study the birational map between cubic surfaces and a plane, [9, 17]. There is an exceptional locus, and the birational map is defined outside the exceptional locus bijective. The exceptional locus of the map on the plane is two conics and a line. The exceptional locus of the map on the surface is two skew lines and one transversal line. We give them explicitly.

The smooth cubic surface has q^2+tq+1 points where t is between -2 and 7, but 6 is never possible [18]. Studying the birational map helps us to prove that the smooth cubic surfaces with 9 lines have q^2+4q+1 points. If the cubic surface has a double-six, then the surface is smooth and has exactly 27 lines. However, if the surface has a double-three, it does not necessarily have exactly 9 lines. It can have more lines, in which case the surface is singular. Hence, a necessary condition for the smoothness of our new form is needed. We give this condition using the rational parameterization of our new form.

In section 2, we will provide some basic theory about the cubic surfaces with 27 lines since the structure of smooth cubic surfaces with 9 lines is the sub-configuration of the structure of cubic surfaces with 27 lines. In section 3, we show the uniqueness of 9 lines and investigate the configuration. In this section, we also give our new form for smooth cubic surfaces with at least 9 lines using six parameters, and we provide the conditions when the surface has exactly 9, 15, or 27 over the given field. In section 4, we provide examples of various fields, including $\mathbb{Q}$ and some finite fields. In section 5, we give the rational parameterization of our new form and the condition when our form is smooth. In section 6, we discuss future work.

2. Preliminaries

In this section, we provide some background material on cubic surfaces and projective geometry over finite fields. For a deeper treatment, we refer to [11, 19, 20].

A finite field is a field with only a finite number of elements. $\mathbb{F}_q$ is a finite field of order $q = p^k$ where p is a prime number. The characteristic of the field is the smallest n such that $\underbrace{1+1+1+\cdots+1}_{n\ times} = 0$. The characteristic of $\mathbb{F}_q$ is p. $\overline{\mathbb{F}}_p = \mathbb{F}_p$ adjoints all the roots of polynomials over $\mathbb{F}_p$. $\overline{\mathbb{F}}_p$ is an algebraically closed field of characteristic p. $\overline{\mathbb{F}}_p$ contains every $\mathbb{F}_{p^e}$, for all $e \geq 1$. Each $\mathbb{F}_p$ has a unique $\overline{\mathbb{F}}_p$.

Let $\mathbb{F}$ be a field. A projective space $\mathrm{PG}(n, \mathbb{F})$ is a partially ordered set of subspaces of a vector space $\mathbf{v}(n+1, \mathbb{F})$. It is a lattice with respect to "join" and "meet". Join is the span of two subspaces. Meet

is the intersection of two subspaces. In $\mathrm{PG}(3,\mathbb{F})$, a point is denoted by $P=\mathbf{P}(\alpha_0,\alpha_1,\alpha_2,\alpha_3)$. A line through the points $\mathbf{P}(\beta_0,\beta_1,\beta_2,\beta_3)$ and $\mathbf{P}(\gamma_0,\gamma_1,\gamma_2,\gamma_3)$ is denoted by

$$\ell \;=\; \mathbf{L}\begin{bmatrix}\beta_0 & \beta_1 & \beta_2 & \beta_3\\ \gamma_0 & \gamma_1 & \gamma_2 & \gamma_3\end{bmatrix}$$

The plane consists of the non-collinear points $\mathbf{P}(\alpha_0,\alpha_1,\alpha_2,\alpha_3)$, $\mathbf{P}(\beta_0,\beta_1,\beta_2,\beta_3)$, and $\mathbf{P}(\gamma_0,\gamma_1,\gamma_2,\gamma_3)$ and is denoted by

$$\pi=\mathbf{v}(c_0x_0+c_1x_1+c_2x_2+c_3x_3)=\begin{bmatrix}\alpha_0 & \alpha_1 & \alpha_2 & \alpha_3\\ \beta_0 & \beta_1 & \beta_2 & \beta_3\\ \gamma_0 & \gamma_1 & \gamma_2 & \gamma_3\end{bmatrix}$$

where c_0, c_1, c_2, and c_3 are elements of the field $\mathbb{F}$.

A conic is a curve of degree 2 in $\mathrm{PG}(2,\mathbb{F})$. It is either an irreducible conic, two distinct lines, or a double line. The space of quadratic polynomials in three variables has dimension 6. To determine conic in the associated projective space, 5 linearly independent conditions are required. A cubic curve is a curve of degree three in $\mathrm{PG}(2,\mathbb{F})$. It is one of the following: an irreducible cubic, a conic, and a line, 3 different lines, or 2 different lines such that one of which is a double or a triple line. To determine a conic in the associated projective space, 9 linearly independent conditions are required. A k-arc in $\mathrm{PG}(2,\mathbb{F})$ is a set of k points where no three are collinear.

Let π be a plane in $\mathrm{PG}(3,\mathbb{F})$, and Q be a point on π. Let ℓ_1 and ℓ_2 be two skew lines in $\mathrm{PG}(3,\mathbb{F})\setminus\pi$. Then, there is a unique transversal line of ℓ_1 and ℓ_2 through Q.

The automorphism group $\mathrm{P\Gamma L}(n+1,\mathbb{F})$ of $\mathrm{PG}(n,\mathbb{F})$ is the group of bijective mappings that preserve collinearity. The collineation group contains $\mathrm{PGL}(n+1,\mathbb{F})$ as subgroup which is the group of projectivities of $\mathrm{PG}(n,\mathbb{F})$. $\mathrm{PGL}(4,\mathbb{F})$ is transitive on the points, lines, and planes of $\mathrm{PG}(3,\mathbb{F})$. In $\mathrm{PG}(n,\mathbb{F})$, any $(n+2)$-arc can be mapped to any other $(n+2)$-arc. The pointwise stabilizer of a hyperplane π in the $\mathrm{PGL}(4,\mathbb{F})$ is transitive on the set of two skew lines of $\mathrm{PG}(3,\mathbb{F})$ not in π which meet the fixed plane π in two points.

Let f be a homogeneous cubic equation in 4 variables over the field $\mathbb{F}$. A *cubic surface* $\mathcal{F}$ in $\mathrm{PG}(3,\mathbb{F})$ is the zero set of f. For instance,

$$\mathcal{F}=\mathbf{v}(f)=\mathbf{v}(x_0^3+x_1^3+x_2^3+x_3^3-(x_0+x_1+x_2+x_3)^3)$$

The cubic surface is smooth if the following system of equations has no solution:

$$\begin{cases} f(x_0,x_1,x_2,x_3)=0\\ \frac{\partial f(x_0,x_1,x_2,x_3)}{\partial x_0}=0\\ \frac{\partial f(x_0,x_1,x_2,x_3)}{\partial x_1}=0\\ \frac{\partial f(x_0,x_1,x_2,x_3)}{\partial x_2}=0\\ \frac{\partial f(x_0,x_1,x_2,x_3)}{\partial x_3}=0 \end{cases}$$

To define a cubic surface $\mathcal{F}$ in $\mathrm{PG}(3,\mathbb{F})$, it is sufficient to specify 19 linearly independent points on it. A line in $\mathrm{PG}(3,\mathbb{F})$ either intersects cubic surfaces in three points, or it is the line of $\mathcal{F}$. Therefore, if the 4 points of the line are on the cubic surface, then the line lies on it. A cubic surface intersects a plane in a cubic curve. If the surface is smooth, then that cubic curve is one of the following: an irreducible cubic, a line, an irreducible conic, or 3 different lines. If the cubic surface intersects a plane in 3 different lines, then that plane is called a tritangent plane.

A "double-six" in PG$(3,\mathbb{F})$ is the set of 12 lines

$$\begin{array}{cccccc} a_1 & a_2 & a_3 & a_4 & a_5 & a_6 \\ b_1 & b_2 & b_3 & b_4 & b_5 & b_6 \end{array}$$

such that a_i intersects b_j if and only if $i \neq j$, a_i are pairwise skew, and b_i are pairwise skew.

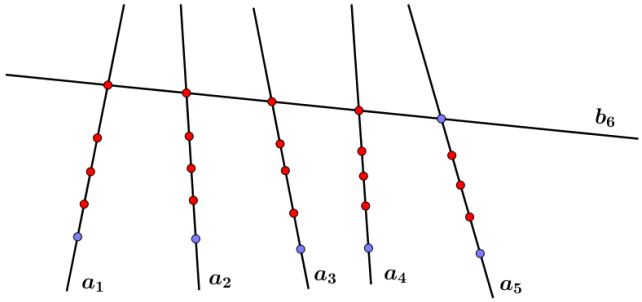

Figure 1. 19 independent points of cubic surfaces with 27 lines

A double-six determines a unique cubic surface with 27 lines. 15 further lines c_{ij} are given by $< a_i, b_j > \cap < a_j, b_i >$ [2]. The red points in Figure 1 represent the 19 independent points that determine the cubic surface with 27 lines.

When three lines of the cubic surface are concurrent at a point, then this point is called an Eckardt point. From line intersection properties, only two cases are possible: either a_i, b_j, and c_{ij} are concurrent where $i \neq j$ or c_{ij}, c_{kl}, and c_{mn} are concurrent where i, j, k, l, m, and n are all different. In the first case, we notate the Eckardt point as E_{ij}, and for the second case, $E_{ij,kl,mn}$.

There is a map between the cubic surface in PG$(3,\mathbb{F})$ and a plane. This map is called Clebsch map in [9]. Here, we refer to [9, 11, 17, 20] and repeat the description of the map. Let $\mathcal{F}$ be a cubic surface and π be a plane in PG$(3,\mathbb{F})$. Let ℓ_1 and ℓ_2 be two skew lines of $\mathcal{F}$ not lying on the plane π, and $P = \mathbf{P}(X)$ be a point of $\mathcal{F}$ which is neither on ℓ_1 nor on ℓ_2. There is a unique line ℓ through P which is the transversal to ℓ_1 and ℓ_2. The line ℓ meets π in a unique point $Q = \mathbf{P}(Y)$. Let Q be the image of P. Therefore,

$$\begin{aligned} \Phi : \mathcal{F} &\to \pi \\ P &\mapsto Q \end{aligned}$$

There is a unique line through Q that is transversal to ℓ_1 and ℓ_2. This line intersect $\mathcal{F}$ in 3 points. Two of them are on ℓ_1 and ℓ_2, let the third one to be P. The inverse Φ^{-1} of this map moves Q to P.

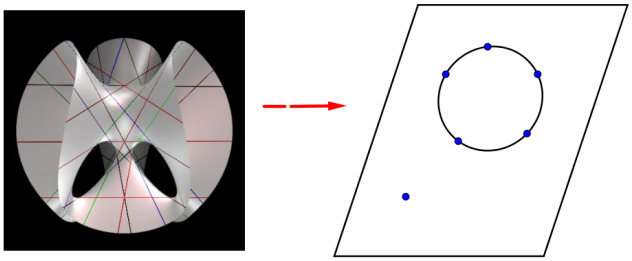

Figure 2. Birational map from cubic surfaces with 27 lines to 6-arc not on a conic

Some properties of this map are as follows: Consider that the surface $\mathcal{F}$ has 27 lines. Each line of the half double-six of $\mathcal{F}$ maps to a single point in π under Φ. These six points form a 6-arc not on a conic in the plane, see Figure 2. Outside these six lines, the map is bijective.

The following lemma is elementary. For a proof of the lemma, see Proposition 7.3 in [21]. For the sake of completeness, we include the reference of the previous paper of the author [11].

Lemma 2.1. [11,21] Let $\mathcal{F}$ be a smooth cubic surface with at least one line. The number of tritangent planes through a line of $\mathcal{F}$ is one of 0, 1, 2, 3, and 5 but never 4.

Lemma 2.2. [1] If two lines of a smooth cubic surface intersect, then they span a tritangent plane.

We introduce the following notation. Two tritangent planes are called disjoint if their line of intersection does not belong to $\mathcal{F}$.

Lemma 2.3. [22] Any two disjoint tritangent planes of $\mathcal{F}$ determine a third.

The three tritangent planes in Lemma 2.3 give rise to 9 lines of $\mathcal{F}$. These 9 lines give rise to three further tritangent planes [11, 20].

A trihedral pair consists of two sets of three tritangent planes, which pairwise intersect in 9 lines of $\mathcal{F}$ [22].

Lemma 2.4. Let $\mathcal{F}$ be a smooth cubic surface with at least 9 lines over the field $\mathbb{F}$. There exist at least four tritangent planes of $\mathcal{F}$.

Proof.
As 9 lines of $\mathcal{F}$ cannot be pairwise skew, there exist two lines ℓ_1 and ℓ_2 which intersect. From Lemma 2.2, there is a third line ℓ_3 such that ℓ_1, ℓ_2, and ℓ_3 form a tritangent plane. Any line not contained in a hyperplane intersects the hyperplane at a point. In the case of a tritangent plane and a line of the surface, this point of intersection must be on one of the three lines of the tritangent plane. Hence, each m_i such that $i \in \{1, \ldots, 6\}$ intersect one of the ℓ_j such that $j \in \{1, 2, 3\}$. This gives rise to 6 pairs (ℓ_j, m_i) of intersecting lines. By Lemma 2.2, these 6 pairs create at least 3 tritangent planes different from the tritangent plane through ℓ_1, ℓ_2, and ℓ_3. □

Lemma 2.5. Let $\mathcal{F}$ be a smooth cubic surface with at least 9 lines over the field $\mathbb{F}$. Lemma 2.4 guarantees that there are at least 4 tritangent planes. If these 4 tritangent planes of $\mathcal{F}$ intersect pairwise in a line of the surface, then they all intersect in the same line of $\mathcal{F}$.

Proof.
Let π_1, π_2, π_3, and π_4 be the tritangent planes arising from Lemma 2.4. Let π_1 and π_2 intersect in the line a_1 of $\mathcal{F}$. Without loss of generality, we may assume that π_1 is spanned by a_1, b_2, and c_{12}, and π_2 is spanned by a_1, b_3, and c_{13}. The lines b_2 and c_{12} are skew to the lines b_3 and c_{13}. Therefore, if the third tritangent plane π_3 intersects π_1 and π_2 in lines of $\mathcal{F}$, this line must be a_1. The same holds true for π_4. □

Lemma 2.6. Let $\mathcal{F}$ be a smooth cubic surface with at least 9 lines over the field $\mathbb{F}$. Then, there is at least one pair of disjoint tritangent planes.

Proof.
From Lemma 2.4, there exist 4 tritangent planes of $\mathcal{F}$. To show that a disjoint pair of tritangent planes exist, we assume the opposite. From Lemma 2.5, these planes are all through the same line. By Lemma 2.1, there exists a fifth tritangent plane in this pencil. This configuration gives rise to 11 lines of the surface. Because of Lemma 2.2, any further line would create another tritangent plane not passing through a_1, contradicting Lemma 2.5, and it is not possible that a smooth cubic surface to have 11 lines. □

3. Construction of a Smooth Cubic Surface with 9 Lines

This section proves the uniqueness of the line intersection graph of a smooth cubic surface with 9 lines and defines double-three. Besides, is provides a new form of smooth cubic surfaces with at least 9 lines involving 6 parameters.

The result of Cayley (and Salmon) in [1] is strengthened for smooth cubic surfaces with 15 lines in [11]. In this section, we will strength this result for cubic surfaces with 9 lines.

Theorem 3.1. The line intersection graph of a smooth cubic surface with exactly 9 lines over $\mathbb{F}$ is unique.

Proof.
Let $\mathcal{F}$ be a smooth cubic surface with 9 lines over $\mathbb{F}$. By Lemma 2.6, there is a pair of disjoint tritangent planes. Because of Lemma 2.3, there is a unique third tritangent plane which is also disjoint to others. The 9 lines obtained in this way give rise to 3 more tritangent planes. Hence, there exists a trihedral pair of $\mathcal{F}$. In addition, there are 2 tritangent planes through each line of $\mathcal{F}$. Moreover, each line in the trihedral pair intersects 4 others and is skew to 4. Therefore, it is unique. □

Let ℓ be a line of $\mathcal{F}$ and $\pi(\mu)$ be the plane through ℓ. $\pi(\mu)$ intersects $\mathcal{F}$ in a conic $C(\mu)$ and the line ℓ. Let $\mathcal{Q}(\mu)$ be a quadratic polynomial which represents $C(\mu)$. We define $\Delta(\mu)$ as the discriminant of the quadratic polynomial $\mathcal{Q}(\mu)$ as in the proof of Lemma 2.1.

Theorem 3.2. Let $\mathbb{F}$ be a non-algebraically closed field, and $\mathcal{F}$ be a smooth cubic surface with at least one line. The smooth cubic surface $\mathcal{F}$ has exactly 9 lines over $\mathbb{F}$ if and only if $\Delta(\mu)$ consists of an irreducible polynomial of degree 3 and 2 linear factors over $\mathbb{F}$.

Proof.
If $\Delta(\mu)$ has two linear factors over the field $\mathbb{F}$, then there exists 2 tritangent planes through ℓ. With a similar argument in the proof of Theorem 11 in [11], we start with a fixed tritangent plane. There is one more tritangent plane through each of the three lines of the fixed plane. This gives 3 tritangent planes different from the one we started with. Each tritangent plane gives rise to 2 new lines. Counting all lines gives $1 + 2 + 3 \cdot 1 \cdot 2 = 9$ lines. If $\mathcal{F}$ has exactly 9 lines, there are 2 tritangent planes through each line of $\mathcal{F}$ from Theorem 3.1. Therefore, there are exactly 2 distinct solutions for $\mu \in \mathbb{F}$ in the $\Delta(\mu)$. Hence, $\Delta(\mu)$ has exactly two distinct linear factors. □

To give the intersection properties of the lines for smooth cubic surfaces with exactly 9 lines, we used the same idea of double-six but for double-three.

Definition 3.3. Let $\mathbb{F}$ be a field. A *double-three* in $\mathrm{PG}(3, \mathbb{F})$ is the set of 6 lines

$$\begin{array}{ccc} a_1 & a_2 & a_3 \\ b_1 & b_2 & b_3 \end{array}$$

such that each line is skew to the ones in the same column or row and meets others. One row from the array is called half double-three.

Once a smooth cubic surface include a double-three, then it follows with 3 more lines which arise from the intersection of the following planes:

$$c_{12} = \langle a_1, b_2 \rangle \cap \langle a_2, b_1 \rangle$$

$$c_{13} = \langle a_1, b_3 \rangle \cap \langle a_3, b_1 \rangle$$

and

$$c_{23} = \langle a_2, b_3 \rangle \cap \langle a_3, b_2 \rangle$$

The intersection table of 9 lines can be seen in Table 1. We insert 1 in the table if the lines intersect; otherwise, 0.

Table 1. Pairwise intersection table of the 9 lines

	a_1	a_2	a_3	b_1	b_2	b_3	c_{12}	c_{13}	c_{23}
a_1	–	0	0	0	1	1	1	1	0
a_2	0	–	0	1	0	1	1	0	1
a_3	0	0	–	1	1	0	0	1	1
b_1	0	1	1	–	0	0	1	1	0
b_2	1	0	1	0	–	0	1	0	1
b_3	1	1	0	0	0	–	0	1	1
c_{12}	1	1	0	1	1	0	–	0	0
c_{13}	1	0	1	1	0	1	0	–	0
c_{23}	0	1	1	0	1	1	0	0	–

The following theorem presents a new form of a smooth cubic surfaces with 9 lines.

Theorem 3.4. Let $\mathbb{F}$ be a field with at least 4 elements. Let $a, c \in \mathbb{F} \setminus \{0, 1\}$, $b, d \in \mathbb{F} \setminus \{0, -1\}$, and $f, g \in \mathbb{F} \setminus \{0\}$ such that $b \neq d$ and $f \neq g$. Let $\mathcal{F}_{a,b,c,d,f,g} = \mathbf{v}(\mathfrak{f}_{a,b,c,d,f,g})$ be the variety over $\mathbb{F}$ given by the equation $\mathfrak{f}_{a,b,c,d,f,g}$

$$\begin{aligned} &d_{002}x_0^2x_2 + d_{012}x_0x_1x_2 + d_{013}x_0x_1x_3 + d_{022}x_0x_2^2 + d_{023}x_0x_2x_3 \\ &+d_{112}x_1^2x_2 + d_{113}x_1^2x_3 + d_{122}x_1x_2^2 + d_{123}x_1x_2x_3 + d_{133}x_1x_3^2 = 0 \end{aligned} \tag{1}$$

where

$$\begin{aligned} d_{002} &= bg\kappa_3 & d_{113} &= d_{112} \\ d_{012} &= g(a+b)\kappa_2 - f(bf+a)\kappa_1 & d_{023} &= -abg\kappa_3 \\ d_{013} &= f\kappa_1\kappa_4 & d_{122} &= -cf\kappa_4 \\ d_{022} &= ag\kappa_3 & d_{133} &= cdf\kappa_4 \\ d_{112} &= -(1+d)f\kappa_4 & d_{123} &= (d-1)cf\kappa_4 \end{aligned}$$

$$\begin{aligned} \kappa_1 &= c + d + 1 \\ \kappa_2 &= dg + c + g \\ \kappa_3 &= cf + df - dg - c + f - g \\ \kappa_4 &= ag - bf + bg - a \\ \kappa_5 &= abd + acd + bcd + ab \\ \kappa_6 &= abc + abd + bcd + ab \end{aligned}$$

$$\kappa_3 \neq 0,\ \kappa_4 \neq 0,\ a\kappa_1 + bc \neq 0, \quad \text{and} \quad a\kappa_2 + bcf \neq 0$$

Let $\mathbf{g}_{a,b,c,d,f,g}$ be the polynomial

$$\mathbf{g}_{a,b,c,d,f,g} = A_3\mu^3 + A_2\mu^2 + A_1\mu + A_0 \tag{2}$$

in μ such that

$$A_0 = -bcdf(ac + ad + cd + a)(ag - bf + bg - a)$$

$$A_1 = g^2A_{12} + g(c^2A_{112} + cA_{111} + A_{110}) + A_{10}$$

$$A_2 = a^2(fA_{221} + A_{220}) - abc(f^2A_{212} + fA_{211} + A_{210}) + A_{20}$$

$$A_3 = (f - g)(ac + ad + bc + a)(adg + bcf + ac + ag)$$

and

$$A_{12} = -a(d+1)b(abd + acd + bcd + ab) \qquad A_{220} = g(dg + c + g)(bc + 2bd + cd + 2b)$$

$$A_{112} = -(a+b)(bd^2f + abd - abf - adf - 2bdf) \qquad A_{212} = (c + d + 1)(b + d - 1)$$

$$A_{111} = a(d+1)(ab^2f - ab^2 + abf + adf + b^2f + bdf) \qquad A_{211} = -2cdg + 2cd + 2cg + dg - c + g$$

$$A_{110} = a^2b^2f(d+1)^2 \qquad A_{210} = -g(dg + c + g)(b + d)$$

$$A_{221} = -(c + d + 1)(2bdg + bc + 2bg + cd + cg - c) \qquad A_{20} = -b^2c^2f(f - g)(2d - 1)$$

$$A_{10} = cf(bf + a)(abcd + abd^2 + bcd^2 - abc - acd - ad^2 - 2bcd - ab - ad)$$

Assume that the surface $\mathcal{F}_{a,b,c,d,f,g}$ is smooth over $\mathbb{F}$. The surface $\mathcal{F}_{a,b,c,d,f,g}$ has at least 9 lines, six of which form a double-three. The conditions on the exact number of lines of $\mathcal{F}_{a,b,c,d,f,g}$ depends on the polynomial $\mathbf{g}_{a,b,c,d,f,g}$ of degree three.

i. If the polynomial $\mathbf{g}_{a,b,c,d,f,g}$ is irreducible over the field $\mathbb{F}$, then the surface $\mathcal{F}_{a,b,c,d,f,g}$ has exactly 9 lines.

ii. If $\mathbf{g}_{a,b,c,d,f,g}$ is reducible into one irreducible quadratic polynomial and one linear over the field $\mathbb{F}$, then the surface $\mathcal{F}_{a,b,c,d,f,g}$ has exactly 15 lines.

iii. If $\mathbf{g}_{a,b,c,d,f,g}$ splits completely to 3 linear factors over the field $\mathbb{F}$, then the surface $\mathcal{F}_{a,b,c,d,f,g}$ has exactly 27 lines.

In Table 2, the parametrization of the 9 lines of $\mathcal{F}_{a,b,c,d,f,g}$ can be observed.

Table 2. Lines of $\mathcal{F}_{a,b,c,d,f,g}$

$$a_1 = \mathbf{L}\begin{bmatrix} a(b+1) & 0 & -b & b \\ a+b & b & 0 & 0 \end{bmatrix} \qquad a_2 = \begin{cases} \mathbf{L}\begin{bmatrix} 1 & 0 & 0 & 0 \\ 0 & d_{133} & 0 & -d_{112} \end{bmatrix}, & \kappa_1 = 0 \\ \mathbf{L}\begin{bmatrix} -cd & 0 & 0 & \kappa_1 \\ 1+d & \kappa_1 & 0 & 0 \end{bmatrix}, & \text{otherwise} \end{cases} \qquad a_3 = \mathbf{L}\begin{bmatrix} 0 & 0 & 0 & 1 \\ 0 & 0 & 1 & 0 \end{bmatrix}$$

$$b_1 = \mathbf{L}\begin{bmatrix} 1 & 0 & 0 & 0 \\ 0 & 0 & 0 & 1 \end{bmatrix} \qquad b_2 = \mathbf{L}\begin{bmatrix} 0 & 1 & 0 & 0 \\ 0 & 0 & -1 & 1 \end{bmatrix} \qquad b_3 = \mathbf{L}\begin{bmatrix} 1 & 1 & 1 & 0 \\ c(b-d)a & 0 & \kappa_6 & a\kappa_1 + bc \end{bmatrix}$$

$$c_{12} = \mathbf{L}\begin{bmatrix} 1 & 0 & 0 & 0 \\ 0 & 1 & 0 & 0 \end{bmatrix} \qquad c_{13} = \mathbf{L}\begin{bmatrix} a & 0 & 0 & 1 \\ 0 & 0 & b & 1 \end{bmatrix} \qquad c_{23} = \mathbf{L}\begin{bmatrix} 0 & 0 & d & 1 \\ 0 & c & -1 & 1 \end{bmatrix}$$

Proof.

The group $\mathrm{PGL}(4, \mathbb{F})$ is transitive on the planes. Therefore, we can start from any hyperplane. Hence, we may pick $\pi = \mathbf{v}(x_3)$. Consider that we want to construct a cubic surface $\mathcal{F}$ with 9 lines, including

the double-three. Considering the sub-configuration of Schlafli configuration and the labeling for 9 lines, we may choose the labels that a_1, a_2, a_3, b_1, b_2, b_3, c_{12}, c_{13}, and c_{23}. To determine this surface $\mathcal{F}$, we have to specify 19 independent conditions. Nine of them should be on the plane π since the cubic surface intersects π in a cubic curve. We can assume that the coordinates of 4 of those 9 points are $P_1 = \mathbf{P}(1,0,0,0)$, $P_2 = \mathbf{P}(1,0,0,0)$, $P_3 = \mathbf{P}(1,0,0,0)$, and $P_4 = \mathbf{P}(1,0,0,0)$ since the projective group of the plane is transitive on the quadrangles. Since $\mathrm{PGL}(4,\mathbb{F})$ is transitive on the lines, we can pick the first line of the surface $\mathcal{F}$ without any constraints. Let assume that the first line of $\mathcal{F}$ is

$$c_{12} = \mathbf{L}\begin{bmatrix} 1 & 0 & 0 & 0 \\ 0 & 1 & 0 & 0 \end{bmatrix}$$

Since c_{12} lies on the surface $\mathcal{F}$, there are 2 more independent points on the intersection $c_{12} \cap \mathcal{F}$. Assume that $P_7 = \mathbf{P}(1,1,0,0)$ and $P_8 = \mathbf{P}(-1,1,0,0)$ are the points of $\mathcal{F}$ as well as c_{12} is transitive. It is known that the pointwise stabilizer of the hyperplane π in the $\mathrm{PGL}(4,\mathbb{F})$ is transitive on the set of two skew lines of $\mathrm{PG}(3,\mathbb{F})$ not in π which meet the fixed plane π in two points P_1 and P_2. Therefore, we are free to choose two skew lines not on the plane π through P_1 and P_2. Let

$$b_1 = \mathbf{L}\begin{bmatrix} 1 & 0 & 0 & 0 \\ 0 & 0 & 0 & 1 \end{bmatrix} \quad \text{and} \quad b_2 = \mathbf{L}\begin{bmatrix} 0 & 1 & 0 & 0 \\ 0 & 0 & -1 & 1 \end{bmatrix}$$

are the two skew lines. b_1 are through P_1 and $P_5 = \mathbf{P}(0,0,0,1)$ and b_2 are through P_2 and $P_6 = \mathbf{P}(0,0,-1,1)$. It is known that there is a unique line through P_2 and transversal to b_1 and b_2. We call this line is a line of $\mathcal{F}$. Because of the configuration of 9 lines, we can label that line as a_3 and it is the line through P_5 and P_6,

$$a_3 = \mathbf{L}\begin{bmatrix} 0 & 0 & 0 & 1 \\ 0 & 0 & -1 & 1 \end{bmatrix}$$

From line intersection properties, we know that there exists a line c_{23} which meets b_2 and a_3 and skew to c_{12}, i.e., not in π. When a_3, b_2, and c_{23} are not concurrent which means the Eckardt point E_{32} does not exist, we may set the line c_{23} through $P_9 = \mathbf{P}(0,c,-1,1)$ and $P_{10} = \mathbf{P}(0,0,d,1)$. Since P_2, P_6, and P_9 are three distinct points from our assumption, we have $0 \neq c \neq 1$.

From line intersection properties, we know that there exists a line c_{13} which meets b_1 and a_3 and skew to c_{12}, i.e., not in π. When a_3, b_1, and c_{13} are not concurrent which means the Eckardt point E_{31} does not exist, we may set the line c_{13} through $P_{11} = \mathbf{P}(a,0,0,1)$ and $p' = \mathbf{P}(0,0,b,1)$. Since P_1, P_5, and P_{11} are three distinct points from our assumption, we have $0 \neq a \neq 1$. Therefore, two lines of $\mathcal{F}$ are

$$c_{13} = \mathbf{L}\begin{bmatrix} a & 0 & 0 & 1 \\ 0 & 0 & b & 1 \end{bmatrix} \quad \text{and} \quad c_{23} = \mathbf{L}\begin{bmatrix} 0 & c & -1 & 1 \\ 0 & 0 & d & 1 \end{bmatrix}$$

Since P_3, P_5, P_6, P_{10}, and p' are five distinct points on the line a_3, we have $b, d \notin \{0,-1\}$ and $b \neq d$. Since there are already 4 independent points on a_3, we do not count the point p'. The plane π intersects the line c_{13} at the point $P_{13} = \mathbf{P}(-a,0,b,0)$ and intersects the line c_{23} at the point $P_{12} = \mathbf{P}(0,-c,d+1,0)$. From line intersection properties, we know that there exists a line b_3 which meets c_{13} and c_{23} and skew to a_3, b_1, b_2, and c_{12}. The line b_3 cannot intersect the line through P_1 and P_3 and the line through P_2 and P_3 since those lines already have 3 points of $\mathcal{F}$ each. The new line b_3 is either P_4 or $P_{19} = \mathbf{P}(f,g,1,0)$. For this new form, we consider the b_3 is through P_4. We know that the line c_{13} and c_{23} are not in π, and they are skew. Hence, the transversal line b_3 to c_{13} and c_{23} through P_4 is uniquely determined. It intersects c_{13} at the point $P_{14} = \mathbf{P}(ac(b-d),0,\kappa_6,a\kappa_1+bc)$ and intersects c_{23} at the point $P_{15} = \mathbf{P}(0,-ac(b-d),\kappa_5,a\kappa_1+bc)$ where $\kappa_1 = c+d+1$, $\kappa_5 = abd+acd+bcd+ab$,

and $\kappa_6 = abc + abd + bcd + ab$. Thus,

$$b_3 = \mathbf{L}\begin{bmatrix} 1 & 1 & 1 & 0 \\ c(b-d)a & 0 & \kappa_6 & a\kappa_1 + bc \end{bmatrix}$$

The line c_{13} already has 4 independent points of $\mathcal{F}$ which are p', P_{11}, P_{13}, and P_{14}. Hence, it is a line of $\mathcal{F}$. The line c_{23} already has 4 independent points of $\mathcal{F}$ which are P_{12}, P_{10}, P_9, and P_{15}. Thus, it is a line of $\mathcal{F}$. The lines b_1, b_2, and b_3 have 3 points of $\mathcal{F}$ each. Therefore, we force the points $P_{16} = \mathbf{P}(1,0,0,1)$, $P_{17} = \mathbf{P}(0,1,-1,1)$, and $P_{18} = a \cdot P_{15} + P_{14}$ to be on the surface $\mathcal{F}$. The following 18 points are chosen to force the lines

$$b_1, b_2, b_3, a_3, c_{12}, c_{13}, \quad \text{and} \quad c_{23}$$

to be on the cubic surface. More conditions arise from the fact that the cubic surface intersects the plane $\mathbf{v}(x_3)$ in a cubic curve which consists of the line c_{12} and an irreducible conic. Besides, we have considered the 8 points on π

$$P_1,\ P_2,\ P_3,\ P_4,\ P_7,\ P_8,\ P_{12}, \quad \text{and} \quad P_{13}$$

We need to force one further point of the surface to lie on this plane. We may pick the point $P_{19} = \mathbf{P}(f,g,1,0)$. The conic through P_3, P_4, P_{12}, P_{13}, and P_{19} is irreducible. This gives the restriction on the parameters a, b, c, d, f, and g such that $a,c,f,g \neq 0$, $f \neq g$, $\kappa_3 \neq 0$, $\kappa_4 \neq 0$, $a\kappa_1 + bc \neq 0$, and $a\kappa_2 + bcf \neq 0$.

The points $P_1, \ldots, P_{19}$ define the cubic surface uniquely since they are linearly independent. Using Maple, we compute the equation $\mathfrak{f}_{a,b,c,d,f,g}$ as in Equation 1 which is the unique equation of a cubic surface $\mathcal{F}_{a,b,c,d,f,g}$ defined by these 19 points. This surface also involves a double-three. By Theorem 3.1, we know that there is only one way to complete the configuration of the lines. By Definition 3.3, further lines will be defined as a_1 and a_2. These further lines a_1 and a_2 can be computed using Maple. All these 9 lines can be seen in Table 2.

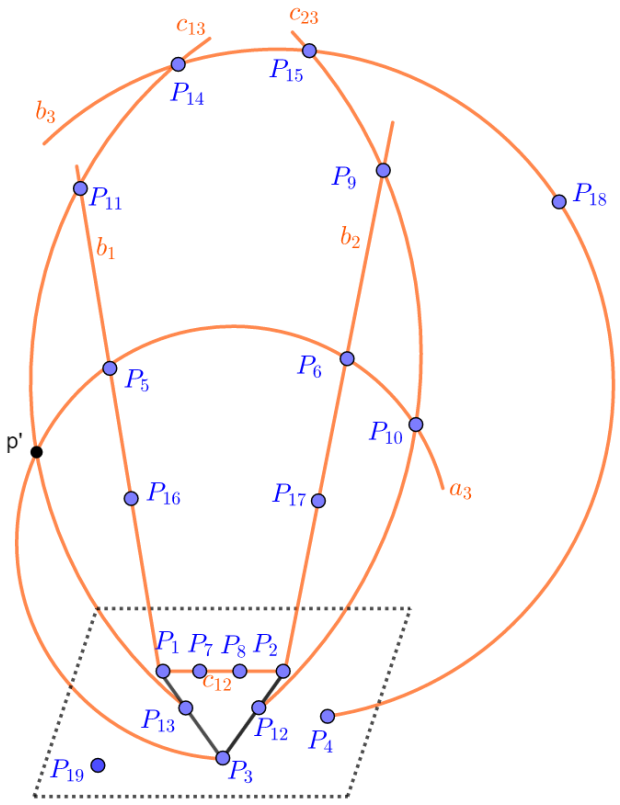

Figure 3. Configuration of 19 points

We check whether the cubic surface $\mathcal{F}_{a,b,c,d,f,g}$ has any further lines. The only possible way would be the surface having 15 or 27 lines. This depends on the discriminant condition. By Theorem 3.2 and Theorem 11 in [11], we know that it depends on the factors of the discirimant. Therefore, we need to compute it. As in the proof of Theorem 3.2, we start with a fixed tritangent plane $\pi = \mathbf{v}(x_3)$. Consider the line

$$c_{12} = \mathbf{L}\begin{bmatrix} 1 & 0 & 0 & 0 \\ 0 & 1 & 0 & 0 \end{bmatrix}$$

and the planes

$$\mathbf{v}(x_2 - \mu x_3)$$

through this line c_{12}. Each of these planes intersects $\mathcal{F}_{a,b,c,d,f,g}$ in c_{12} and in a conic $C(\mu)$. Substituting $x_2 = \mu x_3$ into the equation of Equation 1, we find the conic equation $C(\mu)$ in x_0, x_1, and x_3. Hence, we calculate the discriminant $\Delta(\mu)$ of $C(\mu)$. It has a factor of the polynomial $\mathbf{g}_{a,b,c,d,f,g}$ of degree 3 as in the Equation 2. Similarly, considering the planes through a_1 and b_2, two further polynomials $\mathbf{f}_{a,b,c,d,f,g}$ and $\mathbf{h}_{a,b,c,d,f,g}$ of degree three arise. These polynomials are not stated due to space restrictions. For a given field $\mathbb{F}$, if the polynomial $\mathbf{g}_{a,b,c,d,f,g}$ is irreducible, then $\mathbf{f}_{a,b,c,d,f,g}$ and $\mathbf{h}_{a,b,c,d,f,g}$ are irreducible, and vice versa.

There are 2 tritangent planes of $\mathcal{F}_{a,b,c,d,f,g}$ through each created 9 lines. Hence, there are either one or 3 more tritangent planes through each line. Then, these further lines would arise from the new tritangent planes.

If $\mathbf{g}_{a,b,c,d,f,g}$ is reducible into one linear factor and one irreducible quadratic, then the surface $\mathcal{F}_{a,b,c,d,f,g}$ has 15 lines over $\mathbb{F}$ from Part 2 of Theorem 11 in [11]. The further 6 lines arise as following: Each of c_{12}, a_1, and b_2 lies on one further tritangent planes, and each of which gives two lines to the surface. This gives $3 \cdot 1 \cdot 2 = 6$ further lines of $\mathcal{F}$.

If $\mathbf{g}_{a,b,c,d,f,g}$ is reducible into three linear factors, then the surface $\mathcal{F}_{a,b,c,d,f,g}$ has 27 lines over $\mathbb{F}$ from Part 1 of Theorem 11 in [11]. The further 18 lines arise as following: Each of c_{12}, a_1, and b_2 lies on three further tritangent planes, each of which gives two lines to the surface. This gives $3 \cdot 3 \cdot 2 = 18$ further lines of $\mathcal{F}$.

If the polynomial $\mathbf{g}_{a,b,c,d,f,g}$ is irreducible over $\mathbb{F}$, then the surface $\mathcal{F}_{a,b,c,d,f,g}$ has exactly 9 lines over this field by Theorem 3.2. □

Remark 3.5. Figure 3 summarises the content of Theorem 3.4 by giving the configuration of 19 points on the cubic surface and forcing the surface including the double-three.

Remark 3.6. The cubic surface $\mathcal{F}_{a,b,c,d,f,g}$ cannot have 2 specific Eckardt points. Therefore, we cannot create all possible smooth cubic surfaces with 9 lines using this form.

Remark 3.7. The line b_3 of $\mathcal{F}_{a,b,c,d,f,g}$ could be through P_{19} instead P_4. Considering this way would give another form of such surfaces.

4. Illustrative Examples

This section exemplifies the aforesaid form over finite fields and fields of characteristic zero.

Example 4.1. The surface $\mathcal{F}_{-1,1,-1,2,-1,1}$ given by the equation

$$-2x_0^2x_2 - 2x_0x_1x_2 - 2x_0x_1x_3 + 2x_0x_2^2 - 2x_0x_2x_3 + 3x_1^2x_2 + 3x_1^2x_3 - x_1x_2^2 + x_1x_2x_3 + 2x_1x_3^2 = 0$$

is smooth over $\mathbb{C}$. The polynomial

$$\mathbf{g}_{-1,1,-1,2,-1,1} = -6\mu^3 + 10\mu^2 - 16\mu + 16$$

is irreducible over $\mathbb{Q}$. Hence, the surface $\mathcal{F}_{-1,1,-1,2,-1,1}$ has exactly 9 lines over $\mathbb{Q}$. The polynomial $\mathbf{g}_{-1,1,-1,2,-1,1}$ has one real and two complex roots. Therefore, by Theorem 3.4, it has exactly 15 lines over $\mathbb{R}$ and 27 over $\mathbb{C}$.

Example 4.2. Over $\mathbb{F}_5$, the cubic surface $\mathcal{F}_{2,1,4,2,4,1}$ given by the equation

$$3x_0^2x_2 + 3x_1^2x_2 + 3x_1^2x_3 + x_0x_2^2 + 4x_1x_2^2 + 2x_1x_3^2 + 4x_0x_1x_2 + 3x_0x_1x_3 + 4x_0x_2x_3 + x_1x_2x_3 = 0$$

is smooth. Since the polynomial

$$\mathbf{g}_{2,1,4,2,4,1} = 2\mu^3 + 3\mu^2 + 4\mu + 3$$

is reducible into $(\mu+1)$ and $(2\mu^2+\mu+3)$ over $\mathbb{F}_5$, the surface $\mathcal{F}_{2,1,4,2,4,1}$ has exactly 15 lines over this field by Theorem 3.4.

Let $\tau \in \mathbb{F}_{25}$ satisfy the equation $\tau^2 + \tau + 2 = 0$. The polynomial

$$\begin{aligned}\mathbf{g}_{2,1,4,2,4,1} &= 2\mu^3 + 3\mu^2 + 4\mu + 3\\ &= (\mu+1)(2\mu^2+\mu+3)\\ &= (\mu+1)(\mu+4\tau+1)(\mu+\tau+2)\end{aligned}$$

is reducible into three linear factors over $\mathbb{F}_{25}$. Therefore, by Theorem 3.4, the surface $\mathcal{F}_{2,1,4,2,4,1}$ has exactly 27 lines over this field.

Example 4.3. Over $\mathbb{F}_5$, the cubic surface $\mathcal{F}_{4,1,4,2,4,1}$ given by the equation

$$3x_0^2x_2 + 3x_1^2x_2 + 3x_1^2x_3 + 2x_0x_2^2 + 4x_1x_2^2 + 2x_1x_3^2 + 3x_0x_1x_2 + 3x_0x_1x_3 + 3x_0x_2x_3 + x_1x_2x_3 = 0$$

is smooth. Since the polynomial

$$\mathbf{g}_{4,1,4,2,4,1} = 3\mu^3 + 3\mu + 2$$

is irreducible over $\mathbb{F}_5$, the surface $\mathcal{F}_{4,1,4,2,4,1}$ has exactly 9 lines over this field by Theorem 3.4. Over $\mathbb{F}_{25}$, this polynomial is also irreducible. Therefore, the cubic surface $\mathcal{F}_{4,1,4,2,4,1}$ has exactly 9 lines over this field.

Let $\psi \in \mathbb{F}_{125}$ satisfy the equation $\psi^3 + \psi^2 + 2 = 0$. The polynomial

$$\begin{aligned}\mathbf{g}_{4,1,4,2,4,1} &= 3\mu^3 + 3\mu + 2\\ &= (\mu + 4\psi^2 + 3\psi + 3)(\mu + 4\psi^2 + 2\psi + 1)(\mu + 2\psi^2 + 1)\end{aligned}$$

is reducible into three linear factors over $\mathbb{F}_{125}$. Therefore, the surface $\mathcal{F}_{4,1,4,2,4,1}$ has exactly 27 lines over this field by Theorem 3.4.

5. Rational Parametrization of the New Form

This section provides a parametrization of the rational points at lines of the cubic surface $\mathcal{F}_{a,b,c,d,f,g}$ given in Section 3. The proof of the following theorem is based on the birational map between the cubic surface and a plane. In Subsection 4.2 of [11], rational parametrization of a smooth cubic surface with 15 lines is given explicitly. The proof here and the remarks are similar to the proof of Theorem 8 and its following remarks in [11] but for the cubic surface with at least 9 lines $\mathcal{F}_{a,b,c,d,f,g}$.

Theorem 5.1. Let $\mathbb{F}$ be a field with at least 4 elements. Let $\mathcal{F}_{a,b,c,d,f,g}$ be the variety given in Theorem 3.4. Assume that $\mathcal{F}_{a,b,c,d,f,g}$ is smooth. Let $P = \mathbf{P}(x_0, x_1, x_2, x_3)$ be a point on $\mathcal{F}_{a,b,c,d,f,g}$ and $Q = \mathbf{P}(y_0, y_1, y_2)$ be a point in a plane so that P and Q are the images of each other under a birational map

$$\begin{aligned} \Phi_{a,b,c,d,f,g} : \quad \mathcal{F}_{a,b,c,d,f,g} &\to \mathrm{PG}(2, \mathbb{F}) \\ \mathbf{P}(x_0, x_1, x_2, x_3) &\mapsto \mathbf{P}(y_0, y_1, y_2) \end{aligned}$$

Then, (x_0, x_1, x_2, x_3) can be expressed as

$$\begin{cases} x_0 = -g(a+b)\kappa_3 y_0^2 y_1 + ga(b+1)\kappa_3 y_0^2 y_2 - (1+d)f\kappa_4 y_0 y_1^2 - fc(1+d)\kappa_4 y_0 y_1 y_2 \\ x_1 = abg\kappa_3 y_0 y_1 y_2 - cdf\kappa_4 y_1^2 y_2 - bg\kappa_3 y_0^2 y_1 - f\kappa_1\kappa_4 y_0 y_1^2 \\ x_2 = abg\kappa_3 y_0 y_2^2 - cdf\kappa_4 y_1 y_2^2 - bg\kappa_3 y_0^2 y_2 - f\kappa_1\kappa_4 y_0 y_1 y_2 \\ x_3 = gb\kappa_3 y_0^2 y_2 + ag\kappa_3 y_2^2 y_0 - cf\kappa_4 y_2^2 y_1 + d_{012} y_0 y_1 y_2 - (1+d)f\kappa_4 y_1^2 y_2 \end{cases} \tag{3}$$

and (y_0, y_1, y_2) can be expressed as

$$\begin{cases} y_0 = x_0 x_2 \\ y_1 = x_1 x_2 + x_1 x_3 \\ y_2 = x_2^2 + x_2 x_3 \end{cases} \tag{4}$$

up to a nonzero scalar multiple.

Proof.
No generality is lost by picking the plane as $\mathbf{v}(x_3)$, and the two skew lines b_1 and b_2 of $\mathcal{F}_{a,b,c,d,f,g}$

$$b_1 = \mathbf{L}\begin{bmatrix} 1 & 0 & 0 & 0 \\ 0 & 0 & 0 & 1 \end{bmatrix} \quad \text{and} \quad b_2 = \mathbf{L}\begin{bmatrix} 0 & 1 & 0 & 0 \\ 0 & 0 & -1 & 1 \end{bmatrix}$$

Let $P = \mathbf{P}(x_0, x_1, x_2, x_3)$ be a point on $\mathcal{F}_{a,b,c,d,f,g}$ but neither on b_1 nor on b_2. To find the image Q of P under $\Phi_{a,b,c,d,f,g}$, first we compute the transversal line ℓ of b_1 and b_2 through P. Then, we find the unique point Q where ℓ meets $\mathbf{v}(x_3)$ as follows:

$$\ell = \mathbf{L}\begin{bmatrix} x_0 & 0 & 0 & x_2 + x_3 \\ x_0 x_2 & x_1 x_2 + x_1 x_3 & x_2^2 + x_2 x_3 & 0 \end{bmatrix}$$

and

$$\Phi_{a,b,c,d,f,g}(\mathbf{P}(x_0, x_1, x_2, x_3)) = \mathbf{P}(y_0, y_1, y_2) = \mathbf{P}(x_0 x_2, x_1 x_2 + x_1 x_3, x_2^2 + x_2 x_3)$$

whose coordinates are given in System 4.

Conversely, let $Q = \mathbf{P}(y_0, y_1, y_2, 0)$ be a point in the plane $\mathbf{v}(x_3)$. To find the image Q of P under $\Phi^{-1}_{a,b,c,d,f,g}$, first we compute the transversal line ℓ' of b_1 and b_2 through Q as follows:

$$\ell' = \mathbf{L}\begin{bmatrix} y_0 & 0 & 0 & y_2 \\ y_0 & y_1 & y_2 & 0 \end{bmatrix}$$

Then, we find the three intersection points where ℓ' meets $\mathcal{F}_{a,b,c,d,f,g}$ by substituting the point

$$\mathbf{P}(y_0, 0, 0, y_2) + t \cdot \mathbf{P}(y_0, y_1, y_2, 0)$$

of ℓ' into the equation of $\mathcal{F}_{a,b,c,d,f,g}$. This gives a polynomial of degree three in t, for some $t \in \mathbb{F}$. Solving this polynomial in t gives 3 solutions as follows:

$$t_1 = 0$$

$$t_2 = -1$$

and

$$t_3 = \frac{abg\kappa_3 y_0 y_2 - cdf\kappa_4 y_1 y_2 - bg\kappa_3 y_0^2 - f\kappa_1\kappa_4 y_0 y_1}{gb\kappa_3 y_0^2 + ag\kappa_3 y_2 y_0 - cf\kappa_4 y_2 y_1 + d_{012} y_0 y_1 - (1+d)f\kappa_4 y_1^2}$$

The point $\mathbf{P}(y_0, 0, 0, y_2)$ arising from t_1 is the point where ℓ' meets the line b_1. The point $\mathbf{P}(0, -y_1, -y_2, y_2)$ arising from t_2 is the point where ℓ' meets the line b_2. Let $P = \mathbf{P}(x_0, x_1, x_2, x_3)$ be the third point of intersection of ℓ' with $\mathcal{F}_{a,b,c,d,f,g}$. Hence,

$$x_0 = y_0 + t_3 \cdot y_0$$

$$x_1 = t_3 \cdot y_1$$

$$x_2 = t_3 \cdot y_2$$

and

$$x_3 = y_2$$

as in System 3. Then,

$$\Phi^{-1}_{a,b,c,d,f,g}(\mathbf{P}(y_0, y_1, y_2)) = \mathbf{P}(x_0, x_1 x_2, x_3)$$

□

Remark 5.2. Let $\mathcal{F}_{a,b,c,d,f,g}$ be the smooth cubic surface over the field $\mathbb{F}$ as described in Theorem 3.4, and $\Phi_{a,b,c,d,f,g}$ be the birational map from $\mathcal{F}_{a,b,c,d,f,g}$ to the plane embedded in $\mathrm{PG}(3, \mathbb{F})$ as the hyperplane $\mathbf{v}(x_3)$, described in Theorem 5.1. Consider the lines a_1, a_2, and a_3 of $\mathcal{F}_{a,b,c,d,f,g}$. The map $\Phi_{a,b,c,d,f,g}$ sends the line a_1 to the point $\mathbf{P}(1, 0, 0)$, the line a_2 to the point $\mathbf{P}(0, 1, 0)$, and the line a_3 to the point $\mathbf{P}(0, 0, 1)$.

Remark 5.3. The exceptional locus of $\Phi_{a,b,c,d,f,g}$ on the surface consists of 3 lines of $\mathcal{F}_{a,b,c,d,f,g}$ which are b_1, b_2, and c_{12}. The exceptional locus on the plane can be found explicitly by applying $\Phi^{-1}_{a,b,c,d,f,g}$ to $\mathbf{P}(x_0, x_1, x_2, x_3)$ and then by applying $\Phi_{a,b,c,d,f,g}$ to $\mathbf{P}(y_0, y_1, y_2)$. It consists of one line and two conics in the plane, which are the line L' through $\mathbf{P}(1, 0, 0)$ and $\mathbf{P}(0, 1, 0)$ and two conics

$$D_1 = abg\kappa_3 y_0 y_2 - cdf\kappa_4 y_1 y_2 - bg\kappa_3 y_0^2 - f\kappa_1\kappa_4 y_0 y_1$$

and

$$D_2 = -f(1+d)\kappa_4 y_1^2 + ag(b+1)\kappa_3 y_0 y_2 - cf(1+d)\kappa_4 y_1 y_2 + (-f\kappa_1\kappa_4 + d_{012}) y_0 y_1$$

The points of the lines b_1 and b_2 are mapped to the points of the conics D_1 and D_2 and the points of c_{12} are mapped to the points of L' under $\Phi_{a,b,c,d,f,g}$.

Theorem 5.4. The cubic surface $\mathcal{F}_{a,b,c,d,f,g} = \mathbf{v}(\mathfrak{f}_{a,b,c,d,f,g})$ as described in Theorem 3.4 is non-singular over $\mathbb{F}$ if and only if the certain four sextic curves in $(2, \mathbb{F})$ never intersect at a point of $\mathcal{F}_{a,b,c,d,f,g}$.

Proof.
The idea of the proof is similar to the proof of Theorem 9 in [11] but for $\mathcal{F}_{a,b,c,d,f,g}$. The partial derivatives of $\mathfrak{f}_{a,b,c,d,f,g}$ as follows:

$$\frac{\partial \mathfrak{f}_{a,b,c,d,f,g}}{\partial x_0} = 2d_{002}x_0x_2 + d_{012}x_1x_2 + d_{013}x_1x_3 + d_{022}x_2^2 + d_{023}x_2x_3$$

$$\frac{\partial \mathfrak{f}_{a,b,c,d,f,g}}{\partial x_1} = d_{012}x_0x_2 + d_{013}x_0x_3 + 2d_{112}x_1x_2 + 2d_{113}x_1x_3 + d_{122}x_2^2 + d_{123}x_2x_3 + d_{133}x_3^2$$

$$\frac{\partial \mathfrak{f}_{a,b,c,d,f,g}}{\partial x_2} = d_{002}x_0^2 + d_{012}x_0x_1 + 2d_{022}x_0x_2 + d_{023}x_0x_3 + d_{112}x_1^2 + 2d_{122}x_1x_2 + d_{123}x_1x_3$$

and

$$\frac{\partial \mathfrak{f}_{a,b,c,d,f,g}}{\partial x_3} = d_{013}x_0x_1 + d_{023}x_0x_2 + d_{113}x_1^2 + d_{123}x_1x_2 + 2d_{133}x_1x_3$$

Let $P = \mathbf{P}(x_0, x_1, x_2, x_3)$ be a point of $\mathcal{F}_{a,b,c,d,f,g}$. By substituting the coordinates of the point $\mathbf{P}(y_0, y_1, y_2)$ as given in Theorem 5.1 into the four partial derivatives of $\mathfrak{f}_{a,b,c,d,f,g}$, we get four polynomials S_1, S_2, S_3, and S_4 of degree 6 in three variables y_0, y_1, and y_2. We did not present these polynomials explicitly here so that they do not take up much space. The zeros of these polynomials form curves $\mathcal{S}_1, \mathcal{S}_2, \mathcal{S}_3$, and $\mathcal{S}_4$ of degree six in $\mathrm{PG}(2, \mathbb{F})$. The point $P = \mathbf{P}(x_0, x_1, x_2, x_3)$ is a singular point if and only if it appears on all the partial derivatives of $\mathfrak{f}_{a,b,c,d,f,g}$ if and only if the curves $\mathcal{S}_1, \mathcal{S}_2, \mathcal{S}_3$, and $\mathcal{S}_4$ intersect at P. Therefore, the surface is non singular if and only if the curves $\mathcal{S}_1, \mathcal{S}_2, \mathcal{S}_3$, and $\mathcal{S}_4$ never intersect in a point of $\mathcal{F}_{a,b,c,d,f,g}$. □

6. Conclusion

In this paper, the theorems are proved with a computer-free proof. However, at the beginning of the work, computers are used to produce data. Then, the data is analyzed to make a conjecture. To follow this experimental approach, one needs to have good data. To have good data, one must have the right computer software for computations. We use Orbiter [16], which is an open source. The idea behind that paper has been found this way. This paper shows the uniqueness of the line intersection graph of smooth cubic surfaces with 9 lines. The properties of line intersections are defined. A new form of smooth cubic surfaces $\mathcal{F}_{a,b,c,d,f,g}$ with at least 9 lines is created. The conditions specify when the surface has 9, when 15, and when 27 lines. This form is exemplified over several fields. Besides, the rational parametrization of points and lines of $\mathcal{F}_{a,b,c,d,f,g}$.

The Remarks 3.6 and 3.7 will be considered as a continuation of this work. All possible smooth cubic surfaces with 9 lines can be created by considering Remark 3.6 and 3.7. Studying the sub-configuration of Eckardt points of smooth cubic surfaces with 9 lines and investigating which cases are not covered by the form in this paper are worth reaching that aim. Moreover, the solution can be found for the other cases to generalize. Regarding Remark 3.7, the points P_{14}, P_{15}, and P_{18} need to be reset. Maple can be used to construct another form, covering all possible cases. Once these two remarks are considered, the classification problem of smooth cubic surfaces with 9 lines over the small finite fields can be considered. Therefore, the result herein can be verified by the enumerative formula of Das [15] using the Orbit Stabilizer Theorem. Besides, one may generalize certain cases and find a family over $\mathbb{Q}$.

Even though it was a popular topic in the 19th century, it still maintains its current and interesting nature. For recent related studies, see [23, 24].

Author Contributions

The author read and approved the final version of the paper.

Conflicts of Interest

The author declares no conflict of interest.

References

[1] A. Cayley, *On the Triple Tangent Planes of Surfaces of the Third Order*, Cambridge Journal of Mathematics (4) (1849) 118–138

[2] L. Schlafli, *An Attempt to Determine the Twenty-Seven Lines upon a Surface of the Third Order and to Divide such 35 Surfaces into Species in Reference to the Reality of the Lines upon the Surface*, The Quarterly Journal of Mathematics (2) (1858) 55–110.

[3] B. Segre, *Le rette delle Superficie Cubiche nei Corpi Commutativi*, Bollettino dell'Unione Matematica Italiana 3 (4) (1949) 223–228.

[4] L. A. Rosati, *L'equazione delle 27 Rette della Superficie Cubica Generale in un Corpo Finito*, Bollettino dell'Unione Matematica Italiana 3 (12) (1957) 612–626.

[5] L. E. Dickson, *Projective Classification of Cubic Surfaces Modulo 2*, Annals of Mathematics 16 (1915) 139–157.

[6] F. Karaoğlu, *Non-Singular Cubic Surfaces over* $\mathbb{F}_{2^k}$, Turkish Journal of Mathematics 45 (6) (2021) 2492–2510.

[7] A. Betten, J. W. P. Hirschfeld, F. Karaoğlu, *Classification of Cubic Surfaces with Twenty-Seven Lines over the Finite Field of Order Thirteen*, European Journal of Mathematics (4) (2018) 37–50.

[8] A. Betten, F. Karaoğlu, *Cubic Surfaces over Small Finite Fields*, Designs, Codes and Cryptography 87 (4) (2019) 931–953.

[9] F. Karaoğlu, A. Betten, *The Number of Cubic Surfaces with 27 lines Over a Finite Field*, Journal of Algebraic Combinatorics 56 (1) (2022) 43–57.

[10] A. Betten, F. Karaoğlu, *The Eckardt Point Configuration of Cubic Surfaces Revisited*, Designs, Codes and Cryptography 90 (9) (2022) 2159–2180.

[11] F. Karaoğlu, *Smooth Cubic Surfaces with 15 Lines*, Applicable Algebra in Engineering, Communication and Computing 33 (6) (2022) 823–853.

[12] T. Shioda, *Weierstrass Transformations and Cubib Surfaces*, Commentarii Mathematici Universitatis Sancti Pauli 44 (1) (1995) 109–128.

[13] I. Polo-Blanco, J. Top, *Explicit Real Cubic Surfaces*, Canadian Mathematical Bulletin 51 (1) (2008) 125–133.

[14] R. A. ElManssour, Y. ElMaazouz, E. Kaya, K. Rose, *Lines on p-adic and Real Cubic Surfaces* Abhandlungen aus dem Mathematischen Seminar der Universität Hamburg (in press).

[15] R. Das, *Arithmetic Statistics on Cubic Surfaces*, Research in the Mathematical Sciences 7 (3) (2020) Article Number 23 12 pages.

[16] A. Betten, *The Orbiter Ecosystem for Combinatorial Objects*, in: I. Z. Emiris, L. Zhi (Eds.), ISSAC 2020–Proceedings of the 45th International Symposium on Symbolic and Algebraic Computation, Kalamata, 2020, pp. 30–37.

[17] H. F. Baker. Principles of Geometry: Solid Geometry, Cambridge University Press, Cambridge, 2010.

[18] L. A. Rosati, *Sul Numero dei Punti di una Superficie Cubica in uno Spazio Lineare Finito*, Bollettino dell'Unione 31 Matematica Italiana 3 (11) (1956) 412–418.

[19] J. W. P. Hirschfeld, Projective Geometries over Finite Fields, 2nd Edition, Oxford University Press, Oxford, 1998.

[20] J. W. P. Hirschfeld, Finite Projective Spaces of Three Dimensions, Oxford University Press, New York, 1985.

[21] M. Reid, Undergraduate Algebraic Geometry, Cambridge University Press, Cambridge, 1988.

[22] J. Steiner, *Uber die Flachen dritten Grades*, Journal Für Die Reine Und Angewandte Mathematik (53) (1857) 133–141.

[23] I.V. Dolgachev, Classical Algebraic Geometry: A Modern View, Cambridge University Press, Cambridge, 2012.

[24] I. Dolgachev, A. Duncan, *Automorphisms of Cubic Surfaces in Positive Characteristic*, Izvestiya: Mathematics 83 (3) (2018) 5–82.

Journal of New Theory
ISSN: 2149-1402

44 (2023) 79-86
Journal of New Theory
https://dergipark.org.tr/en/pub/jnt
Open Access

A Novel Sub-Type Mean Estimator for Ranked Set Sampling with Dual Auxiliary Variables

Eda Gizem Koçyiğit[1]

Article Info
Received: 18 Aug 2023
Accepted: 22 Sep 2023
Published: 30 Sep 2023
doi:10.53570/jnt.1346020
Research Article

Abstract – This research introduces a novel sub-estimator designed to estimate the population mean under ranked set sampling, motivated by the new concept of a recently introduced sub-ratio estimator. The mathematical formulas of the proposed estimator's mean square error and bias are presented and theoretically contrasted with an analogous estimator found in the existing best sub-estimator literature. In addition to the theoretical analysis, empirical evidence is provided to validate the superiority of the proposed estimator. This empirical validation is based on numerical computations using Monte Carlo simulations, encompassing synthetic and real data applications. The results underscore the effectiveness of the proposed estimator. Finally, this study discusses the need for further research.

Keywords *Efficiency, Monte Carlo simulation, ranked set sampling, sub-estimator, survey sampling*

Mathematics Subject Classification (2020) 62D05, 94A17

1. Introduction

Ranked set sampling (RSS) represents a recommended option to simple random sampling (SRS), recognized for its capacity to yield more cost-efficient, time-saving, and efficient outcomes in comparison to SRS [1-3]. The RSS technique hinges on the availability of an auxiliary variable (z), ideally easily accessible and correlated with the study variable (g). This auxiliary variable is pivotal in the ranked process and sample selection procedure. However, once the sample selection is finalized, the estimation process exclusively pertains to the study variable. While it is feasible to incorporate the auxiliary variable into the estimation phase through various estimator types (e.g., ratio, product, or regression type estimators using auxiliary variables) [4-13], such approaches often necessitate knowledge of population parameters. The undeniable impact of utilizing auxiliary variable information in enhancing efficiency is well established. It is widely recognized that employing multiple auxiliary variables has the potential to yield even greater efficiency gains than using a single auxiliary variable [14-17]. However, obtaining these parameters for all variables is frequently impractical, limiting the applicability of such estimators on applications.

A novel method has been proposed, displaying that the auxiliary variable, a crucial component of the RSS method, can be effectively employed in the estimation phase without requiring population parameters. This breakthrough not only broadens the scope of utility for such estimators but also elevates the overall efficiency of the estimation process. These estimators developed for the RSS method are called sub-estimators [18]. The primary objective of this study is to introduce an estimator that surpasses the existing population mean estimators found in the literature in terms of efficiency. For this purpose, a novel sub-estimator using two

[1]eda.kocyigit@deu.edu.tr (Corresponding Author)
[1]Department of Statistics, Faculty of Science, Dokuz Eylül University, İzmir, Türkiye

auxiliary variables without their population parameters is proposed to estimate the population mean. Once the theoretical foundations of the proposed estimator have been established, the subsequent aim is to validate its efficiency through numerical investigations.

2. Estimators in Literature

In the RSS method, a simple random sample of m^2 of the observations z is initially drawn and subsequently divided into m sets. Within each set, a ranking is established based on z, leading to the selection of measurements for the g corresponding to the units situated along the diagonal. If the required sample size cannot be achieved with m, the process is repeated c times, and the desired $n = mc$ is obtained. The fundamental mean estimator of the RSS method and its mean square error (MSE) obtained after the cycle c:

$$\hat{g}_{RSS} = \frac{1}{mc}\sum_{j=1}^{c}\sum_{i=1}^{m} g_{[i,i];j}$$

and

$$\mathrm{MSE}(\hat{g}_{RSS}) = \overline{G}^2\left(\gamma C_g^2 - \omega_g^2\right)$$

where $g_{[i];j}$ is the observation value g of i^{th} ranked in i^{th} set and j^{th} cycle, $\gamma = 1/mc$, C_g^2 is the coefficient of variation of g, $\omega_{g(i)}^2 = \frac{1}{m^2 c\overline{G}^2}\sum_{i=1}^{m}\tau_{g(i)}^2$, $\tau_{g(i)}^2 = \mu_{g(i)} - \overline{G}$, and $\mu_{g(i)}$ represents the mean of the i^{th} order statistics of g. The RSS sub-ratio estimator and its MSE are described as the following equations:

$$\hat{g}_{KK1} = \frac{\overline{g}_{RSS}}{\overline{z}_{RSS}}\overline{Z}_{SUB}$$

and

$$\mathrm{MSE}(\hat{g}_{KK1}) = \overline{G}^2\left[\gamma C_{z_{SUB}}^2 - \omega_{z_{SUB}(i)}^2 + \gamma C_g^2 - \omega_{g(i)}^2 - 2\left(\gamma C_{gz_{SUB}} - \omega_{gz_{SUB}(i)}\right)\right] \quad (1)$$

where $\overline{z}_{RSS} = \frac{1}{mc}\sum_{j=1}^{c}\sum_{i=1}^{m} z_{[i,i];j}$ is the ranked set sample mean of z,

$$\overline{Z}_{SUB} = \frac{1}{m^2 c}\sum_{j=1}^{c}\sum_{k=1}^{m}\sum_{i=1}^{m} Z_{[i,k];j}$$

$C_{z_{SUB}}^2 = \frac{S_{z_{SUB}}^2}{\overline{Z}_{SUB}^2}$ is the coefficient of variation of the Z_{SUB},

$$C_{gz_{SUB}} = \rho C_g C_{z_{SUB}}$$

$$\omega_{z_{SUB}(i)}^2 = \frac{1}{m^2 c\overline{Z}_{SUB}^2}\sum_{i=1}^{m}\tau_{z_{SUB}(i)}^2$$

$$\omega_{gz_{SUB}(i)} = \frac{1}{m^2 c\overline{G}\overline{Z}_{SUB}}\sum_{i=1}^{m}\tau_{gz_{SUB}(i)}^2$$

and $\tau_{gz_{SUB}(i)}^2$ represents the cross-product of the deviation [18]. The RSS sub-exponential ratio type estimator and its MSE are formulated as [18]:

$$\hat{g}_{KK2} = \overline{g}_{RSS}\exp\left(\frac{\overline{Z}_{SUB} - \overline{z}_{RSS}}{\overline{Z}_{SUB} + \overline{z}_{RSS}}\right)$$

and

$$\mathrm{MSE}(\hat{g}_{KK2}) = \overline{G}^2\left[\gamma C_{z_{SUB}}^2 - \omega_{z_{SUB}(i)}^2 + \frac{1}{4}\left(\gamma C_g^2 - \omega_{g(i)}^2\right) - \left(\gamma C_{gz_{SUB}} - \omega_{gz_{SUB}(i)}\right)\right] \tag{2}$$

The sub-regression type estimator and its MSE are given as [19]:

$$\hat{g}_{KR} = \overline{g}_{RSS} + \hat{b}\left(\overline{Z}_{SUB} - \overline{z}_{RSS}\right)$$

and

$$MSE(\hat{g}_{KR})_{SUB}^2 = \left[\gamma C_g^2 - \omega_g^2 - \frac{\left(\gamma C_{gz_{SUB}} - \omega_{gz_{SUB}}\right)^2}{\gamma C_{z_{SUB}}^2 - \omega_{z_{SUB}}^2}\right]_{\min} \tag{3}$$

where $\hat{b} = R_{SUB}\frac{\gamma C_{gz_{SUB}} - \omega_{gz_{SUB}}}{\gamma C_{z_{SUB}}^2 - \omega_{z_{SUB}}^2}$ and $R_{SUB} = \frac{\overline{G}}{\overline{Z}_{SUB}}$.

3. Proposed Estimator

Building upon the foundation laid by the sub-ratio, sub-exponential, and sub-regression type estimators [18,19], as well as the multiple auxiliary variable estimators [14-17], we introduce a novel sub-estimator for the population mean under ranked set sampling with two auxiliary variables with the following formulation:

$$\hat{g}_{PRO} = \left[\overline{g}_{RSS}\exp\left(\frac{\overline{Z}_{SUB} - \overline{z}_{RSS}}{\overline{Z}_{SUB} + \overline{z}_{RSS}}\right)\exp\left(\frac{\overline{X}_{SUB} - \overline{x}_{RSS}}{\overline{X}_{SUB} + \overline{x}_{RSS}}\right)\right]$$

where x is the second auxiliary variable,

$$\overline{x}_{RSS} = \frac{1}{mc}\sum_{j=1}^{c}\sum_{i=1}^{m} x_{[i,i];j}$$

and

$$\overline{X}_{SUB} = \frac{1}{m^2 c}\sum_{j=1}^{c}\sum_{k=1}^{m}\sum_{i=1}^{m} X_{[i,k];j}$$

To derive the MSE of the proposed estimator, we introduce the following definitions:

$$\overline{g}_{RSS} = \overline{G}\left(e_g + 1\right), \quad \overline{z}_{RSS} = \overline{Z}_{SUB}(e_z + 1), \quad \text{and} \quad \overline{x}_{RSS} = \overline{X}_{SUB}(e_x + 1) \tag{4}$$

where

$$\begin{gathered}
E\left(e_g\right) = E(e_z) = E(e_x) = 0 \\
E\left(e_g^2\right) = \gamma C_g^2 - \omega_g^2 = V_{200} \\
E(e_z^2) = \gamma C_{z_{SUB}}^2 - \omega_{z_{SUB}}^2 = V_{020} \\
E(e_x^2) = \gamma C_{x_{SUB}}^2 - \omega_{x_{SUB}}^2 = V_{002} \\
E\left(e_g e_z\right) = \gamma C_{gz_{SUB}} - \omega_{gz_{SUB}} = V_{110} \\
E\left(e_g e_x\right) = \gamma C_{gx_{SUB}} - \omega_{gx_{SUB}} = V_{101} \\
E(e_z e_x) = \gamma C_{z_{SUB}x_{SUB}} - \omega_{z_{SUB}x_{SUB}} = V_{011} \\
E\left(e_g e_z e_x\right) = \gamma C_{gz_{SUB}x_{SUB}} - \omega_{gz_{SUB}x_{SUB}} = V_{111}
\end{gathered} \tag{5}$$

By utilizing the provided definitions in Equation 4, we can express the estimator given in Equation 5 in linear form using Taylor series and second-degree approximation:

$$\hat{g}_{PRO} = \left[\overline{G}(e_g+1)\exp\left(\frac{\overline{Z}_{SUB}-\overline{Z}_{SUB}(e_z+1)}{\overline{Z}_{SUB}+\overline{Z}_{SUB}(e_z+1)}\right)\exp\left(\frac{\overline{X}_{SUB}-\overline{X}_{SUB}(e_x+1)}{\overline{X}_{SUB}+\overline{X}_{SUB}(e_x+1)}\right)\right]$$

$$= \overline{G}(e_g+1)\exp\left(\frac{-e_z}{e_z+2}\right)\exp\left(\frac{-e_x}{e_x+2}\right)$$

$$= \overline{G}(e_g+1)\exp\left[\frac{-e_z}{2}\left(\frac{e_z}{2}+1\right)^{-1}\right]\exp\left[\frac{-e_x}{2}\left(\frac{e_x}{2}+1\right)^{-1}\right]$$

$$= \overline{G}(e_g+1)\left(1-\frac{e_z}{2}+\frac{3e_z^2}{8}\right)\left(1-\frac{e_x}{2}+\frac{3e_x^2}{8}\right)$$

$$= \overline{G}+\overline{G}e_g\left(1-\frac{e_z}{2}+\frac{3e_z^2}{8}-\frac{e_x}{2}+\frac{3e_x^2}{8}+\frac{e_ze_x}{4}\right)$$

Hence,

$$\hat{g}_{PRO} = \overline{G}+\overline{G}\left(e_g-\frac{e_z}{2}-\frac{e_x}{2}+\frac{3e_z^2}{8}+\frac{3e_x^2}{8}+\frac{e_ze_x}{4}-\frac{e_ge_x}{2}-\frac{e_ge_z}{2}+\frac{e_ge_ze_x}{4}\right) \quad (6)$$

When subtracting from Equation 5 and then taking the expected value, the bias of the estimator is determined as follows:

$$B(\hat{g}_{PRO}) = \overline{G}^2\left(\frac{3V_{020}}{8}+\frac{3V_{002}}{8}+\frac{V_{011}}{4}-\frac{V_{101}}{2}-\frac{V_{110}}{2}+\frac{V_{111}}{4}\right)$$

After subtracting $\overline{G}$ from Equation 6 and subsequently squaring and taking the expected value, upon substituting the equations provided in Equation 5 into their corresponding positions, we arrive at the MSE equation of the estimator as follows:

$$MSE(\hat{g}_{PRO}) = \overline{G}^2\left(V_{200}+\frac{V_{020}}{4}+\frac{V_{002}}{4}-V_{110}-V_{101}+\frac{V_{011}}{2}\right) \quad (7)$$

For theoretical comparisons, we can express Equations 1–3 in the following forms:

$$MSE(\hat{g}_{KK1}) = \overline{G}^2(V_{200}+V_{020}-2V_{110})$$

$$MSE(\hat{g}_{KK2}) = \overline{G}^2\left(V_{200}+\frac{1}{4}V_{020}-V_{110}\right)$$

and

$$MSE(\hat{g}_{KR})\overline{G}^2\left(V_{200}+\frac{V_{110}^2}{V_{020}}\right)_{min}$$

Subsequently, by employing Equation 7, we can perform concluding the disparities between the estimators:

i. If $MSE(\hat{g}_{PRO}) < MSE(\hat{g}_{KK1})$ then $\frac{V_{002}-4V_{101}+2V_{011}}{3V_{020}-4V_{110}} < 1$.

ii. If $MSE(\hat{g}_{PRO}) < MSE(\hat{g}_{KK2})$ then $\frac{V_{002}+2V_{011}}{4V_{110}} < 1$.

iii. If $MSE(\hat{g}_{PRO}) < MSE(\hat{g}_{KR})$ then $-\frac{V_{020}(V_{002}-4V_{110}-4V_{101}+2V_{011})}{V_{020}^2+4V_{110}^2} > 1$.

4. Numerical Study

This section encompasses the numerical computations performed on synthetic and real data sets using the existing and proposed estimator. All calculations are carried out utilizing the R programming language in numerical studies.

4.1. Monte Carlo Simulation

Trivariate random observations (G, Z, X) are generated from a trivariate normal distribution characterized by parameters: $\mu_g = \mu_z = \mu_x \approx 5$, and $\sigma_g = \sigma_z = \sigma_x \approx 1$, correlation coefficients $\rho_{gz} = \rho_{gx} = \rho_{zx} \approx 0.7$, 0.8, and 0.9, along with population sizes $N = 100$ and 1000. In the existing literature, it is recommended that the set size "m" for the RSS method does not exceed 5, and it is often chosen as 3, 4, or 5. Therefore, 100000 RSS samples were drawn from these populations with a set size of $m \in \{3,4,5\}$ and cycle $c \in \{1,2,3,4\}$. The estimators' values were computed based on these selected RSS samples.

MSE values for the estimators are computed using Equation 8, while the relative efficiency (RE) values are obtained via Equation 9. In the context of the RE comparison, the reference variable is designated as the RSS basic mean estimator ($\hat{g}_{RSS}$). The results of these comparisons are tabulated in Tables 1-3, each corresponding to distinct parameter combinations. These tables encapsulate valuable insights into the performance of the estimators under varying conditions.

$$MSE(\hat{g}_h) = \sum_{j=1}^{100000} \frac{\left(\hat{g}_{hj} - \bar{G}\right)^2}{100000}, \quad h \in \{RSS, KK1, KK2, KR, PRO\} \tag{8}$$

$$RE(\hat{g}_l) = \frac{MSE(\hat{g}_{RSS})}{MSE(\hat{g}_l)}, \quad l \in \{KK1, KK2, KR, PRO\} \tag{9}$$

Table 1. RE results for $\rho_{gz} = \rho_{gx} = \rho_{zx} \approx 0.7$

							$N = 1000$						
RE	m	5	5	5	5	4	4	4	4	3	3	3	3
	c	4	3	2	1	4	3	2	1	4	3	2	1
$\hat{g}_{KK1}$		1.0837	1.0957	1.0845	1.0917	1.1028	1.0906	1.0975	1.0943	1.0933	1.0967	1.1006	1.0927
$\hat{g}_{KK2}$		1.1099	1.1161	1.1117	1.1164	1.1238	1.1174	1.1209	1.1198	1.1194	1.1211	1.1235	1.1197
$\hat{g}_{KR}$		1.1176	1.1254	1.1129	1.1092	1.1248	1.1246	1.1222	1.1034	1.1215	1.1210	1.1175	1.0911
$\hat{g}_{PRO}$		**1.2244**	**1.2398**	**1.2246**	**1.2329**	**1.2361**	**1.2176**	**1.2282**	**1.2255**	**1.2059**	**1.2079**	**1.2070**	**1.2031**
							$N = 100$						
RE	m	5	5	5	5	4	4	4	4	3	3	3	3
	c	4	3	2	1	4	3	2	1	4	3	2	1
$\hat{g}_{KK1}$		1.1683	1.1598	1.1639	1.1613	1.1647	1.1512	1.1560	1.1557	1.1478	1.1431	1.1451	1.1420
$\hat{g}_{KK2}$		1.1552	1.1510	1.1528	1.1513	1.1547	1.1483	1.1500	1.1516	1.1456	1.1430	1.1433	1.1433
$\hat{g}_{KR}$		1.1766	1.1764	1.1722	1.1686	1.1707	1.1720	1.1688	1.1646	1.1641	1.1602	1.1586	1.1442
$\hat{g}_{PRO}$		**1.3396**	**1.3222**	**1.3199**	**1.3174**	**1.3066**	**1.2982**	**1.3071**	**1.2931**	**1.2684**	**1.2649**	**1.2643**	**1.2550**

Boldfaced values indicate the "best" performances.

Table 2. RE results for $\rho_{gz} = \rho_{gx} = \rho_{zx} \approx 0.8$

						$N = 1000$							
RE	m	5	5	5	5	4	4	4	4	3	3	3	3
	c	4	3	2	1	4	3	2	1	4	3	2	1
$\hat{g}_{KK1}$		1.2043	1.1980	1.1993	1.1952	1.2133	1.2088	1.2114	1.2121	1.2072	1.2047	1.2027	1.1977
$\hat{g}_{KK2}$		1.1708	1.1681	1.1675	1.1665	1.1772	1.1751	1.1762	1.1763	1.1729	1.1714	1.1702	1.1680
$\hat{g}_{KR}$		1.2056	1.2044	1.2010	1.1825	1.2071	1.2087	1.2021	1.1875	1.2003	1.1944	1.1877	1.1610
$\hat{g}_{PRO}$		**1.4034**	**1.3979**	**1.3941**	**1.3924**	**1.3828**	**1.3722**	**1.3789**	**1.3789**	**1.3398**	**1.3371**	**1.3369**	**1.3219**
						$N = 100$							
RE	m	5	5	5	5	4	4	4	4	3	3	3	3
	c	4	3	2	1	4	3	2	1	4	3	2	1
$\hat{g}_{KK1}$		1.1904	1.1820	1.1892	1.1844	1.1875	1.1864	1.1852	1.1791	1.1784	1.1752	1.1751	1.1694
$\hat{g}_{KK2}$		1.2306	1.2281	1.2292	1.2279	1.2263	1.2265	1.2256	1.2218	1.2128	1.2099	1.2095	1.2070
$\hat{g}_{KR}$		1.2418	1.2321	1.2248	1.1898	1.2300	1.2258	1.2133	1.1805	1.2137	1.2088	1.1929	1.1546
$\hat{g}_{PRO}$		**1.3452**	**1.3399**	**1.3403**	**1.3375**	**1.3265**	**1.3268**	**1.3285**	**1.3210**	**1.2986**	**1.2898**	**1.2846**	**1.2841**

Boldfaced values indicate the "best" performances.

Table 3. RE results for $\rho_{gz} = \rho_{gx} = \rho_{zx} \approx 0.9$

						$N = 1000$							
RE	m	5	5	5	5	4	4	4	4	3	3	3	3
	c	4	3	2	1	4	3	2	1	4	3	2	1
$\hat{g}_{KK1}$		1.3782	1.3816	1.3722	1.3805	1.3722	1.3744	1.3689	1.3659	1.3416	1.3377	1.3333	1.3252
$\hat{g}_{KK2}$		1.2765	1.2799	1.2761	1.2799	1.2735	1.2738	1.2732	1.2700	1.2518	1.2498	1.2495	1.2436
$\hat{g}_{KR}$		1.3762	1.3730	1.3608	1.3385	1.3634	1.3600	1.3537	1.3086	1.3264	1.3100	1.3028	1.2655
$\hat{g}_{PRO}$		**1.5093**	**1.5155**	**1.5074**	**1.5184**	**1.4786**	**1.4852**	**1.4732**	**1.4799**	**1.4243**	**1.4194**	**1.4140**	**1.4109**
						$N = 100$							
RE	m	5	5	5	5	4	4	4	4	3	3	3	3
	c	4	3	2	1	4	3	2	1	4	3	2	1
$\hat{g}_{KK1}$		1.4533	1.4484	1.4471	1.4368	1.4204	1.4166	1.4186	1.4094	1.3651	1.3651	1.3659	1.3639
$\hat{g}_{KK2}$		1.3240	1.3233	1.3218	1.3190	1.3041	1.3045	1.3053	1.3007	1.2708	1.2693	1.2707	1.2694
$\hat{g}_{KR}$		1.4387	1.4240	1.4113	1.3855	1.4011	1.3968	1.3794	1.33975	1.3455	1.3466	1.3196	1.2751
$\hat{g}_{PRO}$		**1.6143**	**1.6016**	**1.6037**	**1.5920**	**1.5385**	**1.5379**	**1.5418**	**1.5285**	**1.4497**	**1.4537**	**1.4530**	**1.4422**

Boldfaced values indicate the "best" performances.

4.2. Real Data Application

This section extends the simulation study employed in the preceding segment to utilize real rather than synthetic data. The dataset originates from the compilation of data across 81 provinces in Türkiye [20]. The variables used within this context are as follows: $\boldsymbol{G}$: The population of Türkiye in the year 2021; $\boldsymbol{Z}$: The number of registered vehicles in the year 2017, and $\boldsymbol{X}$: The tally of traffic accidents involving fatalities or injuries in 2017. The underlying population parameters are briefly summarized as follows: $\overline{G} = 1045435$, $\overline{Z} = 15400.6$, $\overline{X} = 2255.173$, $\sigma_g = 1914343$, $\sigma_z = 50392.4$, $\sigma_x = 2662.278$, $\rho_{gz} = 0.97$, $\rho_{gx} = 0.87$, and $\rho_{zx} = 0.77$. 100000 RSS samples were drawn from this population ($N = 81$), considering various set sizes $m \in \{3,4,5\}$, and cycle $c \in \{1,2,3,4\}$. After calculating the estimator values from these samples, RE values were computed

utilizing Equations 8 and 9. The outcomes of these computations are presented in Table 4, offering insights into the performance of the estimators within the context of real data.

Table 4. RE results for a real data set

	$N = 1000$											
RE	m	5	5	5	5	4	4	4	4	3	3	3	3
	c	4	3	2	1	4	3	2	1	4	3	2	1
$\hat{g}_{KK1}$		0.8853	0.9082	0.9102	0.8641	0.8205	0.8214	0.7860	0.71628	0.7274	0.6975	0.6608	0.5989
$\hat{g}_{KK2}$		3.7009	3.5807	3.3467	3.1058	2.8741	2.8033	2.6894	2.6239	2.2153	2.1860	2.1698	2.2215
$\hat{g}_{KR}$		1.3834	1.2962	1.2149	1.0786	1.7861	1.8303	1.8906	1.9278	**2.5979**	**2.8551**	**3.2944**	**4.1129**
$\hat{g}_{PRO}$		**3.7707**	**3.7500**	**3.6274**	**3.5907**	**2.9717**	**2.9644**	**2.9386**	**3.0829**	2.3119	2.3417	2.4090	2.6944

Boldfaced values indicate the "best" performances.

5. Conclusion

This study aims to introduce a new sub-estimator that surpasses the existing alternatives available in the literature regarding efficiency. A novel sub-estimator is proposed to achieve this objective, which utilizes two auxiliary variables without relying on population parameters. Once the theoretical framework of this novel estimator is established, the subsequent step involves substantiating its efficiency through numerical investigations.

The outcomes of the numerical studies indicate that, across all scenarios, the proposed estimator consistently outperforms other estimators in terms of effectiveness, as evidenced by simulation results derived from trivariate normal distributions. Considering the simulation study conducted on real data, the proposed estimator is the optimal choice in most cases, except for instances where $m = 3$.

In the simulation study and the real data application, a discernible pattern emerged, underscoring that the effectiveness of the estimator exhibited a positive correlation with the parameter "m", denoting the number of ranked sets employed in the sampling process. Specifically, as the value of "m" increased, there was a notable enhancement in the estimator's performance.

For prospective research, exploring the proposed estimator's behavior in the context of skewed distributions and under varied sampling methodologies is recommended. Furthermore, an intriguing avenue for exploration involves devising sub-estimator adaptations under the ranked set sampling (RSS) of the proposed estimators for other sampling methods, subsequently assessing their efficiencies.

Author Contributions

The author read and approved the final version of the paper.

Conflict of Interest

The author declares no conflict of interest.

References

[1] Z. Chen, Z. Bai, B. K. Sinha, Ranked Set Sampling: Theory and Applications, Springer, New York, 2004.

[2] D. A. Wolfe, *Ranked Set Sampling*, Wiley Interdisciplinary Reviews: Computational Statistics 2 (4) (2010) 460–466.

[3] G. P. Patil, Ranked Set Sampling. Encyclopedia of Environmetrics, 2006.

[4] S. L. Stokes, *Ranked Set Sampling With Concomitant Variables*, Communications in Statistics-Theory and Methods 6 (12) (1977) 1207–1211.

[5] S. Bhushan, A. Kumar, T. Zaman, A. Al Mutairi, *Efficient Difference and Ratio-Type Imputation Methods under Ranked Set Sampling*, Axioms 12 (6) (2023) 558 22 pages.

[6] S. Bhushan, A. Kumar, *A Novel log Type Class of Estimators under Ranked Set Sampling*, Sankhya B 84 (2022) 421–447.

[7] S. Bhushan, A. Kumar, *On Optimal Classes of Estimators under Ranked Set Sampling*, Communications in Statistics - Theory and Methods 51 (8) (2022) 2610–2639.

[8] E. G. Koçyiğit, C. Kadilar, *Ratio Estimators for Ranked Set Sampling in the Presence of Tie Information*, Communications in Statistics-Simulation and Computation 51 (11) (2022) 6826–6839.

[9] T. Zaman, E. Dünder, A. Audu, D. A. Alilah, U. Shahzad, M. Hanif, *Robust Regression-Ratio-Type Estimators of the Mean Utilizing Two Auxiliary Variables: A Simulation Study*, Mathematical Problems in Engineering 2021 (2021) Article ID 6383927 9 pages.

[10] S. K. Yadav, T. Zaman, *Use of Some Conventional and Non-Conventional Parameters for Improving the Efficiency of Ratio-Type Estimators*, Journal of Statistics and Management Systems 24 (5) (2021) 1077–1100.

[11] M. Ijaz, T. Zaman, H. Bulut, A. Ullah, S. M. Asim, *An Improved Class of Regression Estimators Using the Auxiliary Information*, Journal of Science and Arts 20 (4) (2020) 789–800.

[12] K. U. I. Rather, E. G. Koçyiğit, R. Onyango, C. Kadilar, *Improved Regression in Ratio Type Estimators Based on Robust M-Estimation*, PloS ONE 17 (12) (2022) e0278868 16 pages.

[13] K. U. I. Rather, E. G. Koçyiğit., C. Ünal, *New Exponential Ratio Estimator in Ranked Set Sampling*, Pakistan Journal of Statistics and Operation Research 18 (2) (2022) 403–409.

[14] C. Kadilar, H. Cingi, *A New Estimator Using Two Auxiliary Variables*, Applied Mathematics and Computation 162 (2) (2005) 901–908.

[15] L. Khan, J. Shabbir, S. A. Khan, *Efficient Estimators of Population Mean in Ranked Set Sampling Scheme Using Two Concomitant Variables*, Journal of Statistics and Management Systems 22 (8) (2019) 1467–1480.

[16] S. Bhushan, A. Kumar, *New Efficient Logarithmic Estimators Using Multi-Auxiliary Information under Ranked Set Sampling*, Concurrency, and Computation: Practice and Experience 34 (27) (2022) e7337 23 pages.

[17] S. Bhushan, A. Kumar, N. Alsadat, M. S. Mustafa, M. M. Alsolmi, *Some Optimal Classes of Estimators Based on Multi-Auxiliary Information*, Axioms 12 (6) (2013) 515 25 pages.

[18] E. G. Koçyiğit, C. Kadilar, *Information Theory Approach to Ranked Set Sampling and New Sub-Ratio Estimators*, Communications in Statistics-Theory and Methods (2022) 23 pages.

[19] E. G. Koçyiğit, K. U. I. Rather, *The New Sub-Regression Type Estimator in Ranked Set Sampling*, Journal of Statistical Theory and Practice 17 (2) (2023) 27 14 pages.

[20] TÜİK, https://biruni.tuik.gov.tr/medas/, Accessed 16 Aug 2023.

Journal of New Theory
ISSN: 2149-1402

44 (2023) 87-96
Journal of New Theory
https://dergipark.org.tr/en/pub/jnt
Open Access

An Investigation into LRS Bianchi I Universe in Brans-Dicke Theory

Halife Çağlar

Article Info
Received: 30 Aug 2023
Accepted: 20 Sep 2023
Published: 30 Sep 2023
doi:10.53570/jnt.1352470
Research Article

Abstract — In this study, the homogenous and anisotropic locally rotationally symmetric (LRS) Bianchi type-I universe filled with the bulk viscous and the string cloud matter has been investigated in the Brans-Dicke (BD) scalar-tensor theory. The modified Einstein field equations of the constructed model have been solved by using the relation of the scale factors $A = B^m$ and considering the deceleration parameter to be $q = m - 1$. It is found that the string does not survive for the model due to the obtained zero string energy density ($\rho_s = 0$) and agrees with some studies in recent years. Moreover, it is possible to say that string matter may be turned into phantom energy over time, depending on the obtained negative rest energy density of the matter. When BD scalar field Φ is assumed constant, the attained solutions are reduced to General Relativity (GR) solutions for the static vacuum. Thus, the constructed model has not allowed the reduction of the BD solutions to GR solutions, including the matter distributions. In addition, some expansion models for choosing a value of constant m have been obtained and provided. All the results have been analyzed in detail.

Keywords *LRS Bianchi I universe, Brans-Dicke theory, bulk viscous, string cloud, deceleration parameter*

Mathematics Subject Classification (2020) 83C05, 83C15

1. Introduction

Gravitation theories are based on Newton's theory, successful in determining the orbits of planets and other celestial bodies. However, this theory was insufficient to explain some cosmic issues. On the other hand, Einstein's General Relativity (GR) theory [1] was the first theory that succeeded in explaining gravity geometrically. But Einstein's theory has been suggested for a static universe. After studies of Friedman [2], Lemaitre [3], and Hubble [4], when considering the expanding universe model, a function determining the expansion of the universe has been needed to add to the field equations in Einstein's GR theory. Einstein has suggested the cosmological constant Λ as the added function to GR theory. Hence, the GR theory has become the most valid gravitational theory, which provides tests, such as the perihelion progression of planets, the gravitational deflection, and the redshift of light. Firstly, scientists have discussed decelerating expanding universe until some observation, such as Supernova IA observation [5], Cosmic Microwave Background radiation (CMB) [6], Wilkinson Microwave Anisotropy Probe (WMAP) [7], etc. Such studies have proven the expanding universe model by accelerating, and then researchers have been focused on studies on this expansion model. Especially alternative gravitation theories, such as Lyra theory [8], Barber's Theory [9], Creation Field

[1]halife@comu.edu.tr (Corresponding Author)
[1]Department of Electricity and Energy, Biga Vocational School, Çanakkale Onsekiz Mart University, Çanakkale, Türkiye

Theory [10], Yılmaz Theory [11], and Brans-Dicke theory [12] have been investigated with some cosmic matter distribution to explain accelerating expansion of the universe.

In addition, cosmic strings formed during the phase transition have been suggested to cause variations in the density of the particles, which cause the formation of the galaxies [13, 14]. Because of this assumption, it is believed that cosmic strings are important matter structures to investigate and determine the universe's evolution from early to late. Scientists have recently studied the Brans-Dicke (BD) theory with cosmic string for various space-time models. Delice [15] has investigated BD theory for the generalized cylindrical symmetric universe with cosmic string. Reddy and Rao [16] have researched the axially symmetric metric in the presence of a string dust cloud for BD theory. Besides, in BD theory, Rao and Neelima [17] have analyzed the axially symmetric universe model with bulk string matter distribution. Vidya et al. [18] have solved equations of BD theory for the Bianchi type-III universe with bulk string matters. Sharma and Singh [19] have gotten the solutions of Bianchi II universe for the massive string in BD alternative theory. Trivedi and Bhabor [20] have investigated five-dimensional Bianchi III space-time with dark energy fluid and cosmic string in BD theory.

Moreover, Mahanta et al. [21] have calculated plane-symmetric metric with strange quark matter by attaching to string cloud and bulk viscous matter in BD theory. Chakraborty et al. [22] have analyzed BD theory for the Bianchi type-III universe in the presence of perfect fluid matter. Adhav et al. [23] have gotten exact solutions of the Bianchi III cosmological model for vacuum in BD gravity. Çağlar et al. [24] have investigated the locally rotationally symmetric (LRS) Bianchi type I universe in BD theory by assuming strange quark matter (SQM) coupled with string cloud as matter distributions. Çağlar and Aygün [25] have gotten the exact solutions of higher dimensional Friedman–Walker Friedmann-Robertson-Walker (FRW) universe in the presence of SQM with bulk viscous and cosmic string matter in Lyra theory. Furthermore, higher dimensional FRW universe filled with SQM attached to cosmic string matter for Self Creation Cosmology and BD theory, respectively, have been examined by Çağlar and Aygün [26, 27].

Motivated by the studies mentioned above, the LRS Bianchi type-I universe has been studied in BD theory by assuming cosmic string with bulk viscous as matter distribution. This paper is organized as follows: In the second section, the universe model has been constructed, and the modified field equations of the model have been solved. In the last section, all the obtained solutions have been concluded in detail.

2. MEFE's of LRS Bianchi-I Universe for Brans-Dicke Theory

The modified Einstein field equations (MEFE's) in BD theory [12] have been suggested as:

$$R_{ij} - \frac{1}{2}Rg_{ij} = -\frac{8\pi}{\Phi}T_{ij} - \frac{\omega}{\Phi^2}(\Phi_{,i}\Phi_{,j} - \frac{1}{2}g_{ij}\Phi_{,k}\Phi^{,k}) - \frac{1}{\Phi}(\Phi_{i;j} - g_{ij}\Phi^{;k}_{;k})) \tag{1}$$

Here, R, R_{ij}, and ω are Ricci scalar, Ricci tensor, and the coupling constant of BD theory, respectively. It is possible to reduce BD theory to GR theory when $\omega \to \propto$ and $\Phi = constant$ [28]. In addition, Φ symbolizes BD scalar field and it is given as follows [29]:

$$\Phi = \Phi^{;k}_{;k} = \frac{8\pi}{3+2\omega}T \tag{2}$$

Here and after, comma (,) and semicolon (;) represent partial derivative and covariant derivative, respectively. Furthermore, T_{ij} is a tensor characterized stress energy of the matter in Equation 1. In this study, it has been assumed that the string cloud matter with bulk viscous filled the universe and this matter distribution is written as

$$T_{ij} = \rho u_i u_j - \rho_s x_i x_j - \eta u^{k}_{;k}(u_i u_j - g_{ij}) \tag{3}$$

Here, ρ and ρ_s symbolizes the rest energy density of matter and the string energy density, respectively. Moreover, the bulk viscous coefficient has been represented as η. Besides, u_i defines 4-velocity of the particle and x_i is named unit space-like vector determined the string direction [21, 30]. Further, the LRS Bianchi type-I space-time line element can be written as

$$ds^2 = dt^2 - A(t)^2dx^2 - B(t)^2(dy^2 + dz^2) \tag{4}$$

Here, $A(t)$ and $B(t)$ are time-depending scale factors of the universe [31, 32]. Some kinematic quantities, such as spatial volume (V), Hubble parameter (H), expansion scalar (θ), shear scalar (σ^2), and deceleration parameter (q), for LRS Bianchi type-I universe are provided as follows, respectively:

$$V = a^3 = AB^2 \tag{5}$$

$$H = \frac{a_t}{a} = \frac{A_t}{3A} + \frac{2B_t}{3B} \tag{6}$$

$$\theta = \frac{A_t}{3A} + \frac{2B_t}{B}$$

$$\sigma^2 = \frac{1}{3}\left[\frac{A_t}{A} - \frac{B_t}{B}\right]^2$$

and

$$q = \frac{d}{dt}\left(\frac{1}{H}\right) - 1 = \frac{2(AB_t - A_tB)^2 - 3AB(A_{tt}B + 2AB_{tt})}{(2AB_t + A_tB)^2} \tag{7}$$

Here and after, the lower index t represents the derivative with respect to cosmic time t. Besides, a provided in Equations 5 and 6 symbolizes the average scale factor [33]. By using Equations 1-4, the modified Einstein field equations of LRS Bianchi-I space-time for string cloud coupled with bulk viscous matter have been obtained in BD theory as follows:

$$\frac{B_t^2}{B^2} + \frac{2B_{tt}}{B} = \frac{1}{\Phi}\left[8\pi\eta\left(\frac{A_t}{A} + \frac{2B_t}{B}\right) - \frac{\omega\Phi_t^2}{2\Phi} - \frac{2B_t\Phi_t}{B} - \Phi_{tt}\right] \tag{8}$$

$$\frac{B_t^2}{B^2} + \frac{2A_tB_t}{AB} = \frac{1}{\Phi}\left[8\pi\rho + \frac{\omega\Phi_t^2}{2\Phi} - \frac{A_t\Phi_t}{A} - \frac{2B_t\Phi_t}{B}\right] \tag{9}$$

$$\frac{A_{tt}}{A} + \frac{B_{tt}}{B} + \frac{A_tB_t}{AB} = \frac{1}{\Phi}\left[8\pi\eta\left(\frac{A_t}{A} + \frac{2B_t}{B}\right) - \Phi_t\left(\frac{A_t}{A} - \frac{B_t}{B}\right) - \frac{\omega\Phi_t^2}{2\Phi} - \Phi_{tt}\right] \tag{10}$$

$$\frac{A_{tt}}{A} + \frac{B_{tt}}{B} + \frac{A_tB_t}{AB} = \frac{1}{\Phi}\left[8\pi\eta\left(\frac{A_t}{A} + \frac{2B_t}{B}\right) - \Phi_t\left(\frac{A_t}{A} - \frac{B_t}{B}\right) + 8\pi\rho_s - \frac{\omega\Phi_t^2}{2\Phi} - \Phi_{tt}\right] \tag{11}$$

Field equations obtained as in Equations 8-11 have six unknown quantities such as A, B, Φ, ρ, ρ_s, and η. Therefore, two approximations have been used to solve field equations. The first one is the relationship of the scale factors came from a proportion of the shear scalar and the expansion scalar given as follows:

$$A = B^k \tag{12}$$

Here, k is an arbitrary constant [24, 34, 35]. The second assumption is a constant form of deceleration parameter by using Equation 7 given as follows:

$$q = m - 1 \tag{13}$$

where the arbitrary constant m determines the expansion model of the universe. Deceleration parameter q specifies the fate of the universe model as follows [15, 24, 36]:

i. When $m < 0$, one gets $q < -1$ named super-exponential expansion

ii. When $m = 0$, one gets $q = -1$ named exponential expansion

iii. When $0 < m < 1$, one gets $-1 < q < 0$ named accelerating power law expansion

iv. When $m = 1$, one gets $q = 0$ named constant expansion

v. When $m > 1$, one gets $q > 0$ named decelerating expansion

By using Equation 13 with Equation 12, the scale factor B has been calculated as

$$B = (s_1 t + s_2)^{\frac{3}{m(k+2)}} \tag{14}$$

Then, by using Equation 14 in Equation 12, the scale factor A has been attained as follows:

$$A = (s_1 t + s_2)^{\frac{3k}{m(k+2)}} \tag{15}$$

Considering the scale factors' values in Equations 14 and 15 in field Equations 8–11, the BD scalar field Φ, the rest energy density ρ, the string energy density ρ_s, and the bulk viscous coefficient η have been obtained as follows, respectively:

$$\Phi = s_3(s_1 t + s_2)^{\frac{m-3}{m}}$$

$$\rho = \frac{\left[(k+2)^2\left(6\omega + 6m - \omega m^2 - 9\omega\right) - 18k(k+2) - 54\right] s_3 s_1^2}{16\pi m^2 (k+2)^2 (s_1 t + s_2)^{\frac{m+3}{m}}}$$

$$\rho_s = 0$$

and

$$\eta = \frac{\left[(k+2)^2\left(\omega m^2 - 6\omega - 6m + 9\omega\right) + 18k(k+2) + 54\right] s_1 s_3}{48\pi m^2 (k+2)^2 (s_1 t + s_2)^{\frac{3}{m}}}$$

Furthermore, kinematic quantities, such as spatial volume (V), Hubble parameter (H), expansion scalar (θ), and shear scalar (σ^2) for the constructed model are calculated as follows, respectively:

$$V = (s_1 t + s_2)^{\frac{1}{m}}$$

$$H = \frac{s_1}{m(s_1 t + s_2)}$$

$$\theta = \frac{3s_1}{m(s_1 t + s_2)}$$

and

$$\sigma^2 = \frac{3(k-1)^2 s_1^2}{m^2 (k+2)^2 (s_1 t + s_2)^2}$$

All the obtained solutions of constructed model have been investigated in the next section.

3. Discussions

In this paper, the bulk viscous coupled with the string cloud matter distribution has been investigated in BD theory for LRS Bianchi type-I space-time. By considering the scale factor values given in Equations 14 and 15 within Equation 4, the new line element of the LRS Bianchi-I universe can be rewritten as

$$ds^2 = dt^2 - (s_1 t + s_2)^{\frac{6k}{m(k+2)}} dx^2 - (s_1 t + s_2)^{\frac{6}{m(k+2)}} (dy^2 + dz^2) \tag{16}$$

It is obviously seen that s_1 and k in Equation 16 are important constants to determine meaningful the universe model and must be $s_1 \neq 0$, $k \neq -2$, and $k \neq 0$. Besides, it is well know that the universe is expanding with acceleration. When $0 < m < 1$, the deceleration parameter value has given accelerating power law expansion universe. At this condition, the evolution of scale factor $A(t)$ has been shown in Figure 1. As seen in the figure, the expansion of the constructed universe model is as

expected in given situations.

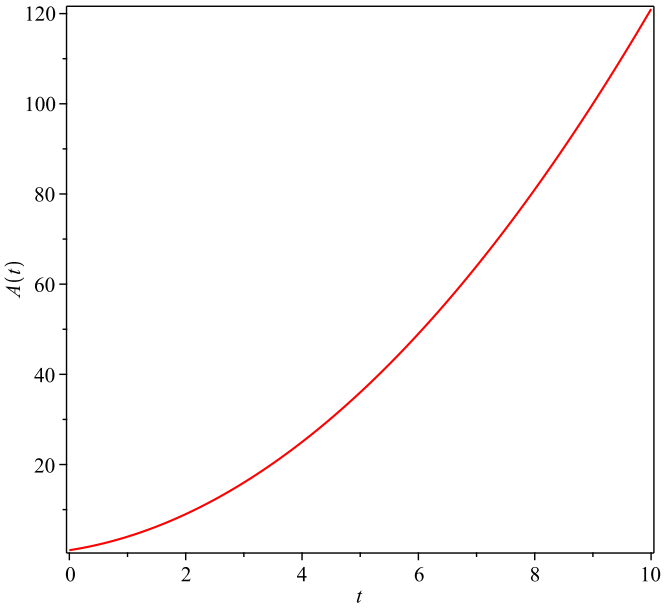

Figure 1. Evolutions of the scale factor $A(t)$ for the accelerating expanding universe ($s_1 = s_2 = k = 1$ and $m = 0.5$)

Moreover, the string energy density ρ_s vanishes for constructed model. Thus, it can be said that the string matter does not survive in the model LRS Bianchi type-I universe for BD theory with the bulk viscous and the string cloud. This finding agrees with the studies of Zel'dovich [13], Çağlar and Aygün [25–27], Sahoo and Mishra [37], Kiran and Reddy [38], etc. In addition, the obtained all the solutions give the negative energy density of particle. Hence, it is possible that the cosmic string may have disappeared by time and turned into a phantom [39]. Rest energy density and bulk viscous coefficient have been shown in Figure 2.

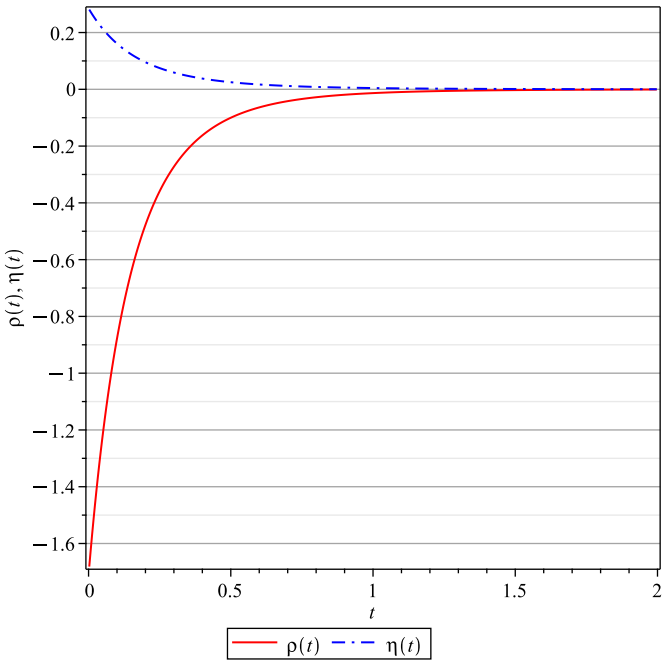

Figure 2. Evolutions of the rest energy density and the bulk viscous coefficient for the accelerating expanding universe ($s_1 = s_2 = s_3 = k = 1, \omega = 2$, and $m = 0.5$)

Furthermore, the BD scalar field Φ has been obtained time dependent and shown in Figure 3 for the accelerating expanding universe. It is observed that the scalar field of the theory is inversely proportional to time, intense at the beginning, and loses its effect over time.

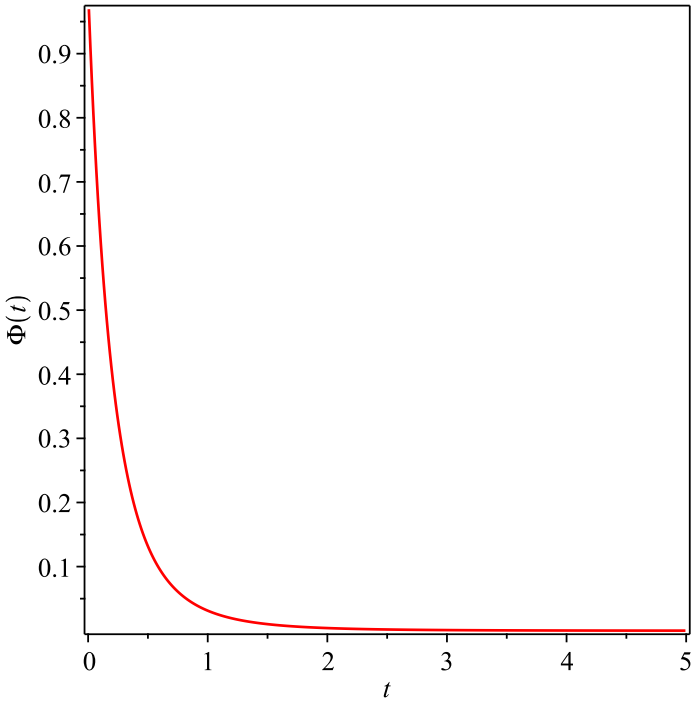

Figure 3. Evolutions of the BD scalar field for the accelerating expanding universe ($s_1 = s_2 = s_3 = 1$ and $m = 0.5$)

Considering the kinematic quantities, it is obtained that the universe has expansion with accelerating. This expansion is observed in Figures 4 and 5. Further, this result agrees with some studies [4–7].

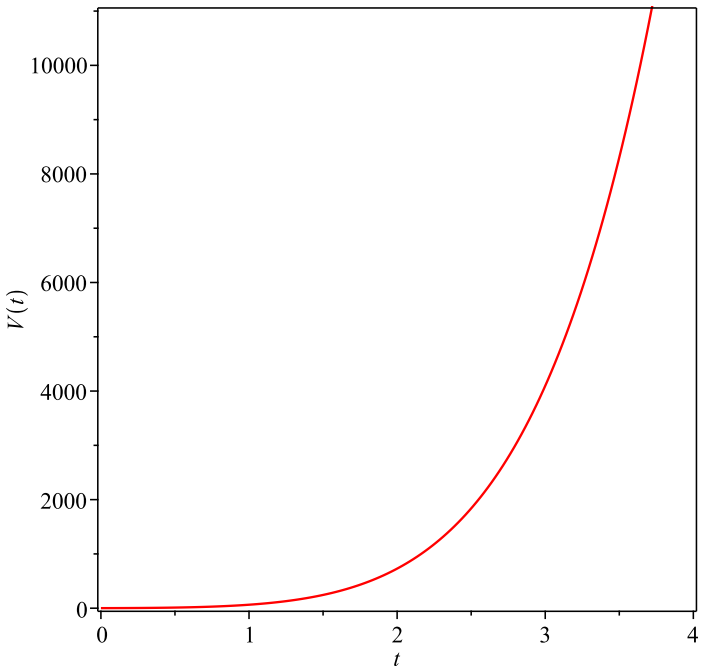

Figure 4. Evolutions of spatial volume for accelerating expanding universe ($s_1 = s_2 = s_3 = 1$ and $m = 0.5$)

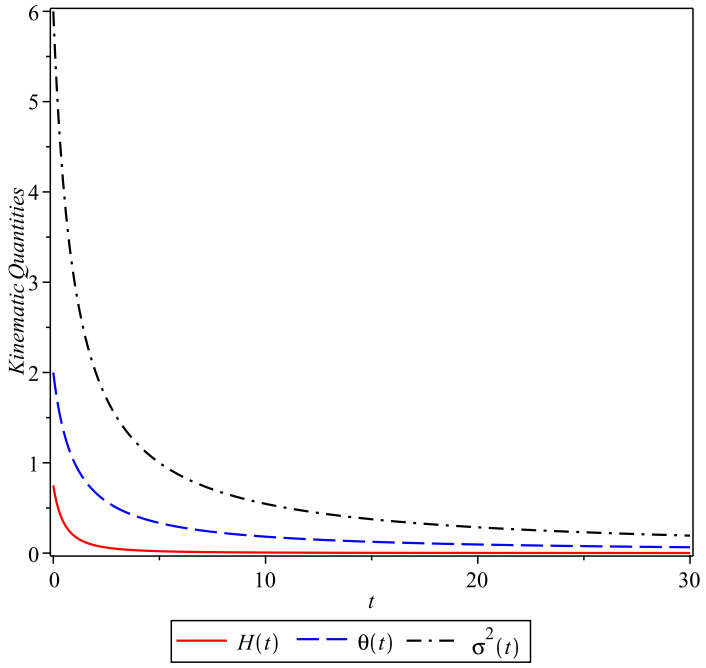

Figure 5. Evolutions of the Hubble parameter, the expansion scalar, and the shear scalar for the accelerating expanding universe ($s_1 = s_2 = s_3 = 1, k = 2$, and $m = 0.5$)

The obtained all the solutions have been calculated depending on some integer values of arbitrary constant m to investigate expansion type of the universe. By assuming $m = 2$, $m = 1$, and $m = 0$, one obtains the results of the constructed model for decelerating expansion, the constant expansion, and the exponential expansion universe, respectively. Additionally, these results have been provided in Table 1.

Table 1. Results of Constructed Model for the Deceleration Parameters

Quantities	**Decelerating Expansion** $q = 1$	**Constant Expansion** $q = 0$	**Exponential Expansion** $q = -1$
Scale Factor A	$(s_1t + s_2)^{\frac{3k}{2k+4}}$	$(s_1t + s_2)^{\frac{3k}{k+2}}$	$s_4^k e^{s_5 kt}$
Scale Factor B	$(s_1t + s_2)^{\frac{3}{2k+4}}$	$(s_1t + s_2)^{\frac{3}{k+2}}$	$s_4 e^{s_5 t}$
BD Scalar Field Φ	$\frac{s_3}{\sqrt{s_1t+s_2}}$	$\frac{s_3}{(s_1t+s_2)^2}$	$\frac{s_6}{e^{(k+2)s_5t}}$
Rest Energy Density ρ	$-\frac{[(\omega+6)k^2+(4\omega-12)k+4\omega+6]s_3s_1^2}{96\pi(k+2)^2(s_1t+s_2)^{\frac{3}{2}}}$	$-\frac{[(\omega+3)2k^2+(4\omega+3)2k+8\omega+15]s_3s_1^2}{8\pi(k+2)^2(s_1t+s_2)^4}$	$-\frac{[(\omega+2)k^2+4(\omega+1)k+4\omega+6)]s_6s_5^2}{16\pi e^{(k+2)s_5t}}$
Bulk Viscous Coefficient η	$\frac{[(\omega+6)k^2+(4\omega-12)k+4\omega+6]s_1s_3}{96\pi(k+2)^2(s_1t+s_2)^{\frac{3}{2}}}$	$\frac{[(\omega+3)2k^2+(4\omega+3)2k+8\omega+15]s_1s_3}{24\pi(k+2)^2(s_1t+s_2)^3}$	$\frac{[(\omega+2)k^2+4(\omega+1)k+4\omega+6)]s_5s_6}{16\pi e^{(k+2)s_5t}}$
Spatial Volume V	$\sqrt{s_1t + s_2}$	$s_1t + s_2$	$s_4 e^{\frac{(k+2)s_5t}{3}}$
Hubble Parameter H	$\frac{s_1}{2(s_1t+s_2)}$	$\frac{s_1}{(s_1t+s_2)}$	$\frac{(k+2)s_5}{3}$
Expansion Scalar θ	$\frac{3s_1}{2(s_1t+s_2)}$	$\frac{3s_1}{(s_1t+s_2)}$	$(k+2)s_5$
Shear Scalar σ^2	$\frac{3(k-1)^2s_1^2}{4(k+2)^2(s_1t+s_2)^2}$	$\frac{3(k-1)^2s_1^2}{(k+2)^2(s_1t+s_2)^2}$	$\frac{(k-1)^2s_5^2}{3}$

It is possible to get GR solutions of the LRS Bianchi type-I space-time with the bulk string cloud matter by assuming $\Phi = constant$ in BD theory. To get the constant BD scalar field, s_3 must be zero in the model results. In this situation, the energy density and the bulk viscous coefficient became zero, and it gives the static vacuum solutions. Thus, the obtained results do not allow GR solutions of the constructed model by reducing BD solutions with $\Phi = constant$.

4. Conclusion

This study investigated BD theory in the LRS Bianchi type-I space-time for bulk viscous and string cloud matter distribution. In the future, it is worth investigating LRS Bianchi I universe filled with bulk string matter or various cosmic matter in alternative gravitation theories such as $f(G)$, $f(Q)$, and $f(Q,T)$.

Author Contributions

The author read and approved the final version of the paper.

Conflicts of Interest

The author declares no conflict of interest.

References

[1] A. Einstein, *The Foundation of the General Theory of Relativity*, Annalen der Physik 49 (7) (1916) 769–822.

[2] A. Friedman, *Über die Krümmung des Raumes*, Zeitschrift für Physik 10 (1922) 377–386.

[3] G. Lemaitre, *Un Univers Homogène de Masse Constante et de Rayon Croissant Rendant Compte de la Vitesse Radiale des Nébuleuses Extra-galactiques*, Annales de la Société Scientifique de Bruxelles A47 (1927) 49–59.

[4] E. Hubble, *A Relation Between Distance and Radial Velocity Among Extra-Galaktik Nebulae*, Proceedings of the National Academy of Sciences of the USA 15 (3) (1929) 168–173.

[5] S. Perlmutter, G. Aldering, G. Goldhaber, R. Knop, P. Nugent, P. G. Castro, S. Deustua, S. Fabbro, A. Goobar, D. E. Groom, I. M. Hook, A. G. Kim, M. Y. Kim, J. C. Lee, N. J. Nunes, R. Pain, C. R. Pennypacker, R. Quimby, C. Lidman, R. S. Ellis, M. Irwin, R. G. McMahon, P. Ruiz-Lapuente, N. Walton, B. Schaefer, B. J. Boyle, A. V. Filippenko, T. Matheson, A. S. Fruchter, N. Panagia, H. J. M. Newberg, W. J. Couch, The Supernova Cosmology Project, *Measurements of* Ω *and* Λ *from* 42 *High-Redshift Supernovae*, The Astrophysical Journal 517 (2) (1999) 565–586.

[6] D. N. Spergel, L. Verde, H. V. Peiris, E. Komatsu, M. Nolta, C. L. Bennett, M. Halpern, G. Hinshaw, N. Jarosik, A. Kogut, M. Limon, S. S. Meyer, L. Page, G. S. Tucker, J. L. Weiland, E. Wollack, E. L. Wright, *First-Year Wilkinson Microwave Anisotropy Probe (WMAP)* Observations: Determination of Cosmological Parameters*, The Astrophysical Journal Supplement Series 148 (1) (2003) 175–194.

[7] R. A. Knop, G. Aldering, R. Amanullah, P. Astier, G. Blanc, M. S. Burns, A. Conley, S. E. Deustua, M. Doi, R. Ellis, S. Fabbro, G. Folatelli, A. S. Fruchter, G. Garavini, S. Garmond, K. Garton, R. Gibbons, G. Goldhaber, A. Goobar, D. E. Groom, D. Hardin, I. Hook, D. A. Howell, A. G. Kim, B. C. Lee, C. Lidman, J. Mendez, S. Nobili, P. E. Nugent, R. Pain, N. Panagia, C. R. Pennypacker, S. Perlmutter, R. Quimby, J. Raux, N. Regnault, P. Ruiz-Lapuente, G. Sainton, B. Schaefer, K. Schahmaneche, E. Smith, A. L. Spadafora, V. Stanishev, M. Sullivan, N. A. Walton, L. Wang, W. M. Wood-Vasey, N. Yasuda, The Supernova Cosmology Project, *New Constraints on* Ω_M, Ω_Λ, *and* w *from an Independent Set of 11 High-Redshift Supernovae Observed with the Hubble Space Telescope*, Astrophysical Journal 598 (2003) 102–137.

[8] G. Lyra, *Uber eine Modifikation der Riemannschen Geometrie*, Mathematische Zeitschrift 54 (1) (1951) 52–64.

[9] G. A. Barber, *On Two "Self-Creation" Cosmologies*, General Relativity and Gravitation 14 (1982) 117–136.

[10] F. Hoyle, J. V. Narlikar, *A Radical Departure from the 'Steady-State' Concept in Cosmology*, Proceedings of the Royal Society of London Series A, Mathematical and Physical Sciences 290 (1421) (1966) 162–176.

[11] H. Yılmaz, *New Approach to General Relativity*, Physical Review 111 (1958) 1417–1426.

[12] C. Brans, R. H. Dicke, *Mach's Principle and a Relativistic Theory of Gravitation*, Physical Review 124 (1961) 925–935.

[13] Ya. B. Zel'dovich, *Cosmological Fluctuations Produced Near a Singularity*, Monthly Notices of the Royal Astronomical Society 192 (4) (1980) 663–667.

[14] T. W. B. Kibble, *Topology of Cosmic Domains and Strings*, Journal of Physics A: Mathematical and General 9 (8) (1976) 1387–1398.

[15] Ö. Delice, *Local Cosmic Strings in Brans-Dicke Theory with a Cosmological Constant*, Physical Review D 74 (6) (2006) 067703 1–4.

[16] D. R. K. Reddy, S. M. V. Rao, *Axially Symmetric String Cosmological Model in Brans-Dicke Theory of Gravitation*, Astrophysics and Space Science 305 (2) (2006) 183–186

[17] V. U. M. Rao, D. Neelima, *Axially Symmetric Bulk Viscous String Cosmological Models in GR and Brans-Dicke Theory of Gravitation*, ISRN Astronomy and Astrophysics 2013 (2013) Article ID 543483 6 pages.

[18] T. S. Vidya, C. P. Rao, R. B. Vijaya, D. R. K. Reddy, *Bianchi Type-III Bulk Viscous String Cosmological Model in Brans-Dicke Theory of Gravitation*, Astrophysics and Space Science 349 (1) (2014) 479–483.

[19] N. K. Sharma, J. K. Singh, *Some Exact Solutions of Bianchi Type-II String Cosmological Models with Magnetic Field in Brans-Dicke Theory of Gravitation*, International Journal of Theoretical Physics 54 (5) (2015) 1633–1643.

[20] D. Trivedi, A. K. Bhabor, *Higher Dimensional Bianchi Type-III String Cosmological Models with Dark Energy in Brans-Dicke Scalar-Tensor Theory of Gravitation*, New Astronomy 89 (2021) Article ID 101658 9 pages.

[21] K. L. Mahanta, A. K. Biswal, P. K. Sahoo, *Bulk Viscous String Cloud with Strange Quark Matter in Brans-Dicke Theory*, European Physical Journal-Plus 129 (2014) 141–146.

[22] N. C. Chakraborty, S. Chakraborty, A. Dolgov, *Brans-Dicke Theory in Bianchi III Model and Inflationary Scenario*, International Journal of Modern Physics D 11 (3) (2002) 391–404.

[23] K. S. Adhav, M. R. Ugale, C. B. Kale, M. P. Bhende, *Plane Symmetric Vacuum Bianchi Type-III Cosmological Model in Brans-Dicke Theory*, International Journal of Theoretical Physics 48 (1) (2009) 178–182

[24] H. Çağlar, S.Aygün, C. Aktaş, D. Taşer, *LRS Binachi I Model with Strange Quark Matter Attached to String Cloud in Brans-Dicke Theory*, International Physics Conference of the Balkan Physical Union 22 (2014) 221014 129–137.

[25] H. Çağlar, S.Aygün, *Exact Solutions of Bulk Viscous with String Cloud Attached to Strange Quark Matter for Higher Dimensional FRW Universe in Lyra Geometry*, AIP Conference Proceedings 1722 (2016) 050001 1–5.

[26] H. Çağlar, S. Aygün, *Bulk Viscous String Cloud with Strange Quark Matter in Self Creation Cosmology*, IOSR Journal of Mathematics 11 (6) (2015) 53–59.

[27] H. Çağlar, S. Aygün, *Non-existence of Brans-Dicke Theory in Higher Dimensional FRW Universe*, Astrophysics and Space Science 361 (2016) 1–6.

[28] S. Weinberg, Gravitation and Cosmology: Principles and Applications of the General Theory of Relativity, John Wiley & Sons, New York, 1972.

[29] V .U. M. Rao, D. Neelima, *Cosmological Models with Strange Quark Matter Attached to String Cloud in GR and Brans-Dicke Theory of Gravitation*, The European Physical Journal-Plus 129 (2014) 122–136.

[30] A. Dixit, R. Zia, A. Pradhan, *Anisotropic Bulk Viscous String Cosmological Models of the Universe under a Time-Dependent Deceleration Parameter*, Pramana 94 (1) (2020) Article Number 25 11 pages.

[31] G. Mohanty, S. K. Sahu, P. K. Saho, *Massive Scalar Field in the Bianchi Type I Space Time*, Astrophysics and Space Science 288 (2003) 421–427.

[32] K. S. Adhav, *LRS Bianchi Type-I Cosmological Model in $f(R,T)$ Theory of Gravity*, Astrophysics and Space Science 339 (2012) 365–369.

[33] O. Özdemir, C. Aktaş, *Anisotropic Universe Models with Magnetized Strange Quark Matter in $f(R)$ Gravity Theory*, Modern Phys. Lett. A 35 (14) (2020) 2050111 9 pages.

[34] D. Taşer, M. U. Doğru, *Scalar Fields in $f(G)$ Gravity*, International Journal of Geometric Methods in Modern Physics 17 (09) (2020) 2050132 17 pages.

[35] R. Bali, *Magnetized Cosmological Model*, International Journal of Theoretical Physics A 25 (1986) 755–761.

[36] K. S. Adhav, *LRS Bianchi Type-I Cosmological Model with Linearly Varying Deceleration Parameter*, The European Physical Journal-Plus 126 (2011) 122–128.

[37] P. K. Sahoo, B. Mishra, *String Cloud and Domain Walls with Quark Matter for Plane Symmetric Cosmological Model in Bimetric Theory*, Journal of Theoretical and Applied Physics 7 (2013) 12–16.

[38] M. Kiran, D. R. K. Reddy, *Non-existence of Bianchi Type-III Bulk Viscous String Cosmological Model in $f(R,T)$ Gravity*, Astrophysics and Space Science 346 (2013) 521–524.

[39] S. M. Carroll, M. Hoffman, *Can the Dark Energy Equation-of-State Parameter w be Less than A1?*, Physical Review D 68 (2003) 023509 1–11.

Journal of New Theory
ISSN: 2149-1402

44 (2023) 97-105
Journal of New Theory
https://dergipark.org.tr/en/pub/jnt
Open Access

An Alternative Method for Determination of the Position Vector of a Slant Helix

Gizem Güzelkardeşler[1], **Burak Şahiner**[2]

Article Info
Received: 7 Sep 2023
Accepted: 22 Sep 2023
Published: 30 Sep 2023
doi:10.53570/jnt.1356697
Research Article

Abstract — In this paper, we provide an alternative method to determine the position vector of a slant helix with the help of an alternative moving frame. We then construct a vector differential equation in terms of the principal normal vector of a slant helix using an alternative moving frame. By solving this vector differential equation, we determine the position vector of the slant helix. Afterward, we obtain parametric representations of some examples of slant helices for chosen curvature and torsion functions as an application of the proposed method. Finally, we discuss the method and whether further research should be conducted or not.

Keywords *Alternative moving frame, intrinsic equations, position vector, slant helix*

Mathematics Subject Classification (2020) 53A04, 34A05

1. Introduction

In differential geometry, the theory of curves is one of the main study areas. The theory of curves is generally studied with the well-known Frenet frame. Many geometric properties of differentiable curves can be defined with the help of this frame. In addition, the determination of the characterization of some special curves can be achieved by the curvatures of the Frenet frame. Among these special curves, various types of helices, including general helices, circular helices, and slant helices, are the curves that attract the most attention from researchers. A general helix (formerly called cylindrical helix) is defined by the property that all tangent vectors along the curve make a constant angle with a fixed direction. A necessary and sufficient condition for a curve to be a general helix is that the ratio of torsion to curvature is a constant [1]. There are numerous uses for general helices in different branches of science, such as biology, fractal geometry, computer-aided geometric design, engineering, and architecture [2–5]. After a long time since the concept of general helix hs been introduced, a new curve called slant helix has been defined with a similar idea. A slant helix is a curve whose principal normal vectors make a constant angle with a fixed straight line, which is the axis of the slant helix [6]. A necessary and sufficient condition for a curve to be a slant helix is that the ratio $\frac{\kappa^2}{(\kappa^2+\tau^2)^{3/2}}(\frac{\tau}{\kappa})'$ is constant, where κ and τ are curvature and torsion functions of the curve, respectively [6].

According to the fundamental theorem for curves, given two continuous functions of one parameter, a space curve can be determined uniquely up to rigid motion for which the two functions are its curvature and torsion [7]. The problem of determining the position vector of this curve is known as

[1]gizemguzelkardesler@ktu.edu.tr; [2]burak.sahiner@cbu.edu.tr (Corresponding Author)
[1]Department of Mathematics, Faculty of Science, Karadeniz Technical University, Trabzon, Türkiye
[2]Department of Mathematics, Faculty of Science and Letters, Manisa Celal Bayar University, Manisa, Türkiye

solving natural or intrinsic equations [1]. Although the problem has a solution for an arbitrary curve in Galilean space, it remains an open problem for Euclidean and Minkowski spaces [8, 9]. For the problem of determining the position vector of a general helix, a method depending on solving a vector differential equations constructed with the help of the Frenet frame has been proposed in [10]. Using this method, the parametric representation of the position vector of a general helix with the known curvature and torsion functions has been found. Then, a similar method has been used to determine a slant helix's position vector in [11]. After that, similar techniques have been applied for determining position vectors of some special curves with the help of various moving frames, such as the Frenet frame, the type-2 Bishop frame, the Darboux frame, and the alternative moving frame, in various spaces, Euclidean space, Minkowski space, and Galilean space [9, 12–19].

In this paper, we propose an alternative method to the existing methods in the literature to determine the position vector of a slant helix. We first rewrite the derivative formulae of the alternative moving frame to obtain a simpler differential equation. Then, we construct a vector differential equation in terms of the principal normal vector with the help of the new derivative formulae of the alternative moving frame. By solving this vector differential equation, we find the principal normal vector of the slant helix and thus determine the position vector of the curve. Finally, applying the proposed method, we obtain parametric representations of some examples of slant helices for chosen curvature and torsion functions.

2. Preliminaries

Let $\alpha = \alpha(s)$ be a unit speed Frenet curve in E^3, that is, $\langle \alpha'(s), \alpha'(s) \rangle = 1$ and $\alpha''(s) \neq 0$. The Frenet frame along the curve α consists of three mutually orthonormal vectors defined by

$$\boldsymbol{T}(s) = \alpha'(s), \quad \boldsymbol{N}(s) = \frac{1}{\| \boldsymbol{T}'(s) \|} \boldsymbol{T}'(s), \quad \text{and} \quad \boldsymbol{B}(s) = \boldsymbol{T}(s) \times \mathbf{N}(s) \tag{1}$$

where $\boldsymbol{T}(s)$, $\boldsymbol{N}(s)$, and $\boldsymbol{B}(s)$ are called tangent vector, principal normal vector, and binormal vector, respectively. The derivative formulae of the Frenet frame also known as Frenet formulae can be provided as follows:

$$\begin{bmatrix} \boldsymbol{T}'(s) \\ \boldsymbol{N}'(s) \\ \boldsymbol{B}'(s) \end{bmatrix} = \begin{bmatrix} 0 & \kappa(s) & 0 \\ -\kappa(s) & 0 & \tau(s) \\ 0 & -\tau(s) & 0 \end{bmatrix} \begin{bmatrix} \boldsymbol{T}(s) \\ \boldsymbol{N}(s) \\ \boldsymbol{B}(s) \end{bmatrix} \tag{2}$$

where κ and τ are called curvature and torsion functions of the curve α, respectively. These functions, also called Frenet curvatures, are defined by

$$\kappa(s) = \| \boldsymbol{T}'(s) \| \quad \text{and} \quad \tau(s) = -\langle \boldsymbol{B}'(s), \boldsymbol{N}(s) \rangle$$

In Euclidean 3-space, apart from the Frenet frame, many moving frames has been defined to study the differential geometric properties of curves. One of them is the alternative moving frame. The alternative moving frame consists of three mutually orthonormal vectors. These vectors are the unit principal normal vector $\boldsymbol{N}(s)$, also included in the Frenet frame, the unit vector $\boldsymbol{C}(s)$ defined by $\boldsymbol{C}(s) = \frac{\boldsymbol{N}'(s)}{\|\boldsymbol{N}'(s)\|}$, and the unit vector $\boldsymbol{W}(s)$ defined by $\boldsymbol{W}(s) = \boldsymbol{N}(s) \times \boldsymbol{C}(s)$, also normalized instantaneous rotation vector of the Frenet frame [20, 21]. The derivative formulae of the alternative moving frame are as follows [20]:

$$\begin{bmatrix} \boldsymbol{N}'(s) \\ \boldsymbol{C}'(s) \\ \boldsymbol{W}'(s) \end{bmatrix} = \begin{bmatrix} 0 & f(s) & 0 \\ -f(s) & 0 & g(s) \\ 0 & -g(s) & 0 \end{bmatrix} \begin{bmatrix} \boldsymbol{N}(s) \\ \boldsymbol{C}(s) \\ \boldsymbol{W}(s) \end{bmatrix} \tag{3}$$

where the functions

$$f = \sqrt{\kappa^2 + \tau^2} \tag{4}$$

and

$$g = \frac{\kappa^2}{\kappa^2 + \tau^2}\left(\frac{\tau}{\kappa}\right)' \tag{5}$$

are called the first and the second alternative curvatures of the curve α, respectively. From Equalities 4 and 5, we have the followings [22]:

$$\kappa(s) = f(s)\cos\left(\int g(s)ds\right) \tag{6}$$

and

$$\tau(s) = f(s)\sin\left(\int g(s)ds\right) \tag{7}$$

The alternative curvatures play a major role in the characterizations of curves. The following theorem supports this idea.

Theorem 2.1. [20] Let α be a curve in E^3 with alternative curvatures f and g. The curve α is a slant helix if and only if the function

$$\sigma = \frac{g}{f} \tag{8}$$

is a constant.

3. Determination of the Position Vector of a Slant Helix

In this section, the problem of determining a slant helix's position vector is solved using a method based on the alternative moving frame. To achieve this, we first rewrite the derivative formulae of the alternative moving frame with a new parameter. Then, we construct a vector differential equation in terms of the principal normal vector by using these new formulae. By solving this vector differential equation, we obtain the position vector of the slant helix in parametric form. Before constructing the vector differential equation, it will be more useful to use new derivative formulae obtained by the parameter transformation $\theta = \int f(s)ds$ instead of the derivative formulae given in Equality 3 where $f(s)$ is the first alternative curvature. According to this new parameter θ, the derivative formulae of the alternative moving frame become the following form [19]:

$$\begin{bmatrix} \boldsymbol{N}'(\theta) \\ \boldsymbol{C}'(\theta) \\ \boldsymbol{W}'(\theta) \end{bmatrix} = \begin{bmatrix} 0 & 1 & 0 \\ -1 & 0 & \sigma(\theta) \\ 0 & -\sigma(\theta) & 0 \end{bmatrix} \begin{bmatrix} \boldsymbol{N}(\theta) \\ \boldsymbol{C}(\theta) \\ \boldsymbol{W}(\theta) \end{bmatrix} \tag{9}$$

such that $\sigma(\theta) = \frac{g(\theta)}{f(\theta)}$.

Theorem 3.1. Let $\alpha = \alpha(s)$ be a unit speed slant helix and $\alpha = \alpha(\theta)$ be another parametric representation of this curve where $\theta = \int f(s)ds$. The principal normal vector $\boldsymbol{N}(\theta)$ satisfies the following vector differential equation

$$\boldsymbol{N}'''(\theta) + (1 + \sigma^2)\boldsymbol{N}'(\theta) = 0 \tag{10}$$

where $\sigma(\theta) = \frac{g(\theta)}{f(\theta)}$.

Proof.

From the second equation of Equality 9, the vector $\boldsymbol{W}(\theta)$ can be written as

$$\boldsymbol{W}(\theta) = \frac{1}{\sigma(\theta)}\left(\boldsymbol{C}'(\theta) + \boldsymbol{N}(\theta)\right) \tag{11}$$

Differentiating the first equation of Equality 9,

$$\boldsymbol{N}''(\theta) = \boldsymbol{C}'(\theta) \tag{12}$$

Substituting Equality 12 into Equality 11,

$$\boldsymbol{W}(\theta) = \frac{1}{\sigma(\theta)} \left(\boldsymbol{N}''(\theta) + \boldsymbol{N}(\theta)\right) \tag{13}$$

By differentiating Equality 13 and by using the first and third equations of Equality 9,

$$\left(\frac{1}{\sigma(\theta)} \left(\boldsymbol{N}''(\theta) + \boldsymbol{N}(\theta)\right)\right)' + \sigma(\theta)\boldsymbol{N}'(\theta) = 0 \tag{14}$$

According to Theorem 2.1, $\sigma(\theta)$ is a constant. Thus, Equality 14 becomes Equality 10 which completes the proof. □

Equality 10 is a third-order vector differential equation with constant coefficients. The principal normal vector $\boldsymbol{N}$ can be found by solving this equation. The following theorem provides a solution for the problem of determining the position vector of a slant helix given the curvature and torsion functions.

Theorem 3.2. Let $\kappa(s) > 0$ and $\tau(s)$ be two differentiable functions on an interval I. On this interval, the position vector $\alpha(s) = (\alpha_1(s), \alpha_2(s), \alpha_3(s))$ of a slant helix for which s, $\kappa(s)$ and $\tau(s)$ become the arc-length, the curvature and the torsion, respectively, can be determined up to rigid motions in Euclidean 3-space as follows:

$$\begin{cases} \alpha_1(s) = \frac{1}{\sqrt{1+\sigma^2}} \int \left(\int f(s) \cos\left(\sigma \int f(s)ds\right) \cos\left(\sqrt{1+\sigma^2} \int f(s)ds\right) ds \right) ds \\ \alpha_2(s) = \frac{1}{\sqrt{1+\sigma^2}} \int \left(\int f(s) \cos\left(\sigma \int f(s)ds\right) \sin\left(\sqrt{1+\sigma^2} \int f(s)ds\right) ds \right) ds \\ \alpha_3(s) = \frac{\sigma}{\sqrt{1+\sigma^2}} \int \left(\int f(s) \cos\left(\sigma \int f(s)ds\right) ds \right) ds \end{cases} \tag{15}$$

where $\sigma = \frac{g}{f}$ and f and g are the alternative curvatures defined in Equalities 4 and 5, respectively.

Proof.
Let $\alpha = \alpha(s)$ be a unit speed slant helix in E^3 and $\alpha = \alpha(\theta)$ be another parametrization of the same where $\theta = \int f(s)ds$. We can write the principal normal vector $\boldsymbol{N}(\theta)$ of the curve $\alpha(\theta)$ with the standard basis of E^3 as $\boldsymbol{N}(\theta) = N_1(\theta)\boldsymbol{e_1} + N_2(\theta)\boldsymbol{e_2} + N_3(\theta)\boldsymbol{e_3}$. We can choose the axis of the slant helix to be parallel to $\boldsymbol{e_3}$ without losing generality. Note that selections of different axes will produce the same slant helix up to rigid motion in Euclidean 3-space. Since the vector $\boldsymbol{N}(\theta)$ makes a constant angle with the axis, then

$$\langle \boldsymbol{N}(\theta), \boldsymbol{e_3} \rangle = N_3(\theta) = n \tag{16}$$

where n is a constant real number. It is clear that $N_3(\theta) = n$ satisfies Equality 10. Additionally, since $\boldsymbol{N}(\theta)$ is a unit vector,

$$N_1^2(\theta) + N_2^2(\theta) = 1 - n^2 \tag{17}$$

From the general solution of Equality 17, the components N_1 and N_2 can be written as

$$N_1(\theta) = \sqrt{1-n^2}\cos(t(\theta)) \quad \text{and} \quad N_2(\theta) = \sqrt{1-n^2}\sin(t(\theta))$$

where t is a function of θ. The components N_1 and N_2 should satisfy Equality 10. Substituting $N_1(\theta)$ and $N_2(\theta)$ into Equality 10, we obtain the following equalities:

$$(3t't'')\cos t + \left(-(t')^3 + t''' + (1 + (\sigma)^2)t'\right)\sin t = 0 \tag{18}$$

$$(3t't'')\sin t - \left(-(t')^3 + t''' + (1+(\sigma)^2)t'\right)\cos t = 0 \tag{19}$$

From Equalities 18 and 19, we have the following equalities:

$$3t''t' = 0 \tag{20}$$

$$t'' - (t')^3 + (1+\sigma^2)t' = 0 \tag{21}$$

From Equality 20,

$$t(\theta) = c_1\theta + c_2 \tag{22}$$

where c_1 and c_2 are constants. If we change the parameter $t \to t + c_2$, then

$$t(\theta) = c_1\theta \tag{23}$$

Substituting Equality 23 into Equality 21,

$$c_1(-{c_1}^2 + 1 + \sigma^2) = 0 \tag{24}$$

Solving Equality 24,

$$c_1 = \pm\sqrt{1+\sigma^2} \tag{25}$$

Substituting Equality 25 into Equality 23, the function $t(\theta)$ can be obtained as

$$t = \pm\sqrt{1+\sigma^2}\theta$$

Therefore, the vector $\boldsymbol{N}(\theta)$ can be found as follows:

$$\boldsymbol{N}(\theta) = \left(\sqrt{1-n^2}\cos\left(\sqrt{1+\sigma^2}\theta\right), \pm\sqrt{1-n^2}\sin\left(\sqrt{1+\sigma^2}\theta\right), n\right) \tag{26}$$

Moreover, the constant n in Equality 26 can be written in terms of σ. Differentiating Equality 16 and using the first equation of Equality 9,

$$\langle \boldsymbol{C}(\theta), \boldsymbol{e_3}\rangle = 0 \tag{27}$$

Differentiating Equality 27 and using the second equation of Equality 9,

$$\langle \boldsymbol{W}(\theta), \boldsymbol{e_3}\rangle = \frac{n}{\sigma}$$

Since the axis of the slant helix is a unit vector,

$$n = \pm\frac{\sigma}{\sqrt{1+\sigma^2}} \tag{28}$$

Substituting Equality 28 into Equality 26, the principal normal vector $\boldsymbol{N}(\theta)$ of the slant helix can be written in terms of the parameter θ as

$$\boldsymbol{N}(\theta) = \frac{1}{\sqrt{1+\sigma^2}}\left(\cos\left(\sqrt{1+\sigma^2}\theta\right), \pm\sin\left(\sqrt{1+\sigma^2}\theta\right), \pm\sigma\right)$$

or in terms of the arc-length parameter s as

$$\boldsymbol{N}(s) = \frac{1}{\sqrt{1+\sigma^2}}\left(\cos\left(\sqrt{1+\sigma^2}\int f(s)ds\right), \pm\sin\left(\sqrt{1+\sigma^2}\int f(s)ds\right), \pm\sigma\right) \tag{29}$$

Moreover, from Equalities 1 and 2, the curve α can be written as

$$\alpha(s) = \int\left(\int \kappa(s)\boldsymbol{N}(s)ds\right)ds$$

By using Equality 4 and the parameter transformation $\theta = \int f(s)ds$,

$$\alpha(\theta) = \int\frac{1}{f(\theta)}\left(\int\cos(\sigma\theta)\boldsymbol{N}(\theta)d\theta\right)d\theta$$

If the curve α is written again in terms of the arc length parameter s,

$$\alpha(s) = \int \left(\int f(s) \cos\left(\sigma \int f(s)ds \right) \boldsymbol{N}(s)ds \right) ds \tag{30}$$

By choosing the positive sign in Equality 29 and substituting it into Equality 30, the position vector $\alpha(s) = (\alpha_1(s), \alpha_2(s), \alpha_3(s))$ of the slant helix can be found as

$$\begin{cases} \alpha_1(s) = \frac{1}{\sqrt{1+\sigma^2}} \int \left(\int f(s) \cos\left(\sigma \int f(s)ds \right) \cos\left(\sqrt{1+\sigma^2} \int f(s)ds \right) ds \right) ds \\ \alpha_2(s) = \frac{1}{\sqrt{1+\sigma^2}} \int \left(\int f(s) \cos\left(\sigma \int f(s)ds \right) \sin\left(\sqrt{1+\sigma^2} \int f(s)ds \right) ds \right) ds \\ \alpha_3(s) = \frac{\sigma}{\sqrt{1+\sigma^2}} \int \left(\int f(s) \cos\left(\sigma \int f(s)ds \right) ds \right) ds \end{cases} \tag{31}$$

Given the curvature and torsion functions, the functions f, g, and σ can be determined using Equalities 4 and 5 and Theorem 2.1. Substituting f and σ into Equality 31, the position vector of the slant helix can be obtained. □

4. Illustrative Examples

In this section, we obtain parametric representations of some examples of slant helices for chosen some special curvature and torsion functions.

Example 4.1. If $\kappa = \cos(s)$ and $\tau = \sin(s)$, then $f = 1$, $g = 1$, and $\sigma = 1$ from Equalities 4, 5, and 8. From Equality 15, the position vector $\alpha(s)$ of the slant helix can be found as

$$\alpha(s) = \left(-\tfrac{3\sqrt{2}}{2} \cos(\sqrt{2}s)\cos(s) - 2\sin(\sqrt{2}s)\sin(s), -\tfrac{3\sqrt{2}}{2} \sin(\sqrt{2}s)\cos(s) + 2\cos(\sqrt{2}s)\sin(s), -\tfrac{\sqrt{2}}{2} \cos(s) \right)$$

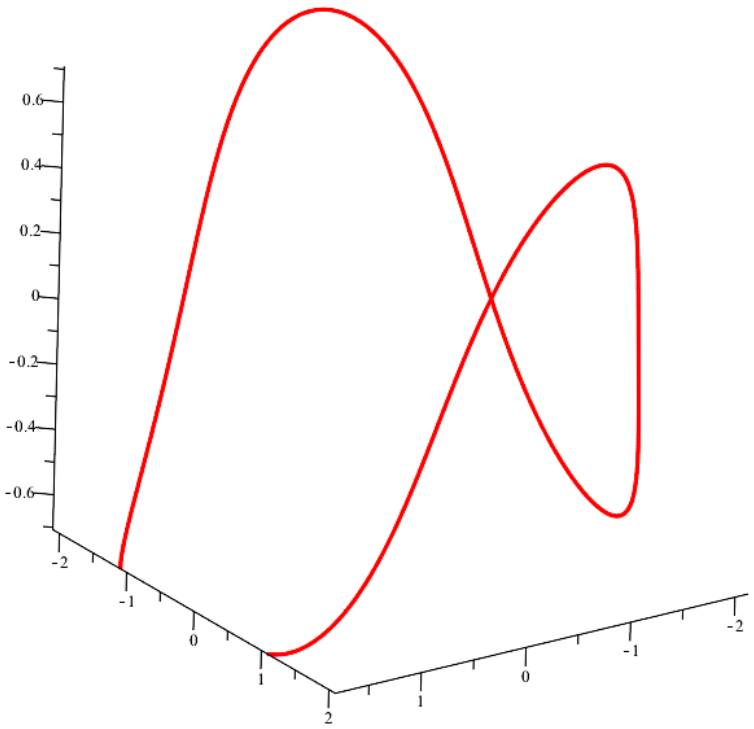

Figure 1. Slant helix with $\kappa = \cos(s)$ and $\tau = \sin(s)$

Example 4.2. Let curvature and torsion functions be given as $\kappa = \frac{1}{(1+s^2)^{3/2}}$ and $\tau = \frac{s}{(1+s^2)^{3/2}}$, respectively. From Equalities 4, 5, and 8, $f = \frac{1}{1+s^2}$, $g = \frac{1}{1+s^2}$, and $\sigma = 1$. Using Equality 15, the

position vector of the slant helix can be obtained in the parametric representation as

$$\alpha(s) = \left(\frac{\sqrt{2}}{2}\sqrt{1+s^2}\cos\left(\sqrt{2}\arctan(s)\right), -\frac{\sqrt{2}}{2}\sqrt{1+s^2}\sin\left(\sqrt{2}\arctan(s)\right), \frac{\sqrt{2}}{2}\sqrt{1+s^2} \right)$$

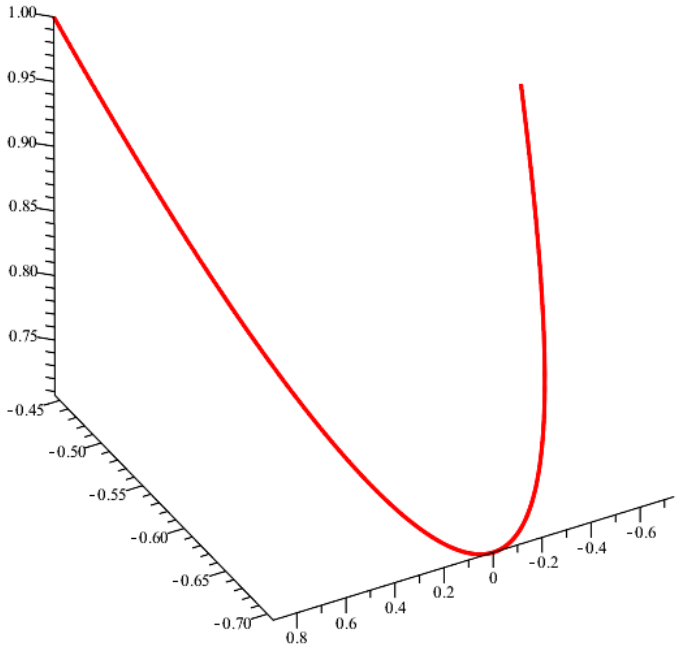

Figure 2. Slant helix with $\kappa = \frac{1}{(1+s^2)^{3/2}}$ and $\tau = \frac{s}{(1+s^2)^{3/2}}$

Example 4.3. Let curvature and torsion functions be given as $\kappa = \frac{\cos(\sqrt{s})}{2\sqrt{s}}$ and $\tau = \frac{\sin(\sqrt{s})}{2\sqrt{s}}$, respectively. The functions f, g, and σ can be found as $f = \frac{1}{2\sqrt{s}}$, $g = \frac{1}{2\sqrt{s}}$, and $\sigma = 1$, respectively. Using Equality 15, the position vector $\alpha(s)$ of the slant helix can be expressed in the parametric representation as

$$\alpha(s) = \left(-\tfrac{\sqrt{2}}{2}\cos\left(\sqrt{2s}\right)\sin\left(\sqrt{s}\right) + \sin\left(\sqrt{2s}\right)\cos\left(\sqrt{s}\right), -\tfrac{\sqrt{2}}{2}\sin\left(\sqrt{2s}\right)\sin\left(\sqrt{s}\right) - \cos\left(\sqrt{2s}\right)\cos\left(\sqrt{s}\right), \tfrac{\sqrt{2}}{2}\sin\left(\sqrt{s}\right)\right)$$

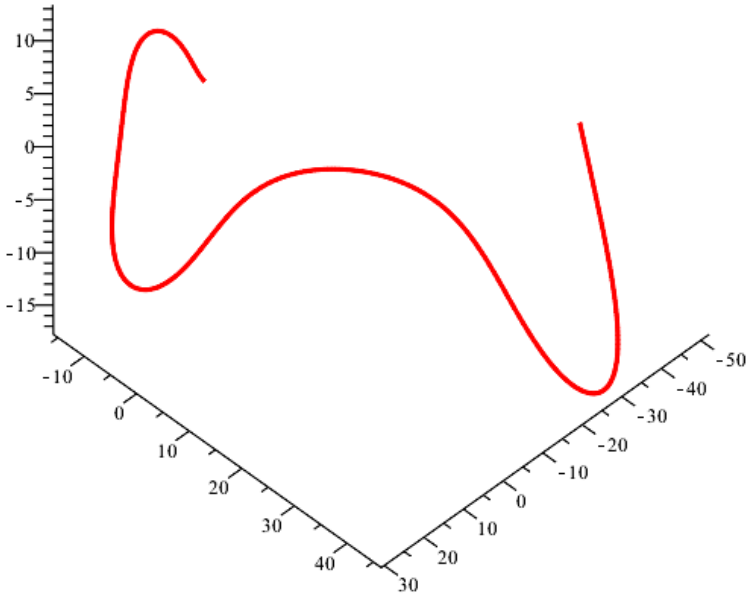

Figure 3. Slant helix with $\kappa = \frac{\cos(\sqrt{s})}{2\sqrt{s}}$ and $\tau = \frac{\sin(\sqrt{s})}{2\sqrt{s}}$

5. Conclusion

In this paper, we give a method for the determination of the position vector of a slant helix. This method basically includes two important steps. The first step is constructing a vector differential equation in terms of the principal normal vector of the curve with the help of the alternative moving frame. The second step is determining the position vector of the slant helix by solving the equation in the first step. Thanks to this method, the problem of determining the position vector of a curve given the curvature and torsion functions is solved for a slant helix case. As an application of the method, some examples of slant helices in parametric form are obtained for given special curvature and torsion functions. It is thought that the obtained examples of slant helices will contribute to the variety of examples of slant helices in the literature.

The problem of determining the position vector of a slant helix, solved in this paper, is also discussed in [11] and [19]. In [11], a method based on solving a vector differential equation in terms of the principal normal vector constructed with the help of Frenet formulae is presented. Since the characterization of a slant helix cannot be used directly in this vector differential equation, this method for determining the position vector of a slant helix involves much more complicated mathematical operations than the method in the present paper. In [19], the authors give a method based on the alternative moving frame to solve the same problem. Unlike the method in the present paper, the vector differential equation is constructed in terms of the vector $\boldsymbol{C}$ of the alternative moving frame in the method given in [19]. Moreover, this method has been developed to determine a slant helix's position vector in Minkowski 3-space, not Euclidean 3-space. The necessity of finding all the vectors of the alternative moving frame to determine the position vector of the slant helix is an important disadvantage of this method. In light of all these comparisons, it is hoped that the method in the present paper will be an important alternative to the methods in the literature for the problem of determining the position vector of a slant helix.

Author Contributions

All the authors equally contributed to this work. This paper is derived from the first author's master's thesis supervised by the second author. They all read and approved the final version of the paper.

Conflicts of Interest

All the authors declare no conflict of interest.

References

[1] D. J. Struik, Lectures on Classical Differential Geometry, 2nd Edition, Dover, New York, 1988.

[2] N. Chouaieb, A. Goriely, J. H. Maddocks, *Helices*, Proceedings of the National Academy of Sciences 103 (25) (2006) 9398–9403.

[3] A. A. Lucas, P. Lambin, *Diffraction by DNA, Carbon Nanotubes and Other Helical Nanostructures*, Reports on Progress in Physics 68 (5) (2005) 1181–1249.

[4] C. D. Toledo-Suarez, *On the Arithmetic of Fractal Dimension Using Hyperhelices*, Chaos, Solitons & Fractals 39 (1) (2009) 342–349.

[5] J. D. Watson, F. H. C. Crick, *Generic Implications of the Structure of Deoxyribonucleic Acid*, Nature 171 (1953) 964–967.

[6] S. Izumiya, N. Takeuchi, *New Special Curves and Developable Surfaces*, Turkish Journal of Mathematics 28 (2) (2004) 153–163.

[7] P. Hartman, A. Wintner, *On the Fundamental Equations of Differential Geometry*, American Journal of Mathematics 72 (4) (1950) 757–774.

[8] L. P. Eisenhart, A Treatise on Differential Geometry of Curves and Surfaces, Dover, New York, 1960.

[9] A. T. Ali, *Position Vectors of Curves in the Galilean Space G_3*, Matematički Vesnik 64 (3) (2012) 200–210.

[10] A. T. Ali, *Position Vectors of General Helices in Euclidean 3-Space*, Bulletin of Mathematical Analysis and Applications 3 (2) (2011) 198–205.

[11] A. T. Ali, *Position Vectors of Slant Helices in Euclidean 3-Space*, Journal of the Egyptian Mathematical Society 20 (1) (2012) 1–6.

[12] A. T. Ali, S. R. Mahmoud, *Position Vector of Spacelike Slant Helices in Minkowski 3-Space*, Honam Mathematical Journal 36 (2) (2014) 233–251.

[13] A. T. Ali, M. Turgut, *Position Vector of a Time-like Slant Helix in Minkowski 3-Space*, Journal of Mathematical Analysis and Applications 365 (2) (2010) 559–569.

[14] H. G. Bozok, S. A. Sepet, M. Ergüt, *Position Vectors of General Helices According to Type-2 Bishop Frame in E^3*, Mathematical Sciences and Applications E-Notes 6 (1) (2018) 64–69.

[15] A. El Haimi, A. O. Chahdi, *Parametric Equations of Special Curves Lying on a Regular Surface in Euclidean 3-Space*, Nonlinear Functional Analysis and Applications 26 (2) (2021) 225–236.

[16] A. El Haimi, M. Izid, A. O. Chahdi, *Position Vectors of Curves Generalizing General Helices and Slant Helices in Euclidean 3-Space*, Tamkang Journal of Mathematics 52 (4) (2021) 467–478.

[17] H. Öztekin, S. Tatlıpınar, *Determination of the Position Vectors of Curves from Intrinsic Equations in G_3*, Walailak Journal of Science and Technology 11 (12) (2014) 1011–1018.

[18] T. Şahin, B. C. Dirişen, *Position Vectors of Curves with respect to Darboux Frame in the Galilean space G^3*, Communications Faculty of Sciences University of Ankara Series A1: Mathematics and Statistics 68 (2) (2019) 2079–2093.

[19] B. Yılmaz, A. Has, *New Approach to Slant Helix*, International Electronic Journal of Geometry 12 (1) (2019) 111–115.

[20] B. Uzunoğlu, İ. Gök, Y. Yaylı, *A New Approach on Curves of Constant Precession*, Applied Mathematics and Computation 275 (2016) 317–323.

[21] P. D. Scofield, *Curves of Constant Precession*, American Mathematical Monthly 102 (6) (1995) 531–537.

[22] B. Şahiner, *Ruled Surfaces According to Alternative Moving Frame* (2019) 16 pages, https://arxiv.org/abs/1910.06589.